

---

[All ETDs from UAB](#)

[UAB Theses & Dissertations](#)

---

1970

## Cardiac Output Derived From The Aortic Pressure.

Wilmer Wayne Nichols  
*University of Alabama at Birmingham*

Follow this and additional works at: <https://digitalcommons.library.uab.edu/etd-collection>

---

### Recommended Citation

Nichols, Wilmer Wayne, "Cardiac Output Derived From The Aortic Pressure." (1970). *All ETDs from UAB*. 5619.  
<https://digitalcommons.library.uab.edu/etd-collection/5619>

This content has been accepted for inclusion by an authorized administrator of the UAB Digital Commons, and is provided as a free open access item. All inquiries regarding this item or the UAB Digital Commons should be directed to the [UAB Libraries Office of Scholarly Communication](#).

70-25,574

NICHOLS, Wilmer Wayne, 1934-  
CARDIAC OUTPUT DERIVED FROM THE AORTIC  
PRESSURE.

University of Alabama, Ph.D., 1970  
Physiology

University Microfilms, A XEROX Company, Ann Arbor, Michigan

CARDIAC OUTPUT DERIVED FROM THE AORTIC PRESSURE

BY

WILMER WAYNE NICHOLS

A DISSERTATION

Submitted in partial fulfillment of the requirements for  
the degree of Doctor of Philosophy in the Department of  
Physiology and Biophysics in the Graduate School of the  
University of Alabama in Birmingham

BIRMINGHAM, ALABAMA

1970

To Arlene, Cami and Cory

## ACKNOWLEDGMENTS

I am deeply indebted to Dr. D. A. McDonald for introducing me to the field of Hemodynamics. I would like to express my appreciation to him for his superb guidance in this research project.

I would also like to thank Mr. John Burdeshaw for writing the computer programs, without which this investigation would not have been possible.

In addition, my deep appreciation goes to Dr. Henry Outlaw, for his strong influence on my undergraduate education, and to Dr. Patrick Crawford for indirectly guiding me into the biological sciences.

Lastly, I would like to thank my wife, Arlene, for her continued inspiration and understanding throughout my graduate training, especially during the last few months of 1969.

## TABLE OF CONTENTS

	Page
ACKNOWLEDGMENTS . . . . .	iii
LIST OF TABLES . . . . .	vi
LIST OF ILLUSTRATIONS . . . . .	viii
INTRODUCTION . . . . .	1
HISTORICAL SURVEY . . . . .	4
DISCOVERY OF THE CIRCULATION AND SOME EARLY ESTIMATES OF CARDIAC OUTPUT . . . . .	4
SOME MODERN METHODS FOR MEASURING CARDIAC OUTPUT . . .	6
The Fick Principle . . . . .	6
Indicator-Dilution Method . . . . .	8
The Electromagnetic Flowmeter . . . . .	10
Ultrasonic Flowmeters . . . . .	11
CARDIAC OUTPUT COMPUTED FROM THE CENTRAL AORTIC PRESSURE . . . . .	12
Pressure Pulse Contour Method . . . . .	12
The Pressure-Gradient Method . . . . .	13
THEORETICAL DISCUSSION . . . . .	19
METHODS . . . . .	39
EXPERIMENTAL PROCEDURES . . . . .	75
RESULTS . . . . .	79
DISCUSSION . . . . .	125
Objectives of the research. Present results compared to other methods . . . . .	125

	Page
Effect of no flow probe and a small interval (3 cm) between the two pressure taps . . . . .	131
Effect of the flow probe on the pressure contour and the phase velocity . . . . .	132
Accuracy of the Fourier series fit to the pressure and flow curves . . . . .	150
Individual faulty experiments . . . . .	151
Possible causes of scatter in the computed mean flow at high stroke outputs . . . . .	151
Possible causes of errors in the computed mean flow during the infusion of metaraminol and glucagon . . . . .	152
Possible causes of errors in the computed peak flow . . . . .	152
Validity of the Womersley equations when applied to the arterial system . . . . .	160
SUMMARY . . . . .	163
APPENDIX . . . . .	166
1. Derivation of the flow equation . . . . .	166
2. A review of Fourier Series . . . . .	172
3. The velocity of wave propagation in an elastic tube . . . . .	177
4. The method of calculating an oscillatory flow from the time-derivative of the pressure . .	179
5. The computer program . . . . .	185
BIBLIOGRAPHY . . . . .	204

# LIST OF TABLES

Table		Page
1	Average apparent phase velocities and foot-to-foot velocities during vagal stimulation . . . .	29
2	Resonance frequencies of the manometer-catheter systems . . . . .	42
3	Fourier components of measured variables and the computed impedance . . . . .	50
4	Fourier components of the synthesized flow and the computed impedance . . . . .	51
5	Accumulated sum of the squares of the moduli as percentage of the total variance . . . . .	54
6	Changes in mean flow, heart rate, and mean arterial pressure produced by the various interventions .	76
7	Statistical analysis of the computed mean flow versus the electromagnetic flowmeter in the individual animals . . . . .	80
8	A computer print-out of the statistical data of all the mean flow comparisons . . . . .	88
9	Statistical analysis of the computed mean flow versus the electromagnetic flowmeter with the ten interventions . . . . .	100
10	Statistical analysis of the computed peak flow versus the electromagnetic flowmeter in the individual animals . . . . .	112
11	Statistical analysis of the computed peak flow versus the electromagnetic flowmeter with the ten interventions . . . . .	114
12	A computer print-out of the statistical data of all the peak flow comparisons . . . . .	124



Table		Page
13	Ordinate values for the two pressures . . . . .	181
14	Oscillatory components of pressure number 1 for the first harmonic . . . . .	182
15	Fourier components of pressure number 1 . . . . .	183
16	Fourier components of pressure number 2 . . . . .	184
17	Fourier components of the computed flow curve . . .	186
18	Oscillatory component of the flow for the first harmonic . . . . .	187
19	Oscillatory components of the flow for the remaining five harmonics . . . . .	188

## LIST OF ILLUSTRATIONS

Figure		Page
1	The oscillatory pressure-gradient . . . . .	20
2	Apparent phase velocities under control conditions	25
3	Apparent phase velocities during vagal stimulation	27
4	Relationship between the apparent phase velocity and the impedance modulus under control conditions . . . . .	33
5	Relationship between the apparent phase velocity and the measured impedance modulus during vagal stimulation . . . . .	35
6	Relationship between the apparent phase velocity and the measured impedance modulus during the infusion of epinephrine . . . . .	37
7	Arrangement of the experimental apparatus for recording the two pressures and the flow in the ascending aorta . . . . .	40
8	Block diagram of the experimental set-up . . . . .	46
9	Recording of the EKG, the two pressures and the flow in the ascending aorta . . . . .	48
10	Comparison of total variance to series variance of a flow curve with a pulse frequency of 2.37 Hz	55
11	Comparison of total variance to series variance of a flow curve with a pulse frequency of 1.28 Hz	57
12	Comparison of total variance to series variance of a pressure curve . . . . .	59
13	Comparison of the resynthesized flow curve to the measured flow curve . . . . .	61

Figure		Page
14	The resynthesized pressure curve and the computed flow curve for one harmonic . . . . .	63
15	The resynthesized pressure curve and the computed flow curve for two harmonics . . . . .	65
16	The resynthesized pressure curve and the computed flow curve for three harmonics . . . . .	67
17	The resynthesized pressure curve and the computed flow curve for four harmonics . . . . .	69
18	The resynthesized pressure curve and the computed flow curve for five harmonics . . . . .	71
19	The resynthesized pressure curve and the computed flow curve for ten harmonics . . . . .	73
20	A comparison of the mean flow as determined by the dye-dilution method with that computed from the pressure-gradient method . . . . .	83
21	A scattergram of all the computed mean flows (pressure-gradient method) versus the measured mean flows (dye-dilution and electromagnetic flowmeter) . . . . .	86
22	Comparison of the computed flow moduli to the measured flow moduli under control conditions . .	90
23	Comparison of the computed flow moduli to the measured flow moduli during vagal stimulation . .	92
24	Comparison of the computed flow moduli to the measured flow moduli during the infusion of norepinephrine . . . . .	94
25	Pulsatile flow curves computed using the pressure-gradient method . . . . .	96
26	Comparison of the computed mean flow to the measured mean flow during the introduction of several different interventions . . . . .	98
27	Comparison of the computed mean flow to the measured mean flow during the infusion of dextran	102

Figure		Page
28	Comparison of the computed mean flow to the measured mean flow after hemorrhage . . . . .	104
29	Comparison of the computed mean flow to the measured mean flow during vagal stimulation . . .	106
30	Comparison of the computed mean flow to the measured mean flow during the infusion of isoproterenol . . . . .	108
31	Comparison of the computed mean flow to the measured mean flow during the infusion of norepinephrine . . . . .	110
32	Comparison of the computed peak flow to the measured peak flow under control conditions . . .	116
33	Comparison of the computed peak flow to the measured peak flow during vagal stimulation . . .	118
34	Comparison of the computed peak flow to the measured peak flow with the vagal stimulation determinations omitted . . . . .	120
35	A scattergram of all the computed flows (pressure-gradient method) versus the measured peak flows (electromagnetic flowmeter) . . . . .	122
36	Apparent phase velocities from 3 runs measured in the ascending aorta using an interval of 3 cm between the two pressure taps . . . . .	133
37	The two pressures ( $P_1$ and $P_2$ ) recorded in the ascending aorta before placement of the flow probe . . . . .	136
38	The two pressures ( $P_1$ and $P_2$ ) recorded in the ascending aorta after placement of the flow probe . . . . .	138
39	Moduli of pressure number 1 recorded in the ascending aorta before and after placement of the flow probe . . . . .	140

Figure		Page
40	Moduli of pressure number 2 recorded in the ascending aorta before and after placement of the flow probe . . . . .	142
41	Phase angles of pressure number 1 recorded in the ascending aorta before and after placement of the flow probe . . . . .	144
42	Phase angles of pressure number 2 recorded in the ascending aorta before and after placement of the flow probe . . . . .	146
43	Computed flow moduli before and after placement of the flow probe . . . . .	148
44	Modulus and phase of the input impedance in the dog ascending aorta under control conditions and during vagal stimulation . . . . .	154
45	A flow curve computed using the pressure-gradient technique during vagal stimulation before and after a phase correction . . . . .	156
46	The computed flow curve after a phase correction compared to the flow curve measured with the electromagnetic flowmeter . . . . .	158
47	The first and second harmonic components of the computed flow curve and the sum of the two components . . . . .	189
48	The third harmonic component of the computed flow curve. The sum of the first three harmonics and the final summation of the six harmonics . .	191
49	A flow chart of the computer program . . . . .	193

## INTRODUCTION

The main objective of this investigation was to find a method for recording cardiac output continuously in patients who had undergone open intracardiac operations or patients with acute myocardial infarctions. The electromagnetic (Kolin, 1960; Westersten et al., 1960; Yanof, 1961; Kolin and Wisshaupt, 1963, and Scher et al., 1963) and ultrasonic (Marshall and Shepherd, 1959; Franklin et al., 1961; Franklin et al., 1962, and Franklin et al., 1963) flowmeters are useful instruments for this measurement in animals. However, the orthodox sensing probes used with these instruments require surgical placement on the ascending aorta and, therefore, have limited application in patients. The intravascular sensing probes (Mills, 1966; Mills and Shillingford, 1967; Pardue et al., 1967; Stegall et al., 1967; Bond and Barefoot, 1967; Kolin, 1969; Warbasse et al., 1969; Nolan et al., 1969; Stein and Schuette, 1969, and Benchimol et al., 1969), which were recently introduced, need to be tested more in animals before they can be used in patients with any confidence.

The method used here employs the hydrodynamic equation derived by Womersley (1954, 1955a) relating the flow of a viscous liquid in a rigid tube to a sinusoidal pressure-gradient (see Appendix 1 for a detailed derivation of the equation). Measuring the pressure-

gradient accurately within the limits of the ascending aorta requires extremely accurate calibration matching of the two manometers.

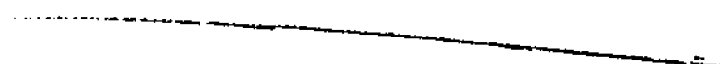
Therefore, it was derived from the time-derivative of the pulse and the phase velocity (McDonald and Taylor, 1959; McDonald, 1960, 1967; McDonald et al., 1968a,b, and Nichols, 1968) since the modern high-frequency manometers that we use have very small phase errors. This procedure for computing pulsatile flow from the pressure-gradient is different from other procedures (e.g. Jones et al., 1959; Jones and Griffin, 1962, and Jones et al., 1966) in that it is independent of other flow methods for calibration and therefore is still valid in profound circulatory changes. If the pulsatile flow could be calculated in the ascending aorta along with the pressure from the same region, then certain important parameters could be determined. Among these are the power output of the heart, the external work, and the input impedance. Therefore, this method would give much more information than a method which estimates stroke volume alone.

An inherent assumption of this method is that the modulus of the input impedance is directly related to the apparent phase velocity ( $c'$ ) (see Theoretical Discussion). This has been demonstrated by Taylor in a transmission line system (1957a) and by us in the ascending aorta (Nichols and McDonald, 1969). Also, when computing the flow from the pressure-gradient it is necessary to know the phase velocity of each harmonic component. We found that the phase velocities were fairly constant for frequencies above 2Hz but below 2Hz they rose sharply, due to reflections from branches and termi-

nations of the system (Nichols et al., 1969, and Nichols and McDonald, 1970).

The computed mean flows from the first seven experiments were compared to those simultaneously determined by the dye-dilution technique (Hamilton, 1953). The mean flows and peak flows from the next thirty-three experiments were compared to those obtained from an electromagnetic flowmeter.

During the experiments, different interventions were introduced to produce changes in the hemodynamic variables. Statistical analysis was performed by the computer on the data collected before and during each intervention.





## HISTORICAL SURVEY

### DISCOVERY OF THE CIRCULATION AND SOME EARLY ESTIMATES OF CARDIAC OUTPUT

Galen (130-200 A.D.), about 165 A.D. (Guthrie, 1945, and Walker, 1955), working with apes and pigs, corrected the error current up to that time that the arteries contained air and proved that they were filled instead with blood. In his opinion, the vital principle was the "pneuma" which entered the lungs in the act of breathing and there mingled with the blood. The blood, he believed, was formed in the liver from foodstuff or chyle; hence, it was endowed with natural spirit and passed to the right ventricle for distribution to the tissues and organs, and also the lungs, in order that the impurities might be exhaled in the breath.

He also proclaimed that there was an ebb and flow movement of the blood in the body and that this movement was brought about by the pumping action of the heart. But he completely missed the point that the blood made a complete circuit of the body. Like his predecessors and like all other medical men of the day, Galen believed that the blood percolated through the intervening septum from one side of the heart to the other. This explanation of the vascular system caused confusion for hundreds of years.

Dr. William Harvey (1578-1657) of St. Bartholomew's Hospital in London announced at his first Lumleian lecture on April 16, 1616, that the movement of the blood was a circular one (motion, as it were, in a circle) and not, as his predecessors had imagined, a slow tidal movement of ebb and flow. He published this great discovery in his book Exercitatio Anatomica de Motu Cordis et Sanguinis in Animalibus in 1628.

In addition to describing the circulation of the blood, he made measurements of how much blood the left ventricle held in its dilated state, i.e. when it was full. He found this to be approximately 92ml in a cadaver. He reasoned that about one-fourth of this amount (i.e. 23ml) was ejected with each contraction and by recording the heart rate he was able to estimate the cardiac output. He gave values up to 3 l/min for the cardiac output. Contrary to his expectations, his book was accepted by the great majority of medical men. This initiated modern cardiovascular physiology, and it was relatively soon after this that the Reverend Stephen Hales (1677-1761), without any previous technical training or equipment, started out to investigate the very difficult problem of the dynamics of the circulation (Hales, 1733). In order to determine the blood pressure, he inserted brass cannulae into the arteries and the veins of various animals (including horses) and then connected these cannulae to vertical glass tubes. By this means he was able to measure and to compare the blood-pressures in different parts of the vascular system. He also computed the

circulation rate, measuring the velocity of the blood as it passed along the veins, arteries, and capillaries. In addition, Hales, using techniques that were essentially similar in principle to those of Harvey, made valuable observations on the measurement of cardiac output (horse - 5.7 l/min; dog - 1.9 l/min). He also introduced the concept of the peripheral resistance in arterioles and discussed the functional significance of the elastic arterial walls.

One of the first efforts to record the pulsatile changes in the velocity of arterial blood is credited to Chauveau (Luciani, 1911) and his pupils about 1860. The apparatus which they used for this was called a hemodromograph. The published records made by this instrument are very good but they are not calibrated.

#### SOME MODERN METHODS FOR MEASURING CARDIAC OUTPUT

##### The Fick Principle

Adolph Fick of Cassel, Germany, devoted a scholarly lifetime to the study of work and heat production in muscles (Rose, 1956). Yet, out of his thoughts came a diversion in 1870 into the field of cardiac output measurement. This led to a brief paper as a principle by which the output of the heart could be calculated (Fick, 1870). The principle states that the flow in a given period of time is equal to the amount of substance entering the stream of flow in the same period of time divided by the difference between the concentrations of the substance before and after the point of

entry. Thus, the "Fick Principle" was introduced, but Fick himself never used it to measure the cardiac output. Instead, it was first used by Grehant and Quinquart in 1886 to measure the cardiac output in six dogs. One of the first, and still the most popular, substances used to calculate the cardiac output using the Fick Principle is oxygen (Guyton, 1963). The formula for calculating cardiac output using oxygen is

$$\text{cardiac output (l/min)} = \frac{\text{O}_2 \text{ consumption (ml/min)}}{\text{arterial O}_2 \text{ (ml/l)} - \text{venous O}_2 \text{ (ml/l)}}$$

In order to use this formula with confidence the samples of blood taken on both sides of the heart must be well mixed. The arterial sample may be taken from any systemic artery since the blood is well mixed in the left ventricle. But, in order to get a well-mixed sample of venous blood, the sample must be taken from the ventricle or the pulmonary arterial system. The usual method for doing this is through a catheter. Forssman (1929) first proved that this could be done by passing a rubber tube into his own forearm vein and threaded it into his own right atrium. A year later, Klein (1930) showed that an adequate sample of mixed venous blood for determining cardiac output can be removed from the right ventricle through a catheter. Cournand and his associates (Cournand and Ranges, 1941; Cournand, 1945, and Cournand et al., 1945) established the safety of the procedure and stimulated widespread utilization of the method, and Guyton et al. (1959) have

developed a continuous cardiac output recorder that utilizes the Fick Principle.

When using the Fick Principle to calculate cardiac output, all the necessary factors may be measured directly (direct Fick method) or some of them may be inferred from other factors rather than being measured directly (indirect Fick method).

Although oxygen is the most widely used substance in calculating cardiac output, using the Fick method (direct or indirect), other substances have also been used. Among these are carbon dioxide (Medkins, 1922), para-amino-hippuric acid (Grossman, 1953) and acetylene (Grollman, 1929).

#### Indicator-Dilution Method

In the simplest of the indicator-dilution methods for determining cardiac output, an indicator substance is injected rapidly into the venous blood, and then its concentration in the blood is measured continuously as it passes into the arterial system. The greater the cardiac output, the more rapidly the "dilution" curve of the substance appears and disappears in the arterial blood. This is the origin of the term "indicator-dilution" method. Any type of substance that can be injected into the circulation without altering circulation dynamics, that does not disappear from the blood as it passes to the point of sampling, and that can be analyzed in the blood can be used as the indicator.

Two different types of indicator-dilution methods have been used with success. (1) the single injection method in which the indicator substance is injected in a single rapid injection, and (2) the continuous infusion method in which a continuous infusion of an indicator substance is suddenly begun and continued for a third of a minute or more.

Stewart (1897) was the first to use an indicator-dilution method for measuring cardiac output; he used the continuous infusion procedure. In his early experiments, he used as indicators different dyes or glucose, but because of technical difficulties, he later chose a hypertonic saline solution as his preferred indicator. He determined its concentration in the arterial blood by measuring the change in electrical conductivity of the blood.

Though Stewart stated in a second paper in 1921 that he had used the single injection technique for measuring cardiac output in his earlier studies, he did not describe this method in his publication of 1897.

The first recorded use of the single injection method was by Henriques (1913). He derived the formula that is used today in the single injection dilution method and also recognized and discussed the importance of recirculation of the indicator as a possible error in the method.

In 1928 Hamilton and his colleagues (1953, 1962) began a long series of studies to prove the validity of the single injection indicator-dilution method for accurate measurement of cardiac output.

In his many studies, Hamilton investigated essentially all suggested possibilities of error in the method, and very early in his work he made a particularly important contribution to the procedure by devising a technique to correct for recirculation of the indicator (Kinsman et al., 1929), thereby greatly improving the accuracy of the method.

### The Electromagnetic Flowmeter

The electromagnetic flowmeter is at present the most widely used device for measuring pulsatile blood flow. The instrument was first introduced in the United States by Kolin in 1936 and in Germany by Wetterer in 1937 (Jochim, 1948) and since then many different versions have been described (Scher et al., 1963; Westersten et al., 1960, and Yanof, 1961).

This device depends on the principle that when a conductor moves at right angles to the lines of force of a uniform magnetic field an electrical potential is induced. This potential difference is given by the following equation (Jochim, 1948):

$$E = H L V 10^{-8}$$

where H is the strength of the magnetic field in gauss, L the length of the conductor in cm, i.e. the internal diameter of the vessel, and V the velocity of the conductor in cm/sec. If H and L are kept constant it can be seen that the voltage E varies linearly with the velocity of flow, and, in fact, the velocity recorded is the average

velocity across the pipe, provided the profile is symmetrical (Kolin, 1945). The calibration curve is thus a straight line passing through the origin.

The general principle of electromagnetic induction as a measure of flow is said (Shercliff, 1962) to have been suggested by Faraday in 1832, who unsuccessfully attempted to measure electric currents from the flow of the Thames in the earth's magnetic field.

The advantages of the electromagnetic flowmeter are (a) the linear calibration mentioned above; (b) it records back flow as well as forward flow; (c) the probe can be applied to the outside of the vessel or inserted into it (Mills, 1966; Mills and Shillingford, 1967; Nolan et al., 1969; Stein and Schuette, 1969, and Kolin, 1969); and (d) it can be calibrated in vitro (Malooly et al., 1963) and in vivo (Weber et al., 1968).

#### Ultrasonic Flowmeters

In the past few years, another type of flowmeter, the ultrasonic flowmeter, that might prove to be as valuable as the electromagnetic flowmeter, has been developed.

The theory of operation of the ultrasonic flowmeter is based upon two physical phenomena: (1) the effective velocity of sound propagated through a medium in motion is equal to the sum of the velocity of the medium and the velocity of sound in the medium; (2) the change in frequency of an ultrasound wave as it is reflected back toward the sending direction from the moving particles in the



flowing liquid (Doppler effect).

The pulsed transit time (Franklin et al., 1962) and continuous phase-shift (Marshall and Shepherd, 1959) flowmeters both make use of the first phenomenon and the Doppler shift flowmeter (Franklin et al., 1961, and Franklin et al., 1963) makes use of the second.

This instrument is similar to the electromagnetic flowmeter in that both inside (Stegall et al., 1967, and Pardue et al., 1967) and outside probes may be used.

#### CARDIAC OUTPUT COMPUTED FROM THE CENTRAL AORTIC PRESSURE

##### Pressure Pulse Contour Method

Erlanger and Hooker (1904) appear to be the first to have suggested a method by which the cardiac output could be estimated from the pressure pulse. This method was later used by Dawson and Gorham (1908) and Rosen and White (1926). They assumed that cardiac output was directly proportional to the pulse pressure times the pulse rate. Unfortunately, these authors did not compare their measurements with measurements made by some reliable method. More recently, Starr (1954a,b,c) proposed a modification of the Erlanger and Hooker method, taking into consideration age as well as pressure measurements. The results from this study were not very good as compared to the Fick method. On the other hand, according to Hamilton and Remington (1947) pulse pressure correlated roughly with stroke volume determined by the dye-dilution technique ( $r = 0.88$ ).

They recognized that prediction of stroke volume from pressure pulses must depend upon evaluation of the "individual arterial distensibility, knowledge of the pulse pressure in the arterial tree and its several parts, and the estimation of arteriolar drainage."

The method employed by Warner et al. (1953) was a simplified technique which facilitated analysis of the pressure pulse. Comparison of this method with the Fick method under a wide range of physiological conditions showed the two measurements to differ from each other by a standard deviation of only  $\pm 9\%$ .

The best results using the pressure pulse contour method were reported recently by Kouchoukos et al. in dogs (1970) and in post-operative patients (1969). They used an equation taken from Warner et al. (1953). They made 541 determinations in 12 dogs and compared these to the stroke volume obtained with an electromagnetic flowmeter under normal and altered circulatory conditions employing 12 different interventions. They reported an overall correlation coefficient of 0.93 in dogs, and 0.92 in patients.

#### The Pressure-Gradient Method

The next work of significance, after Stephen Hales, in the physical analysis of the circulation, began about 1830 with the researches of Poiseuille (1799-1869)(Hatschek, 1928) on the laws governing the flow of liquids through cylindrical pipes. His experiments on glass capillary tubes established that the flow varied

as the fourth power of the diameter ( $D$ ) of the tube. The fact that it varied linearly with the drop in pressure ( $P_1 - P_2$ ) and inversely with the length ( $L$ ) of the tube was already established when he published his first results in 1842. Expressed mathematically, the law as determined by Poiseuille was

$$Q = K \frac{(P_1 - P_2)D^4}{L} \quad . . . . . (1)$$

About 18 years after Poiseuille published this empirical relation, Hagenbach (Hatschek, 1928) made a theoretical analysis of the problem. His result was expressed in the form with which we are familiar

$$Q = \frac{\pi R^4 (P_1 - P_2)}{8\mu L} \quad . . . . . (2)$$

where  $R$  is the radius of the tube and  $\mu$  is the viscosity of the liquid. (This may be obtained by solving equation (34) of Appendix 1).

The above equation is true only if the flow rate is invariant with time (i.e. the pressure-gradient is constant). If the pressure-gradient varies with time (e.g. in a simple harmonic manner) the derivation of the equation relating flow to the pressure-gradient becomes much more difficult but is still essentially similar to the method of deriving Poiseuille's equation (see Appendix 1). It appears that Witzig (1914) was the first to study the relationship between oscillatory flow and the pressure-gradient. He was primarily interested in wave motion and velocity profiles in elastic tubes

filled with incompressible fluids. The solution that he gives for the velocity is essentially the same as that given in Appendix 1 (equation 46). This solution has also been derived by a number of other workers. Richardson and Tyler (1929) used it in their study of oscillatory airflows and Schonfeld (1948) used it to study tidal flows in canals. The solution was also derived by Lambossy (1952) in connection with the resistance term in manometer systems. The form of the solution given in Appendix 1 follows that of Womersley (1954, 1955a,b, 1958) with a few modifications. The solution that he gives for the velocity when the pressure-gradient varies in a simple harmonic manner is

$$v = \frac{\gamma R^2}{\mu \alpha^2} \left[ 1 - \frac{J_0(\alpha i^{3/2})}{J_0(\alpha i^{3/2})} \right] e^{i\omega t} \dots \dots \dots (3)$$

This solution was derived independently and was taken further in that he also integrated equation (3) to give the solution for the volume flow which is necessary for application to the arterial system. The volume flow is

$$Q = \frac{\pi R^4 \gamma}{\mu \alpha^2} \left[ 1 - \frac{2J_1(\alpha i^{3/2})}{\alpha i^{3/2} J_0(\alpha i^{3/2})} \right] e^{i\omega t} \dots \dots \dots (4)$$

These equations (3,4) may be computed by separation into real and imaginary parts in terms of ber and bei functions. This is the method used by Witzig (1914) and Lambossy (1952). In their solutions they used  $\alpha$  for the non-dimensional parameter  $\alpha$  that Womersley used.

In a later paper Womersley (1958) tabulates the bracketed term of equation (4), thereby greatly facilitating the method used by Witzig (1914) and Lambossy (1952). The conventional separation into real and imaginary parts leads to a very clumsy form for the results, and therefore Womersley expressed the results in terms of modulus and phase. By using this technique, equation (4) becomes

$$Q = \frac{\pi MR^4}{\mu} \frac{M'_{10}}{\alpha^2} \sin(\omega t - \phi + \epsilon_{10}) \dots \dots \dots (5)$$

It should be noted that this equation represents only one harmonic component of the synthesized flow curve (see Appendix 1 for identification of terms used in equations 3, 4, and 5).

The first tests of equation (5) were made by Helps and McDonald (1954), McDonald (1955), Hale et al. (1955), McDonald and Taylor (1959) and McDonald (1960) on measurements of the pressure-gradient in the femoral artery of the dog. Since then it has been applied to the human aorta (Gabe et al., 1964), the common carotid artery (Sugahara, 1968), the external iliac artery (Gabe, 1965), and the pulmonary artery (Milnor et al., 1969). Excellent reviews on this method have been written by Fry and Greenfield (1964), Rudinger (1966), Skalak (1966) and Oka (1967).

The assumption that the flow in the proximal aorta may be regarded as largely unsheared has been used implicitly in dogs by Fry et al. (1956), Fry et al. (1957), Fry (1959), Greenfield et al. (1962), and Greenfield and Fry (1965) in deriving a pressure-flow

relation that is simpler than the more general form given by Womersley. The pressure-gradient along the tube is treated as the sum of two components - a large inertial term resulting from the acceleration and deceleration of the blood and a smaller frictional term which is taken as proportional to the velocity of the blood. This may be written as

$$-\frac{\partial P}{\partial z} = L \frac{\partial q}{\partial t} + Rq \quad . . . . . (6)$$

Where  $L$ , the fluid inductance, is  $\frac{(1.1)\rho}{g\pi r^2}$ , and  $R$ , the fluid resistance, is  $\frac{(1.6)8\mu}{g\pi r^4}$ , ( $\rho$  is the density of the blood and  $g$  is the gravitational constant). The solution of equation (6) for flow can be achieved on an analogue computer. This method has been used for flow measurements in the aorta of man by Barnett et al. (1961), Hernandez et al. (1964), and Snell and Luchsinger (1965). Greenfield and Fry (1965) found that there were insignificant differences in the flow data obtained by the more elaborate computations of Womersley and those obtained from this simpler approach. They also found that the instantaneous flows computed by either method compared reasonably well with the flows estimated by electromagnetic flowmeter methods.

Porjé and Rudewald (1957, 1961) used the following equation to compute the volume blood flow in man

$$q = \frac{\pi r^2}{\rho L} \int \Delta P dt + C \quad . . . . . (7)$$

where  $q$  is the instantaneous volume flow through a tube of radius,  $r$ .  $\Delta P$  is the pressure drop along the length,  $L$ , of the tube and  $C$  is the constant of integration. Thus, simple numerical or electrical integration of the measured pressure drop will produce an estimate of volume blood flow.

In 1959, Jones et al. introduced a method for computing blood velocity from the pressure which is more attractive in that it uses only one pressure. They used the following equation:

$$\frac{\partial P}{\partial t} = \rho s \frac{du}{dt} + asu \dots \dots \dots (8)$$

where  $u$  is the blood velocity,  $s$  is the pulse wave velocity (considered to be constant) and  $a$  is a blood friction constant. This equation may be instantaneously and continuously solved for the velocity,  $u$ , by an analogue computer. The stroke volumes obtained in this manner in dogs were compared to those obtained from an electromagnetic flowmeter (Jones and Griffin, 1962) and dye-dilution (Boyett et al., 1966). This method has also been used to compute the stroke volume in man (Jones et al., 1964).

The three pressure-gradient methods mentioned above were reviewed by McDonald (1968b).

## THEORETICAL DISCUSSION

If the flow velocity is invariant with time (i.e.  $\frac{dv}{dt} = 0$ ) in a given tube, then the volume flow is directly related to the pressure-gradient (Hatschek, 1928), i.e.

$$Q = \frac{\pi(P_1 - P_2)R^4}{8L\mu} \dots \dots \dots (9)$$

where R is the internal radius, L is the length of the tube,  $\mu$  is the viscosity of the liquid, and  $P_1 - P_2$  is the pressure-gradient along the length, L, of the tube. It is this difference in pressure that determines the flow and not the absolute level of the pressure.

In the arterial system, the situation is quite different since the pressure is pulsatile owing to the pumping action of the heart. Therefore, a relationship as simple as equation (9) can no longer be used to represent flow.

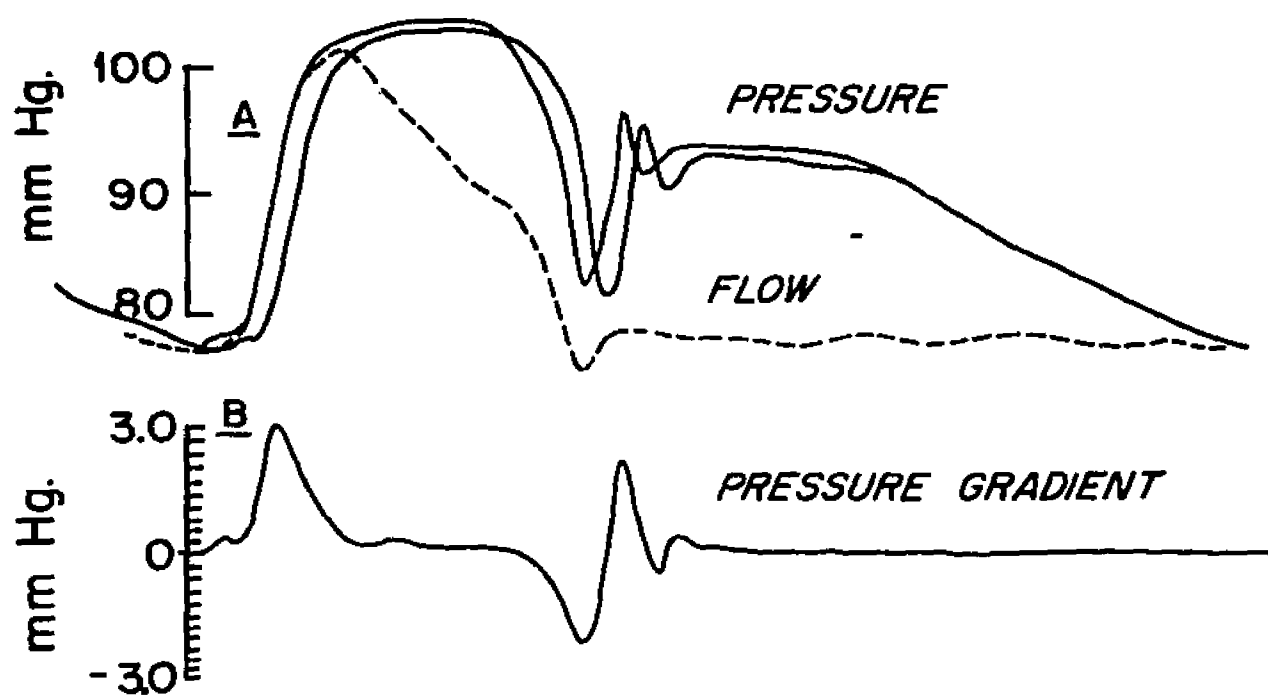
If the pulsatile flow and pressure are recorded at the same site, we see that the peak flow leads the peak pressure but lags the pressure-gradient (Fig. 1). This is due to the fact that, as in the application of Poiseuille's law (equation 9), it is the pressure-gradient along the artery that is related to the flow of the liquid and not the pressure level. Therefore, the velocity of blood may be deduced when the pressure-gradient, viscosity, and density are known



Figure 1

The Oscillatory Pressure-Gradient

- A. Two pressures and flow recorded in the ascending aorta of a dog. The interval between the two pressure taps was 3 cm.
- B. The pressure-gradient was derived by subtracting the pressure at the downstream point from that of the upstream one at 10 msec intervals and dividing by the distance between recording points (3 cm).



at every instant and at every point in the flow. The mathematical relationships between these factors are expressed by the fundamental equation of hydrodynamics (Lamb, 1932)(see Appendix 1). This equation is general and applies to all types of flow (see Historical Survey). Lambossy (1952) applied this equation to flow in a rigid tube to obtain velocity from the pressure-gradient for refinement of manometer theory. Womersley (1954, 1955a,b, 1958) applied it to blood flow in the vascular system.

If an harmonic component of the pressure-gradient is

$$\frac{dP}{dz} = M_g \cos (\omega t - \phi_g) \quad . . . . . (10)$$

(see Appendix 1), then, according to Womersley's derivation, the corresponding harmonic component of the flow is given by

$$Q = \frac{\pi R^2 M_g M'_{10}}{\omega \rho} \sin (\omega t - \phi_g + \epsilon_{10}) \quad . . . . . (11)$$

where  $\omega = 2\pi f$  is the angular frequency,

$f$  is the pulse frequency,

$r$  is the internal radius,

$M_g$  and  $\phi_g$  are the modulus and phase angle of the pressure-gradient

$M'_{10}$  and  $\epsilon_{10}$  are the modulus and phase of the Bessel function dependent on the non-dimensional parameter,  $\alpha$ , approximated as follows for values of  $\alpha > 8.0$ .

$$M'_{10} = 1 - \frac{\sqrt{2}}{\alpha} + \frac{1}{\alpha^2} \quad \dots \dots \dots (12)$$

$$\epsilon_{10} = \frac{\sqrt{2}}{\alpha} + \frac{1}{\alpha^2} + \frac{19}{24} \frac{1}{\sqrt{2}\alpha^3} \quad \dots \dots \dots (13)$$

$$\alpha^2 = R^2 \frac{\omega \rho}{\mu} \quad \dots \dots \dots (14)$$

where  $\rho$  is the density of the blood and  $\mu$  is the viscosity.

Now the pressure-gradient may be written as

$$\frac{dP}{d\mathbf{x}} = \frac{dt}{d\mathbf{x}} \cdot \frac{dP}{dt} = \frac{1}{c'} \frac{dP}{dt} \quad \dots \dots \dots (15)$$

where  $c'$  is the apparent phase velocity and is given by

$$c' = \frac{2\pi f \Delta \mathbf{x}}{\Delta \phi} \quad \dots \dots \dots (16)$$

$\Delta \mathbf{x}$  is the distance between the two pressure measuring points and

$\Delta \phi$  is the measured phase shift between the two pressures for a particular harmonic component.

Porjé (1946) appears to have been the first to measure the phase velocity in this manner. His measurements were made in human beings ranging in age from 21 to 76 years. He recorded the pulse-wave in the subclavian and femoral arteries and the abdominal aorta, by external application of a piezo-electric crystal transducer. The smallest interval that he used between the two pressures was 11 cm. He used only three harmonics in his analysis and he found that the pulse-velocity for the first harmonic was always higher than

for the second and that it was also higher than the usual values for the foot-to-foot velocity. He attributed this phenomenon to the influence of reflected waves.

McDonald and Taylor (1959) have made measurements of the apparent phase-velocity over much smaller intervals (7 - 10cm) in the abdominal aorta of the dog. They also found that the phase-velocity for the fundamental was much higher than the foot-to-foot velocity. This was also derived theoretically from the transmission line, or telegraph equations, by Taylor (1957a) and verified experimentally by him in a rubber-tube model (1957b). Nichols and McDonald (1970) have recorded apparent phase-velocities over intervals ranging from 3 to 5 cm in the ascending aorta of the dog. We found that the velocities remained fairly constant when the pulse frequency was above approximately 2 Hz (Fig. 2), but when the heart rate was slowed by vagal stimulation below 2 Hz (Fig. 3) the velocities rose sharply due to reflected waves. The foot-to-foot velocity (McDonald, 1968a), which is not influenced by reflections (see Appendix 3), was approximately the same as the average apparent phase-velocity above 2 Hz (Table 1). Therefore, above 2 Hz the phase-velocity is dependent primarily on the elastic properties of the vessel wall and is influenced very little by reflected waves.

An harmonic component of the leading pressure ( $P_1$ ) may be represented as

$$P = M_p \cos (\omega t - \phi_p) \dots \dots \dots (17)$$

Figure 2

Average apparent phase velocities in the ascending  
aorta of an anesthetized open-chest dog under con-  
trol conditions

Each data point represents the average of ten velocities.  
Vertical bars represent  $\pm 1$  S.E.M. (Standard Error of the Mean).  
The mean apparent phase velocity ( $c'$ ) was 3.69 m/sec. The foot-  
to-foot velocity was 3.50 m/sec, and the mean aortic pressure  
was 105 mmHg.

# PHASE VELOCITIES

(Control)

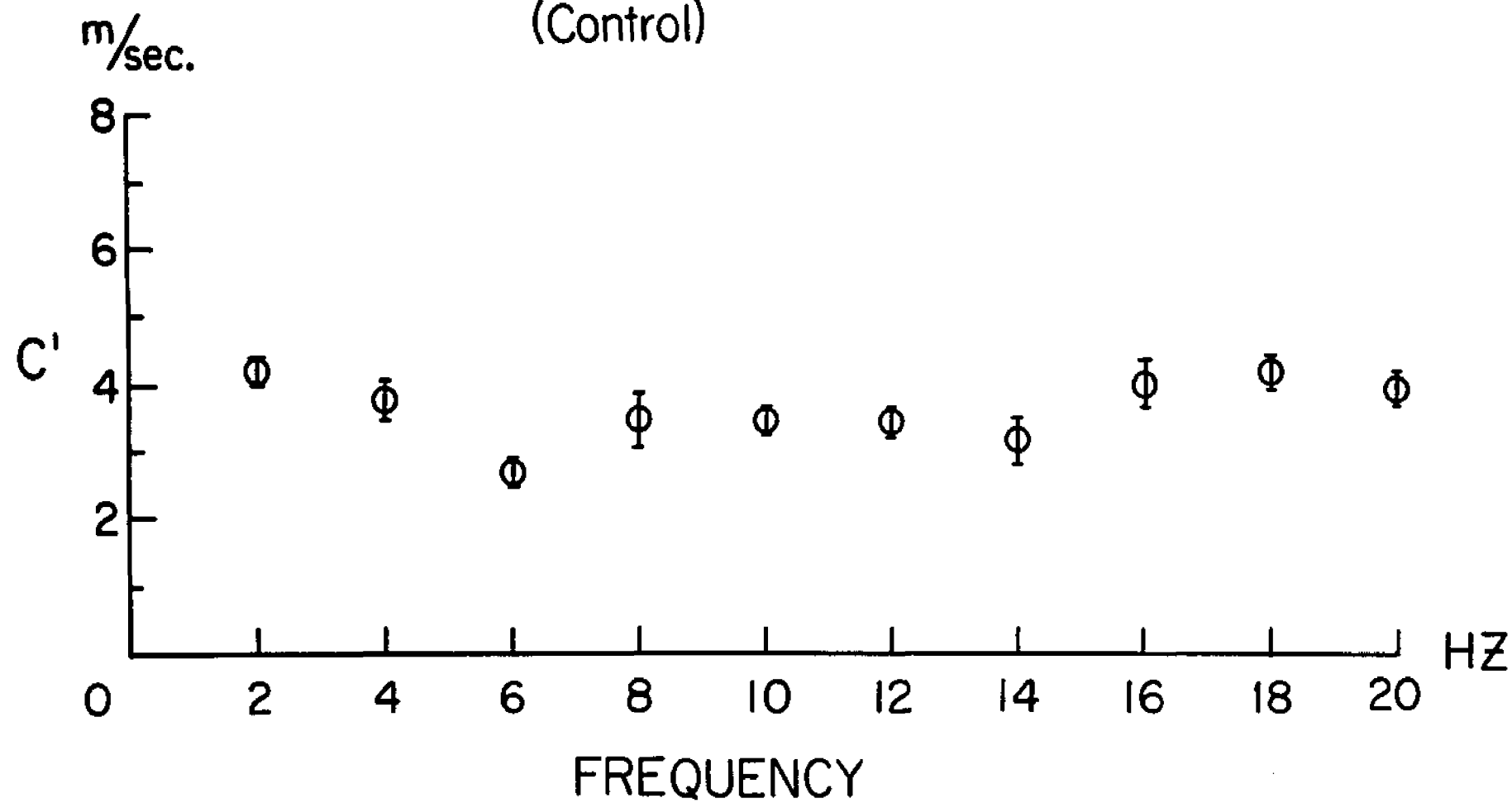


## Figure 3

Average apparent phase velocities in the ascending aorta during vagal stimulation in the same dog as in Figure 1.

The mean apparent phase velocity ( $\bar{c}'$ ) was 5.01 m/sec, the mean apparent phase velocity above 2 Hz was 3.72 m/sec, the foot-to-foot velocity was 3.63 m/sec, and the mean aortic pressure was 95 mmHg. Each data point represents the average of ten velocities and the vertical bars represent  $\pm 1$  S.E.M. (Standard Error of the Mean).



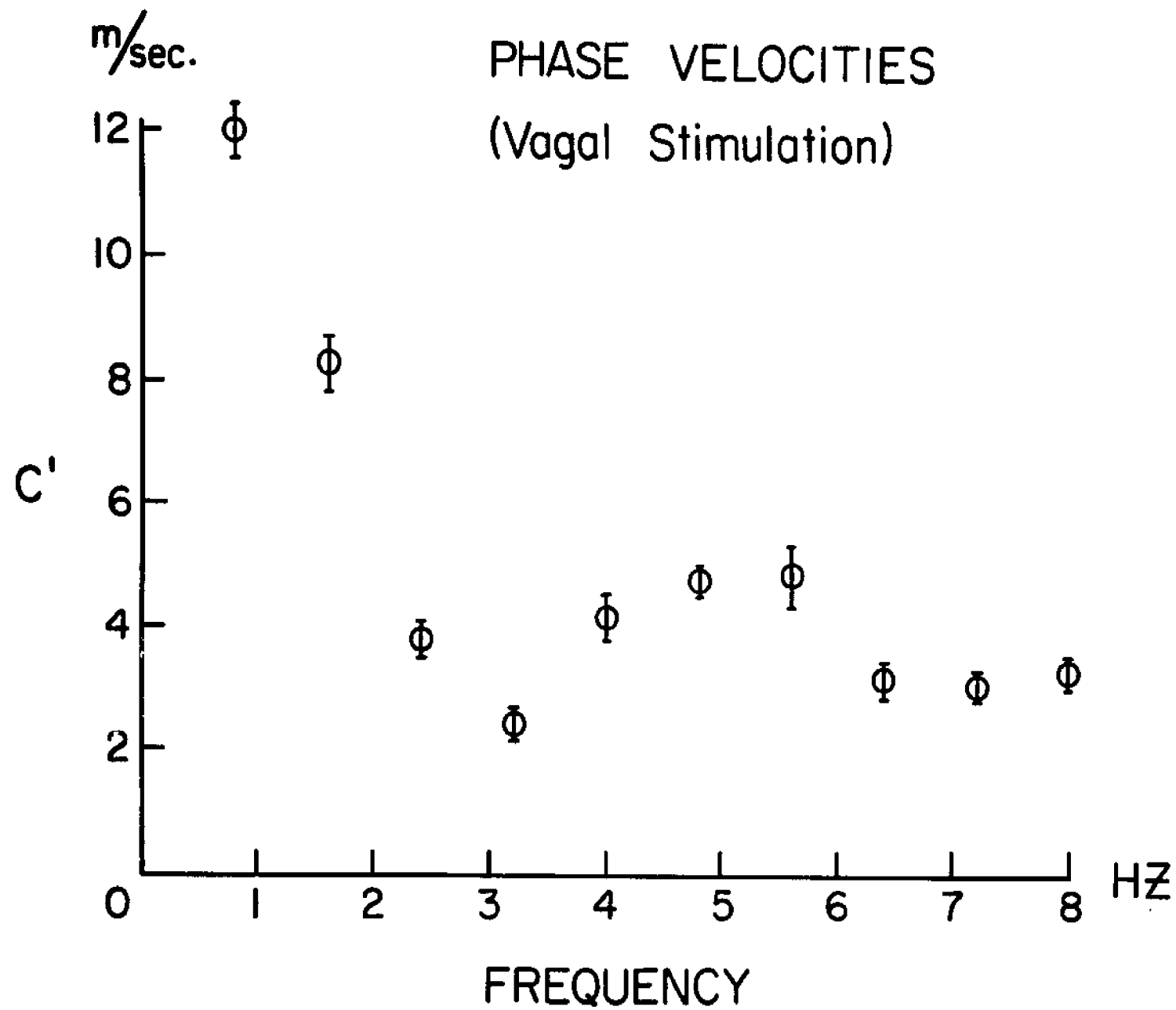


Table 1

Average Apparent Phase Velocities and Foot-to-Foot Velocities  
during Vagal Stimulation\*

Dog #	$\bar{c}'$ m/sec	$\bar{c}'_{>2Hz}$ m/sec	foot-to-foot velocity(m/sec)	H.R. (Hz)	MAP (mmHg)
18	4.35	4.15	4.30	1.3	90
19	5.52	4.30	4.72	0.7	80
20	5.01	3.72	3.63	0.8	95
Avg.	4.96	4.06	4.22		

\* - open chest, flow probe on

$\bar{c}'$  - mean apparent phase velocity for ten harmonics

H.R.- heart rate

MAP - mean aortic pressure

where  $M_p$  and  $\phi_p$  are the modulus and phase angle of the pressure.

If we differentiate equation (17) with respect to time we get

$$\frac{dP}{dt} = -\omega M_p \sin(\omega t - \phi_p) = \omega M_p \cos(\omega t - \phi_p + \pi/2) \quad (18)$$

Now, if we substitute equation (10) and equation (18) into equation (15), we get

$$M_g \cos(\omega t - \phi_g) = \frac{\Delta\phi}{\Delta z} M_p \cos(\omega t - \phi_p + \pi/2) \quad (19)$$

By definition, two oscillatory functions are equal if, and only if, their moduli and phases are equal (Indritz, 1963); therefore,

$$M_g = \frac{\Delta\phi}{\Delta z} M_p \text{ and } \phi_g = \phi_p - \pi/2 \quad (20)$$

If we substitute these values into equation (11) then the harmonic component for the flow becomes

$$Q = \frac{RR^2}{2\pi f\rho} \frac{\Delta\phi M_p M_{10}}{\Delta z} \sin(\omega t - \phi_p + \frac{\pi}{2} + \epsilon_{10}) \quad (21)$$

This is the equation that was used in this study to compute the oscillatory flow curve.

The input impedance of the systemic circulation expresses the opposition to blood flow from the left ventricle into the ascending aorta. For steady flow, opposition is the viscous resistance to blood flow through the systemic circulation. For pulsatile flow, opposition depends upon the interaction of blood, the elastic and

viscous properties of the arterial walls, and wave reflection. The fluctuations in modulus and phase of the input impedance were found by O'Rourke and Taylor (1967) to result from the presence of two functionally discrete reflecting sites in the systemic circulation, one in the upper part of the body and the other in the lower.

In complex notation (Attinger et al., 1966) an harmonic component of the pressure is

$$P = M_p e^{i(\omega t - \phi_p)} \quad . . . . . (22)$$

and the measured flow is

$$Q = M_q e^{i(\omega t - \phi_q)} \quad . . . . . (23)$$

The input impedance for this particular harmonic component is defined as the ratio of the pressure to the flow, i.e.

$$Z = \frac{P}{Q} = \frac{M_p}{M_q} \frac{e^{i(\omega t - \phi_q)}}{e^{i(\omega t - \phi_p)}} = \frac{M_p}{M_q} e^{i(\phi_q - \phi_p)} \quad . . . . . (24)$$

The real part of equation (24) is

$$Z = \frac{M_p}{M_q} \cos (\phi_q - \phi_p) \quad . . . . . (25)$$

where  $\frac{M_p}{M_q}$  is the modulus and  $(\phi_q - \phi_p)$  is the phase of the impedance.

Since  $\sin (\theta + \pi/2) = \cos \theta$  and  $c' = \frac{2\pi f \Delta z}{\Delta \phi}$ , equation (21) may be written as

$$Q = \frac{\pi R^2 M_p M'_{10}}{\rho c'} \cos (\omega t - \phi_p + \epsilon_{10}) \dots \dots \dots (26)$$

and since the modulus of the measured flow and the modulus of the computed flow are equal, the modulus of the impedance may be written as

$$|Z| = \frac{\rho c'}{\pi R^2 M'_{10}} \dots \dots \dots (27)$$

The value of  $\alpha$  in the dog's ascending aorta varies between about 8 and 19 for the first harmonic and increases with the harmonic number (see Table 4). If  $\alpha$  is 8, then  $M'_{10}$  is found to be 0.85, and as  $\alpha$  gets larger  $M'_{10}$  approaches 1.0, i.e.

$$\lim_{\alpha \rightarrow \infty} M'_{10} = 1.0 \dots \dots \dots (28)$$

Therefore, it can be seen that the variation of the apparent phase velocity ( $c'$ ) is the main determinant of the impedance modulus (Nichols et al., 1969). Figures 4, 5, and 6 show the relationship between the apparent phase velocity and the measured impedance modulus under control conditions, during vagal stimulation, and during the infusion of epinephrine. Also, Figure 4 shows the close relationship between the measured impedance modulus and the impedance modulus computed using equation (27).

Figure 4

Relationship between the apparent phase velocity and the impedance modulus under control conditions.

The closed circles represent the measured impedance and the open circles represent the computed impedance (see text).

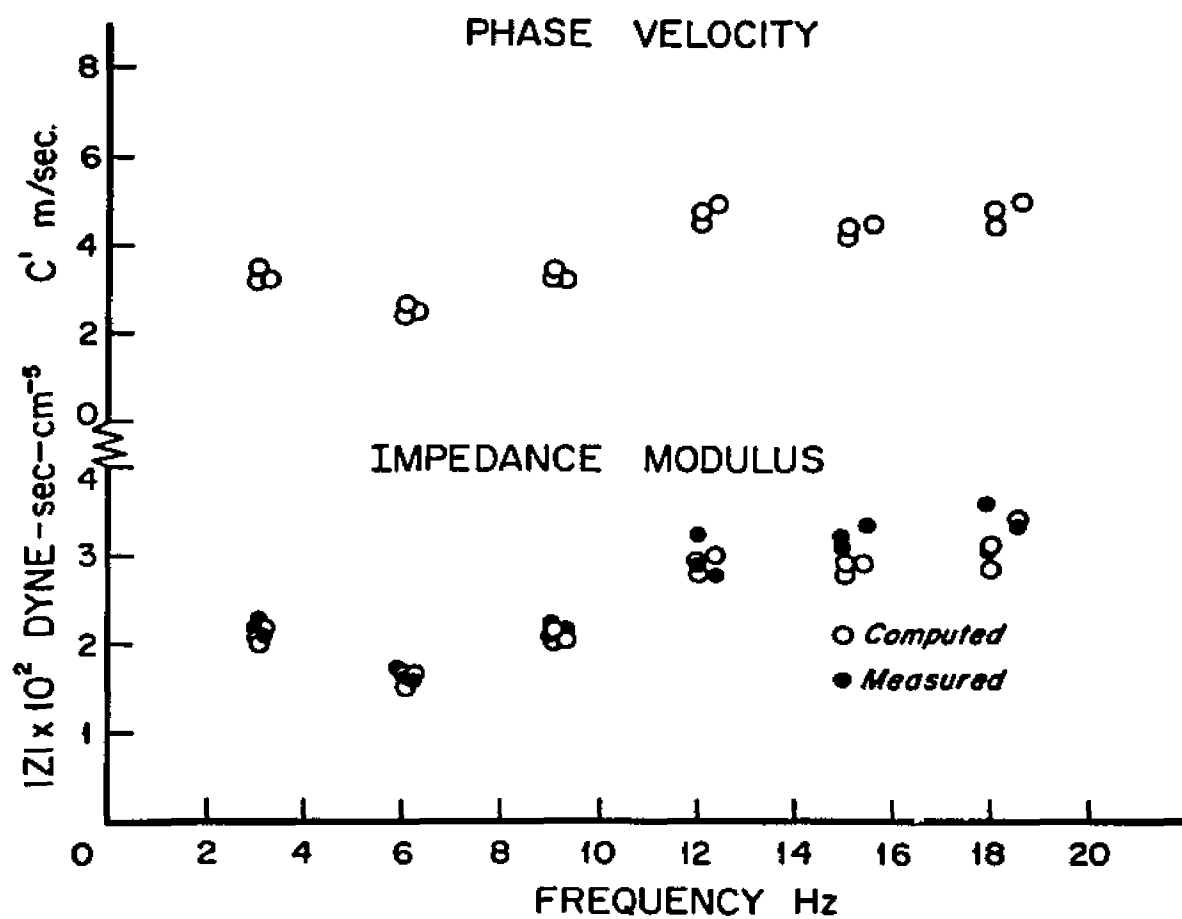


Figure 5

Relationship between the apparent phase velocity and  
the measured impedance modulus during vagal stimulation

Each data point represents the average of ten determinations



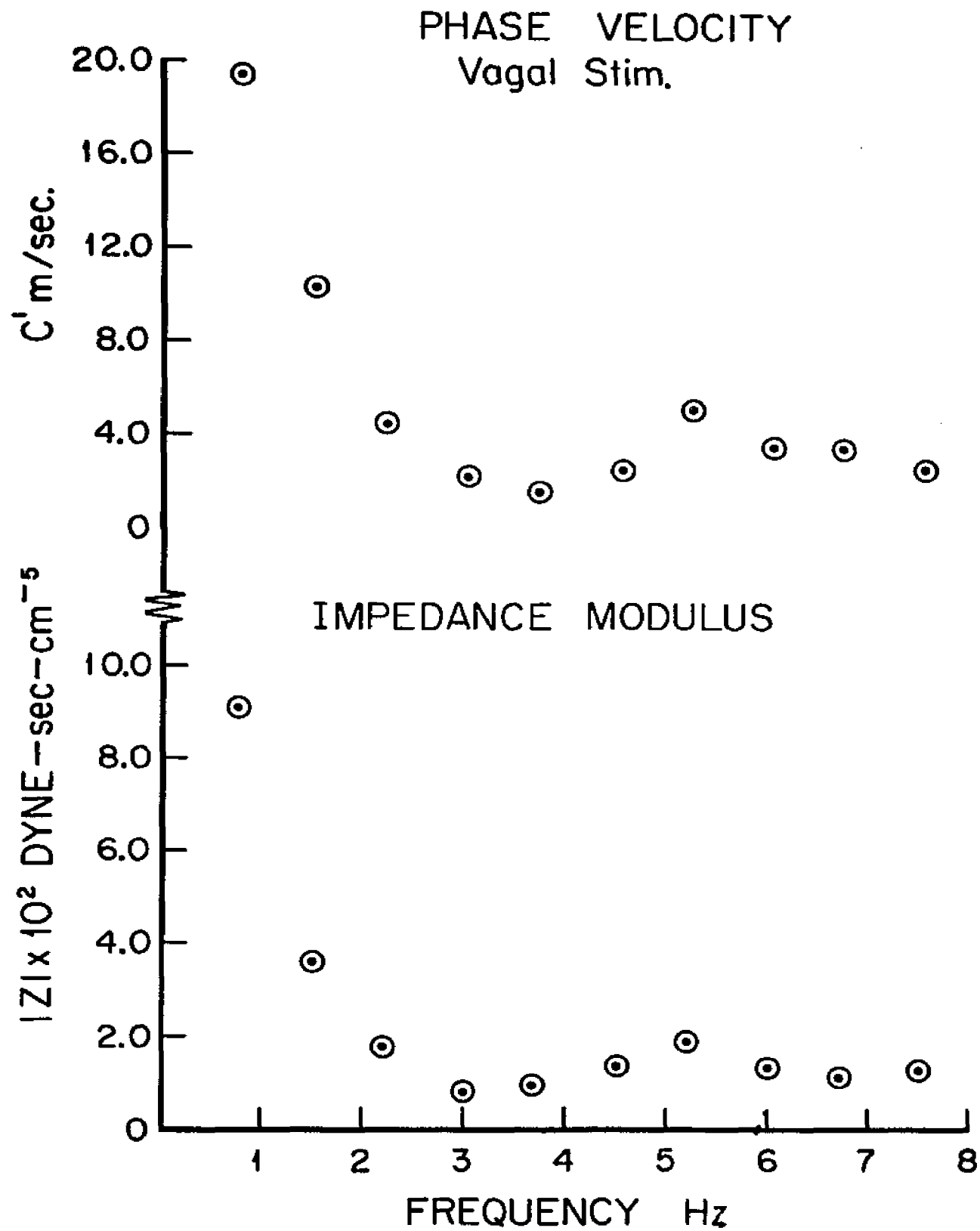
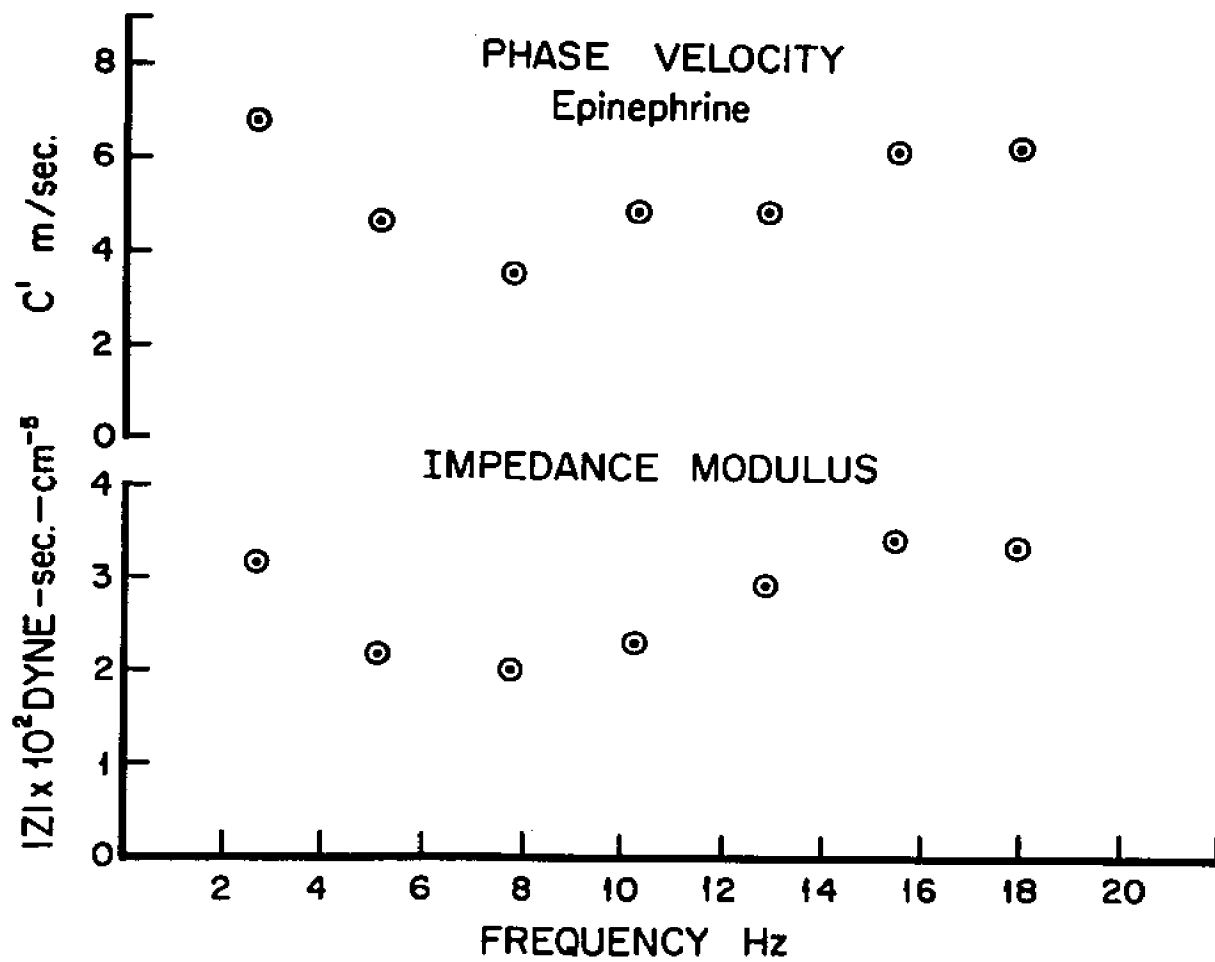


Figure 6

Relationship between the apparent phase velocity and  
the measured impedance modulus during the infusion of  
epinephrine

Each data point represents the average of ten determinations



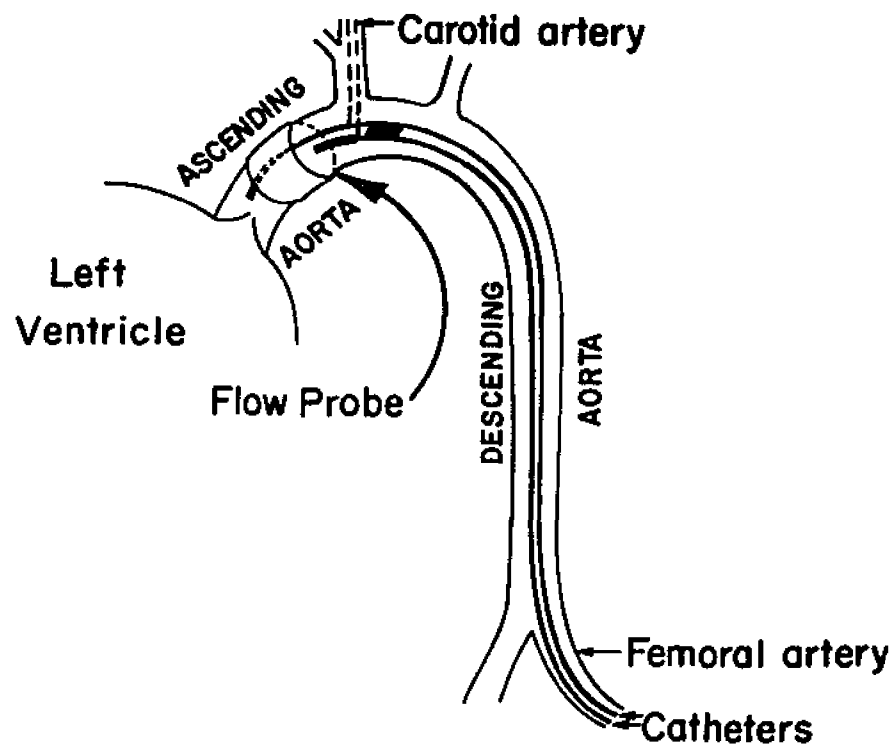
## METHODS

Thirty-nine adult mongrel dogs weighing 15 to 32 Kg (average: 22.4 Kg) and one pig weighing 56 Kg were studied. They were intravenously anesthetized with sodium pentobarbital (30 mm/kg) and maintained with a Harvard intermittent positive pressure respirator. Before the dog was heparinized (3 mg/kg) a median sternotomy was performed and the ascending aorta was exposed.

The basic experimental arrangement is schematically illustrated in Figure 7. Table 2 shows the various catheters and manometers that were used to monitor the two pressures. The procedure was as follows: two catheters were taped together with Blenderm surgical tape so that their tips were a fixed distance apart (3 - 5 cm). They were then inserted either through the left common carotid or the right femoral artery and manually positioned in the ascending aorta. Two catheters side by side have a figure-eight cross-section and therefore heavy bleeding will occur from the artery unless lateral pressure is applied. This was done by stretching two rubber bands a few centimeters apart over small pieces of gauze on the artery close to the point of insertion. The rubber bands were held with hemostats. When the catheter tip manometers were used the mean arterial pressure was recorded through the lumen of one of them with a Statham P-23Gb transducer. This transducer was also used as a reference since the

Figure 7

Arrangement of the experimental apparatus for recording the two pressures and the flow in the ascending aorta



**Arrangement of the experimental apparatus for recording pressures and flow in the ascending aorta.**

Table 2  
Resonance Frequencies of Manometer-Catheter Systems

Manometer	Catheter	Resonance Frequency (Hz)
SF-1	Catheter-tip	1200
SF-4	7F	130
SF-4	Double lumen	100-105
P-23Db	7F	83
P-23Db	4F	48
P-23Gb	7F	125
P-23Gb	6F	114
P-23Gb	5F	90
P-23Gb	4F	85
P-23Gb	Double lumen	72-76

\* All catheters were approximately 100 cm long

baseline of the pressure recorded with the SF-1's tends to drift with changes in temperature. Honeywell Accudata M105 gage control units were used to activate the manometers. This unit is a signal conditioning device containing bridge balance and calibration circuitry to control gage excitation and balance. The output of the M105 was amplified with a Honeywell Accudata M104 DC amplifier. If desired, further amplification could be obtained with a Philbrick amplifier. The phase shift between the input and output of the amplifiers was checked using Lissajous figures (Tang, 1966) and no detectable phase shift was seen until the frequency of the input signal exceeded 1 KHz. The amplified pressure signals were monitored on a Tektronix RM-565 Dual-beam Oscilloscope, while they were being recorded on a Honeywell 7600 Magnetic Tape Unit. Permanent records were obtained with a Honeywell Model 1508 Visicorder. The Visicorder is a direct-writing oscillograph which simultaneously records up to 24 channels of data at frequencies ranging from DC to 5000 cycles per second. The galvanometers that were used to record the pressures had an undamped natural frequency of 40 Hz and a frequency response that was flat to 24 Hz ( $\pm 5\%$ ).

The catheters and manometers, amplifiers and recording equipment were calibrated as a system for each experiment. The resonance frequencies for the various catheter-manometer systems were determined using either the free-vibration method (McDonald et al., 1970) or the forced oscillation method (Yanof et al., 1963, and McDonald et al., 1970). These frequencies are shown in Table 2.



The aortic blood flow was monitored with a Statham M-4001 electromagnetic flowmeter and a Series Q probe. The fat pad was removed from the ascending aorta before the probe was positioned. Restriction of the aorta was prevented by using the largest possible flow probe. Placement of the probe did not alter the pressure contour or the pulse wave velocity (see Discussion). The output of the flowmeter was amplified with a Philbrick amplifier before it was recorded on magnetic tape. The flow was also monitored on the oscilloscope and permanent records were collected from the Visicorder. The galvanometers that were used to record the flow had an undamped natural frequency of 100 Hz and a frequency response that was flat to 60 Hz ( $\pm 5\%$ ). The probes were dynamically calibrated in vitro using a sine-wave pump similar to the one used by Yanof et al. (1963) in their study on the response of manometers. The responses of the probes were linear over a wide range of flows using both physiological saline and whole blood with several hematocrits in the physiologic range (Spencer and Denison, 1959; Olmstead, 1960; Westersten et al., 1960, and Khouri and Gregg, 1963). Calibration factors were determined and used for each probe. The frequency response of the flowmeter was determined using the method of Gessner and Bergel (1964). It was found that the output lagged behind the input by approximately  $3.6^\circ$  per cycle per second. This correction was made and inserted into the computer program. The mean radius was determined from the in vivo circumference of the vessel.

Lead II of the electrocardiogram was recorded with a Honeywell

M-108 AC amplifier. The peak of the QRS complex was used to determine the length of the cardiac cycle, i.e. the computer sampled the data 100 times per second between two consecutive QRS complexes. A block diagram of the experimental set-up is shown in Figure 8.

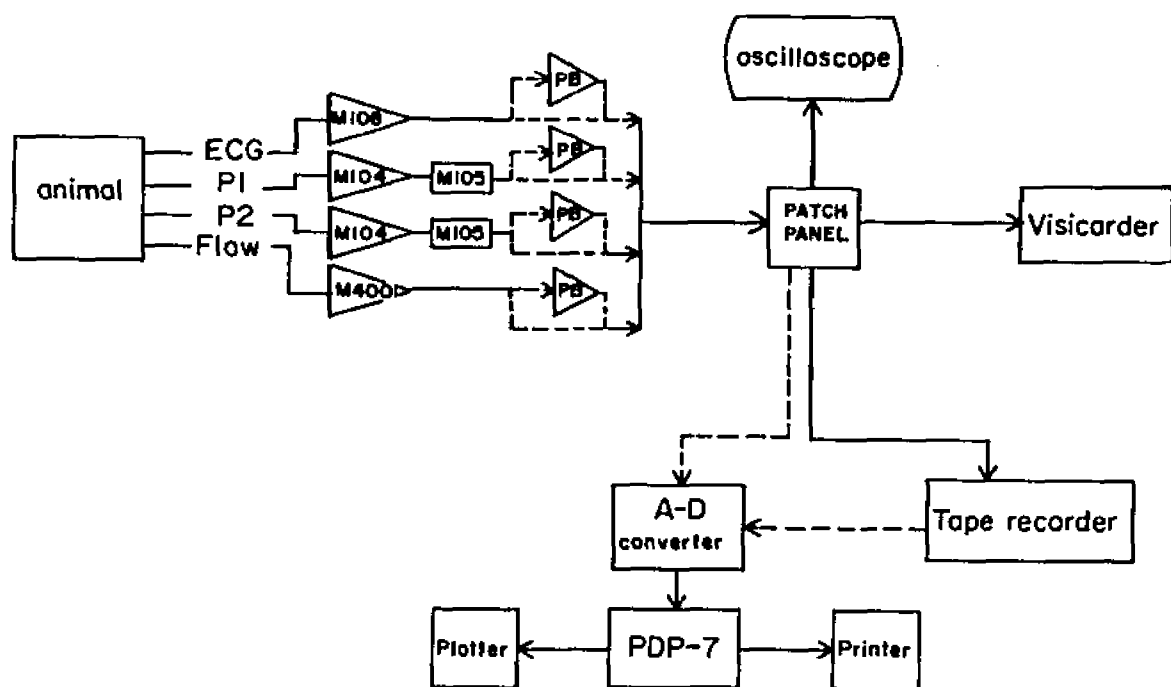
Harmonic analysis (Sokolnikoff, 1939, and Pipes, 1958) was performed by the computer on the two pressures and the flow (see Appendix 2) using the QRS complex as a trigger. The recorded data are shown in Figure 9. Only one cardiac cycle was analyzed each time; ten harmonics were used. A flow chart of the program is shown in Appendix 5 and a print-out of the measured data is shown in Table 3. The modified Womersley equation (see Theoretical Discussion) was then used to calculate each harmonic flow term and a flow curve was synthesized by summing these terms. The mean of the synthesized flow curve is zero; therefore, the mean flow is calculated as the average absolute value of the negative ordinates of the synthesized flow curve. The flow curve is then adjusted by adding this mean value to each of the ordinates. The modulus and phase of the input impedance were calculated from the leading pressure ( $P_1$ ) and the flow (McDonald, 1960; Patel et al., 1963; Milnor et al., 1966, and O'Rourke and Taylor, 1967). A print-out of the calculated data is shown in Table 4.

In the early experiments (1 - 7) the Visicorder records were hand digitized using a Gerber digitizer. These data were punched on IBM cards for analysis on an IBM 1800 computer. The data from later experiments (8 - 40) were recorded on magnetic tape (7½ ips) and played into a PDP-7 computer for analysis.

Figure 8

Block diagram of the experimental set-up

# BLOCK DIAGRAM OF EXPERIMENTAL SET-UP



PB - Philbrick

Figure 9

Recording of the EKG, the two pressures and the flow  
in the ascending aorta

Pressure number 2 has been shifted downward in this record to make  
hand digitizing easier. The interval between the two pressure taps  
was 3 cm.

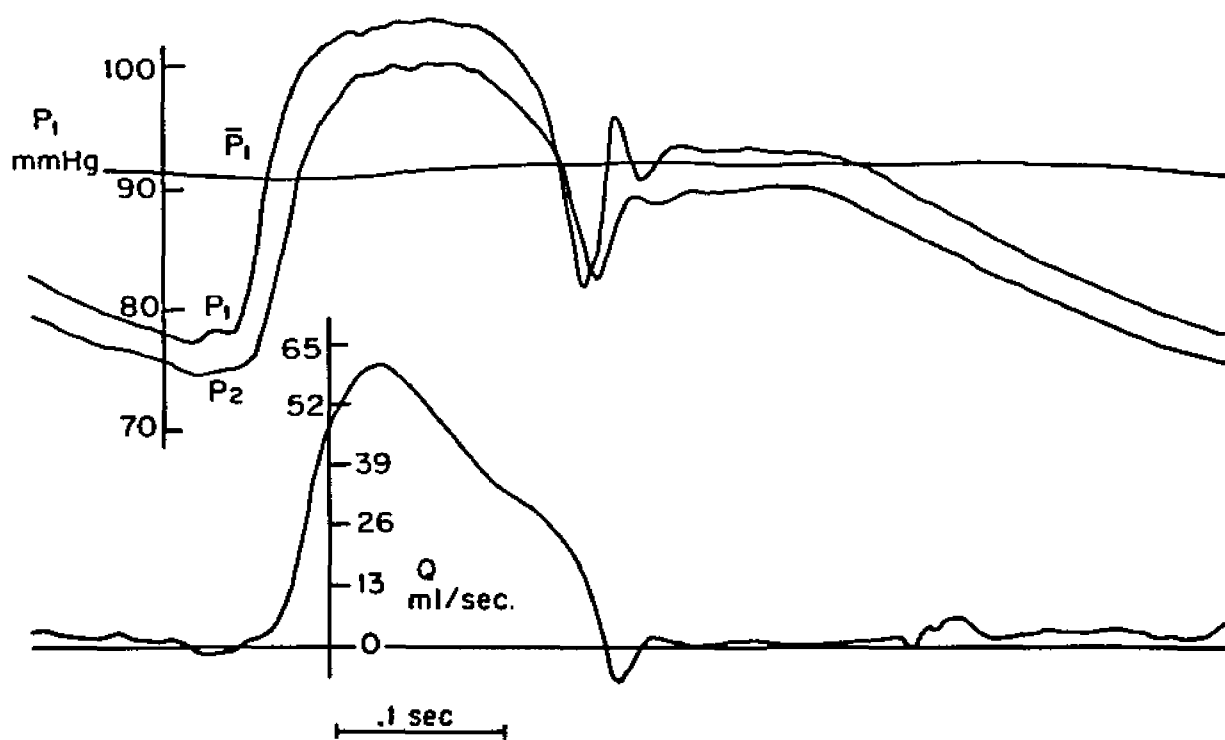


Table 3

Fourier Components of Measured Variables and the Computed Impedance\*

n	Frequency Hz	P1		P2		Q		z <sup>+</sup>	
		M Dynes- cm <sup>-2</sup> × 10 <sup>3</sup>	φ Radians	M Dynes- cm <sup>-2</sup> × 10 <sup>3</sup>	φ Radians	M ml. sec. <sup>-1</sup>	φ Radians	M Dynes- sec. <sup>-5</sup> × 10 <sup>2</sup>	φ Radians
0		122.84		120.62		50.4		24.34	
1	2.50	21.40	2.18	21.10	2.36	74.16	1.82	2.88	-0.51
2	5.00	12.87	3.13	12.18	3.64	49.52	3.61	2.60	0.16
3	7.50	5.58	4.07	4.88	4.71	19.11	4.64	2.92	0.09
4	10.00	5.46	4.65	4.69	5.29	20.29	5.58	2.69	0.30
5	12.50	3.62	6.00	3.05	0.43	10.18	0.76	3.55	0.25
6	15.00	1.39	5.67	1.97	0.44	7.53	1.01	1.84	0.69
7	17.50	2.63	0.93	2.26	1.98	9.71	2.80	2.70	0.77
8	20.00	0.45	0.89	0.51	2.48	2.39	2.90	1.88	0.76
9	22.50	2.55	1.75	1.45	3.38	6.62	4.43	3.85	1.27
10	25.00	0.41	4.58	0.38	5.89	0.81	0.12	5.07	0.26

\* Example of computer print-out

+ Computed from measured pressure and measured flow

Table 4

Fourier Components of the Synthesized Flow and the Computed Impedance\*

n	Frequency	$\alpha$	$M'_{10}$	$\epsilon_{10}$	$\Delta\phi$ Radians	$c'$ $\frac{m}{sec^{-1}}$	$\overset{Q}{M}$ $ml-sec^{-1}$	$\phi$ Radians	$\overset{z^+}{M}$ $\frac{Dynes-}{sec.cm^{-5}}$ $\times 10^2$	$\phi$ Radians
0									22.78	
1	2.50	15.46	0.913	0.096	0.183	4.27	78.68	-0.51	2.72	-2.64
2	5.00	21.87	0.937	0.067	0.505	3.11	66.76	-1.50	1.93	1.65
3	7.50	26.79	0.949	0.054	0.634	3.71	24.50	-2.45	2.28	-0.24
4	10.00	30.93	0.955	0.047	0.636	4.94	18.15	-3.03	3.00	-1.40
5	12.50	34.59	0.960	0.042	0.709	5.53	10.79	-4.39	3.35	-4.11
6	15.00	37.89	0.963	0.038	1.054	4.47	5.14	-4.06	2.70	-3.44
7	17.50	40.92	0.966	0.035	1.054	5.21	8.36	0.68	3.13	-0.24
8	20.00	43.75	0.968	0.033	1.587	3.96	1.89	0.71	2.38	-0.18
9	22.50	46.40	0.970	0.031	1.632	4.33	9.82	-0.15	2.60	-1.89
10	25.00	48.91	0.972	0.029	1.314	5.98	1.15	-2.98	3.58	-1.27

\* Example of computer print-out

+ Computed from measured pressure and computed flow



The computed mean flows from the first seven experiments were compared to those simultaneously determined by the dye-dilution technique. The mean flows and peak flows from the remaining thirty-three experiments were compared to those obtained from an electromagnetic flowmeter. During the experiments, different interventions were introduced to produce changes in mean flow, peak flow, heart rate, mean aortic pressure, apparent phase velocity, and input impedance. Statistical analysis (Brownlee, 1966) was performed by the computer on the data collected before and during each intervention.

When a given curve is to be represented by harmonic components, the question arises as to how many components should be used to represent the curve. This question may be answered by the use of Parseval's theorem, which states that the variance of a finite set of  $n$  harmonic components is given by (McDonald, 1960),

$$V_s = \frac{1}{2} \sum_{n=1}^{n=N} M_n^2 \quad \dots \dots \dots (29)$$

where  $M_n$  is the modulus of the  $n$ th harmonic component (see Appendix 2).

In order to get the variance of the entire curve we use the relation

$$V_T = \frac{1}{m} \sum_{i=1}^m y_i^2 - \left[ \frac{1}{m} \sum_{i=1}^m y_i \right]^2 \quad \dots \dots \dots (30)$$

where  $m$  is the number of ordinates and  $y_i$  is the value of the  $i$ th

ordinate.

The variance of the series that is calculated from equation (29) can be expressed as a fraction, or percentage, of the total variance of the recorded curve (equation 30).

The accumulated sum of the squares of the moduli as a percentage of the total variance of two flow curves and one pressure curve are given in Table 5. It should be noted that the pulse frequency for the two flow curves is different. Histograms representing the comparison of total variance to series variance up to ten harmonics of the two flow curves from Table 5 are shown in Figure 10 and Figure 11. Figure 12 is a histogram representing  $V_s/V_t$  up to 20 harmonics of the pressure curve from Table 5. The close comparison of the resynthesized flow curve to the measured flow curve is shown in Figure 13. Ten harmonics were used in the resynthesis.

The two pressure curves were resolved into their harmonic components by a Fourier analysis and a flow curve was synthesized using the method outlined in Appendix 4. The resynthesized pressure curves and the computed flow curves are shown graphically in Figures 14 through 19. The measured mean flow was 18.4 ml/sec and the measured peak flow was 87.3 ml/sec.

Table 5

Accumulated Sum of the Squares of the Moduli as Percentage of the Total Variance

Harmonics	1	1+2	1+..+3	1+..+4	1+..+5	1+..+6	1+..+7	1+..+8	1+..+9	1+..+10	1+..+20	Frequency Range (Hz)
Flow	52.2	82.7	88.7	94.6	97.7	98.2	99.0	99.6	99.7	99.8	99.9	2.37-23.7
Flow	41.3	69.6	85.8	87.5	91.8	96.6	97.4	99.0	99.3	99.7	99.9	1.28-12.8
Pressure	66.1	92.7	93.8	96.4	96.7	97.2	97.4	97.6	97.7	97.8	99.9	2.37-23.7

-

Figure 10

Comparison of total variance to series variance of a  
flow curve with a pulse frequency of 2.37 Hz.

Flow

$f_0 = 2.37$  Hz

Comparison of Total  
Variance to Series Variance

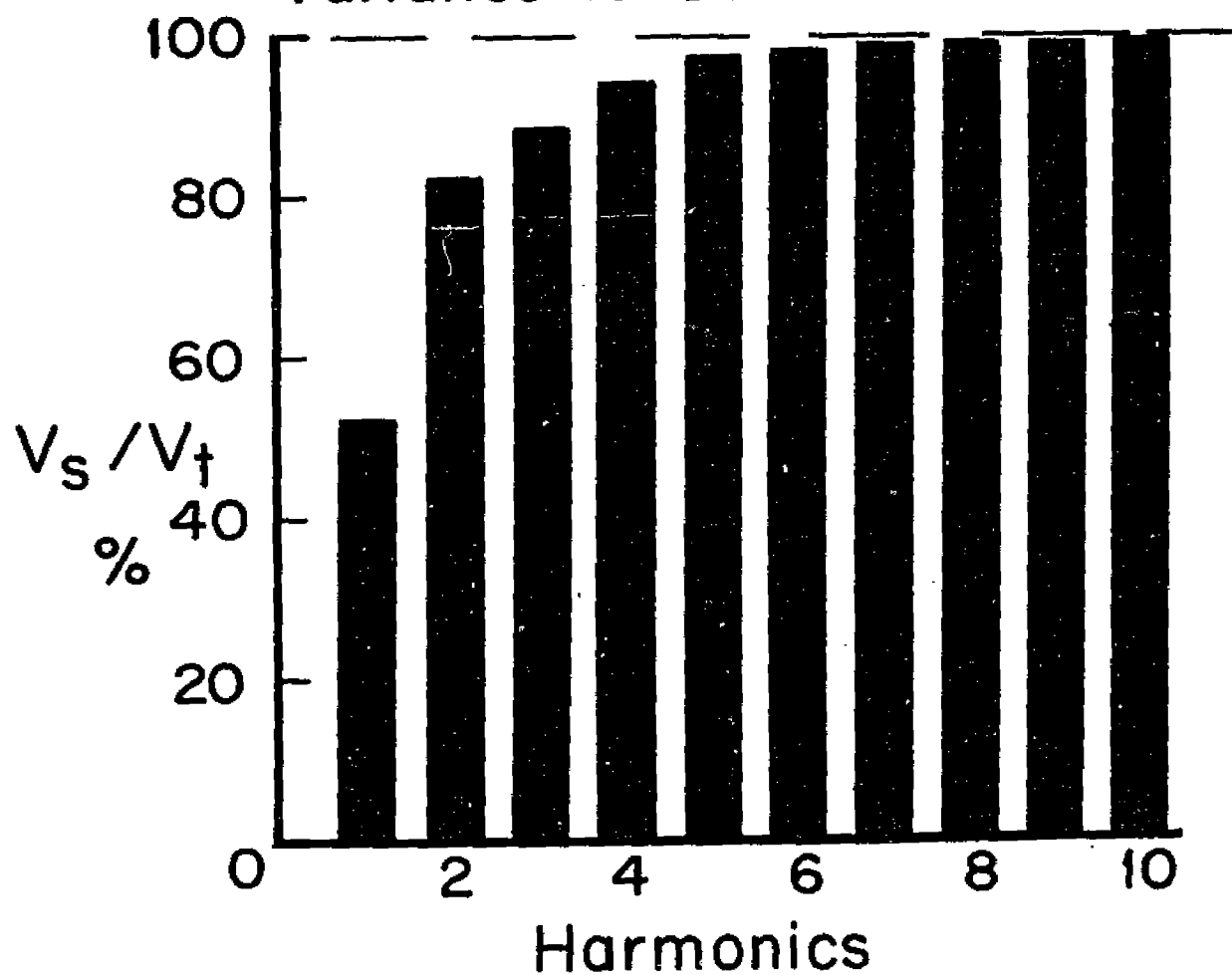


Figure 11

Comparison of total variance to series variance of a flow curve with a pulse frequency of 1.28 Hz.

Flow

$f_0 = 1.28 \text{ Hz}$

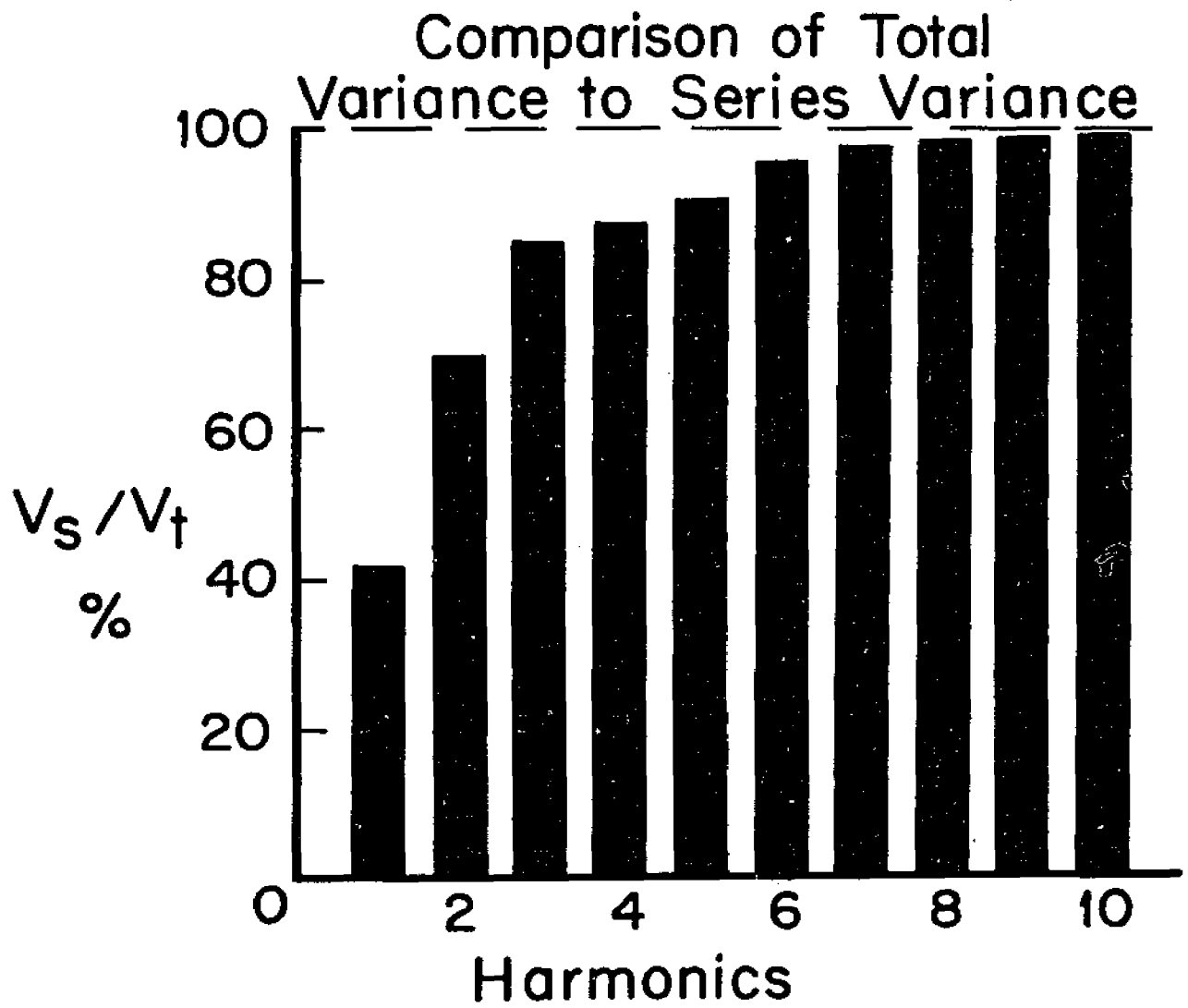


Figure 12

Comparison of total variance to series variance of a  
pressure curve



Pressure

$f_0 = 2.37$  Hz

Comparison of Total Variance to Series Variance

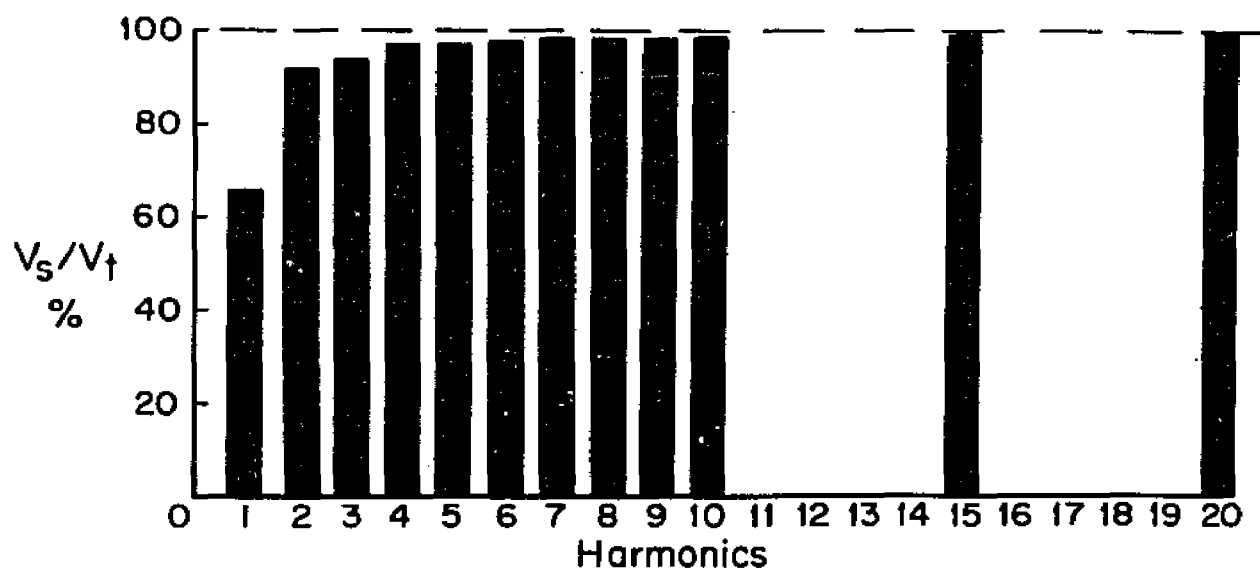


Figure 13

Comparison of the resynthesized flow curve to the  
measured flow curve

(10 harmonics were used in the resynthesis)

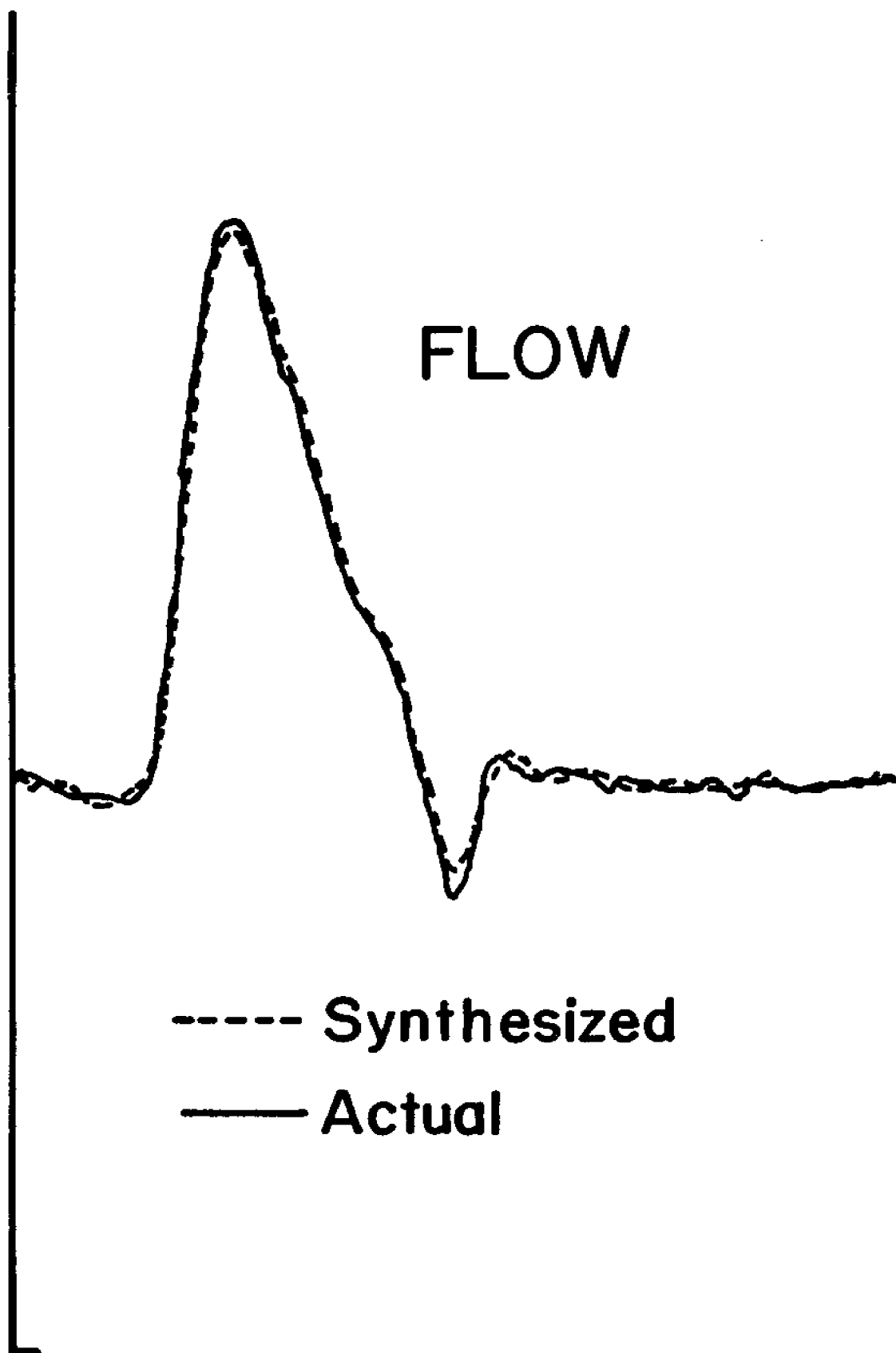


Figure 14

The resynthesized pressure curves and the computed  
flow curve for one harmonic

The solid curve is the measured pressure and the broken curve is the resynthesized pressure. The variance of pressure number 1 ( $P_1$ ) is 46.9 percent and the variance of pressure number 2 ( $P_2$ ) is 47.4 percent. The computed mean flow is 27.6 ml/sec and the computed peak flow is 71.9 ml/sec.

mm Hg.

ml./sec.

$n = 1$

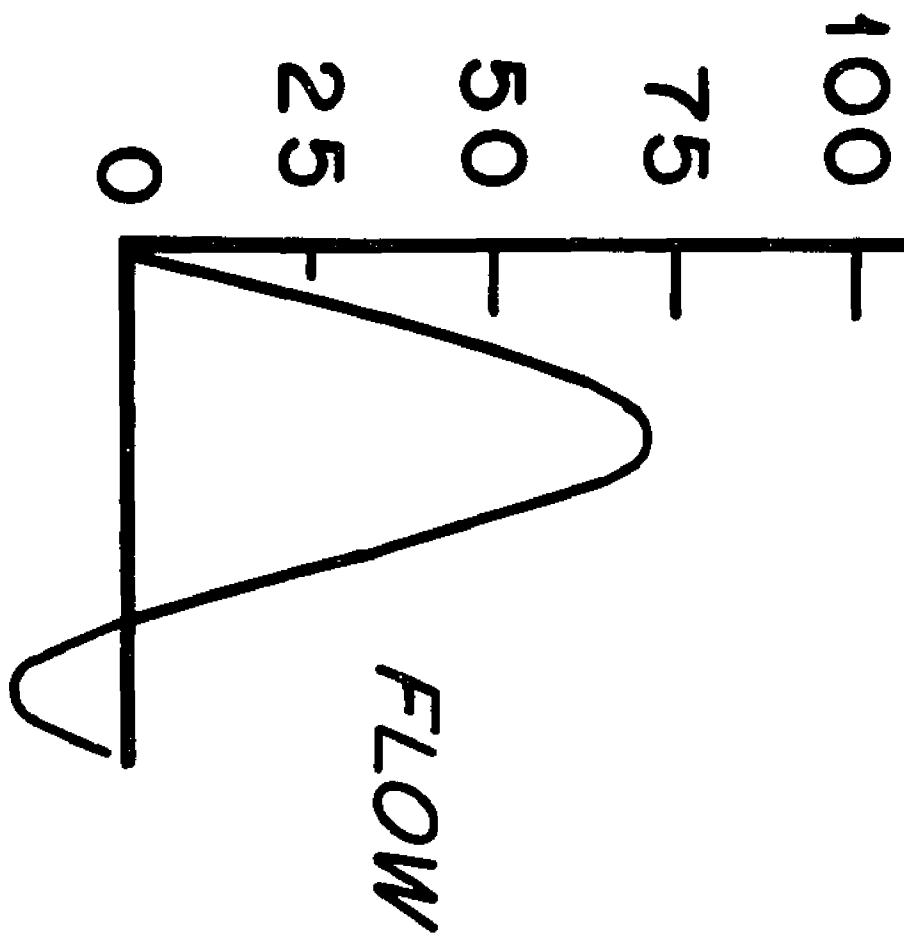


Figure 15

The resynthesized pressure curves and the computed  
flow curve for two harmonics

The solid curve is the measured pressure and the broken curve is the resynthesized pressure. The variance of  $P_1$  is 89.4 percent and the variance of  $P_2$  is 91.3 percent. The computed mean flow is 20.9 ml/sec and the computed peak flow is 80.2 ml/sec.

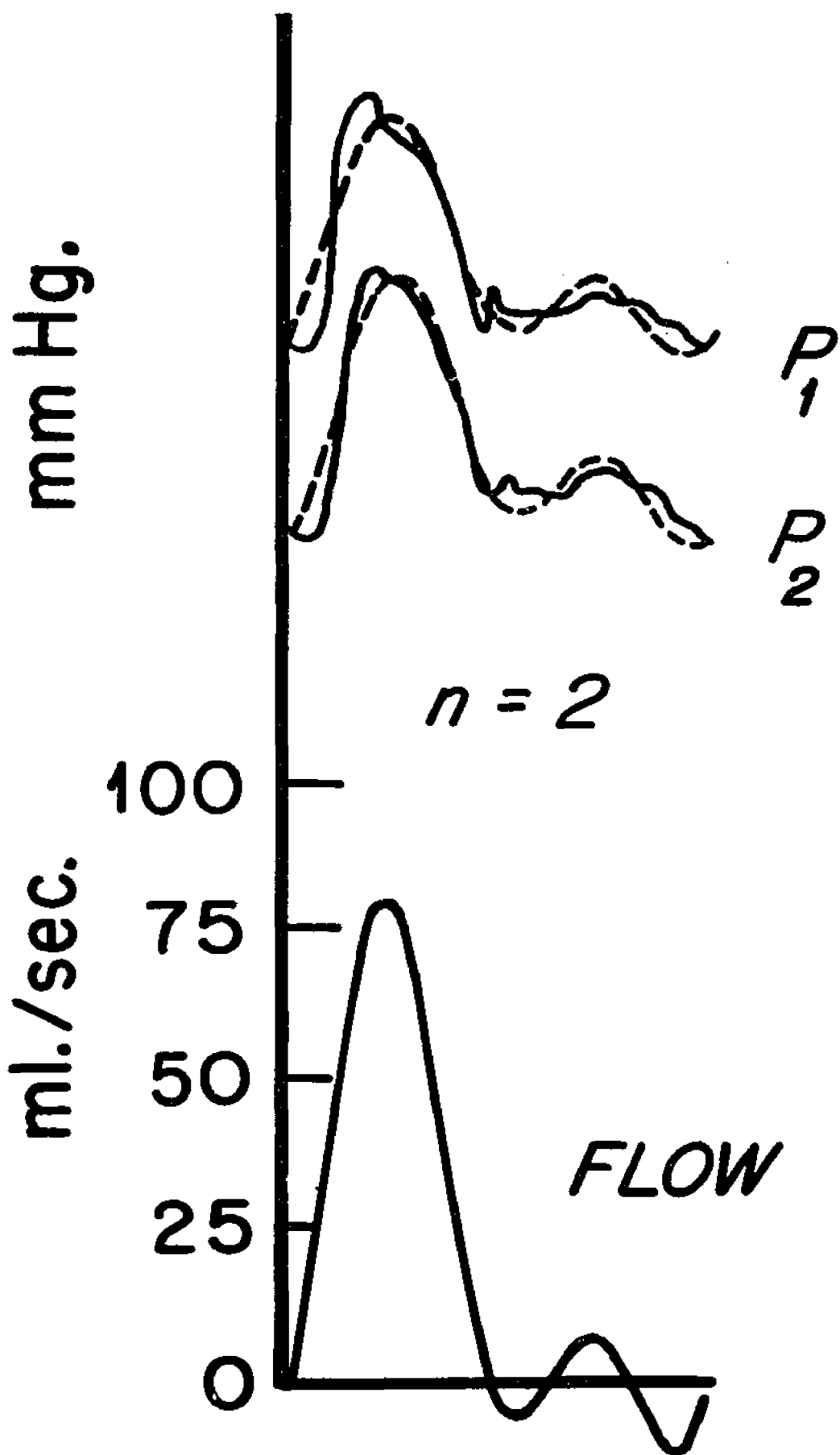


Figure 16

The resynthesized pressure curves and the computed  
flow curve for three harmonics

The solid curve is the measured pressure and the broken curve is the resynthesized pressure. The variance for  $P_1$  is 94.5 percent and the variance for  $P_2$  is 94.8 percent. The computed mean flow is 21.8 ml/sec and the computed peak flow is 95.8 ml/sec.



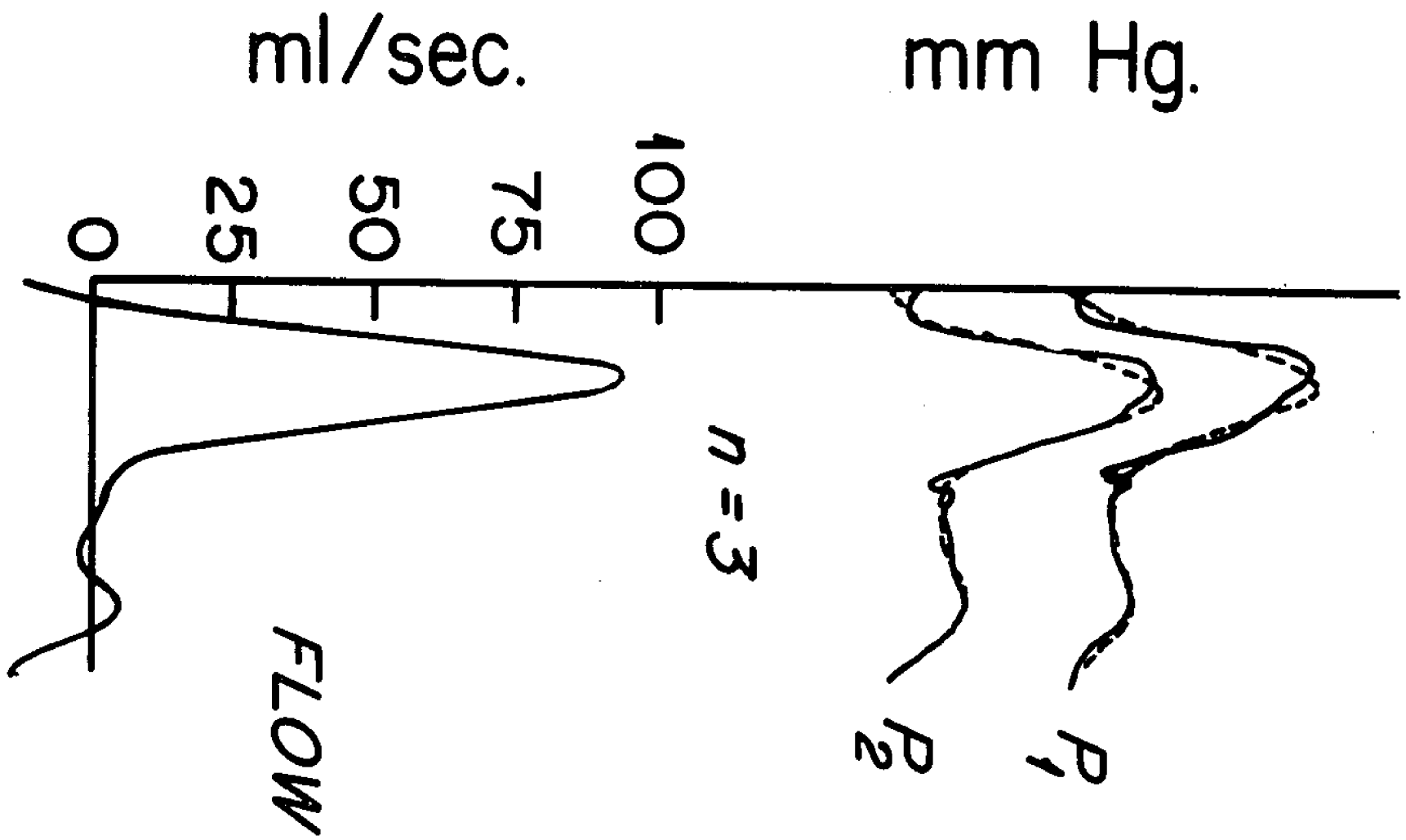
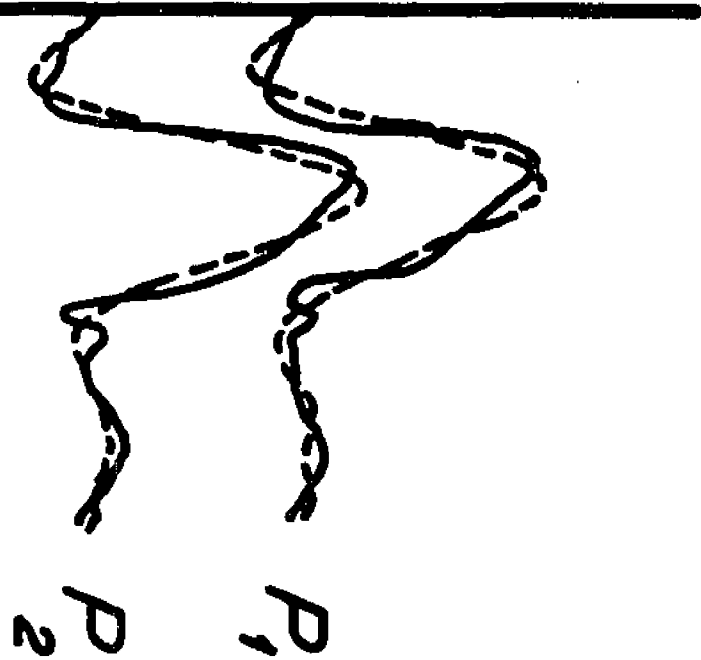


Figure 17

The resynthesized pressure curves and the computed  
flow curve for four harmonics

The solid curve is the measured pressure and the broken curve is the resynthesized pressure. The variance for  $P_1$  is 97.6 percent and the variance for  $P_2$  is 97.1 percent. The computed mean flow is 19.4 ml/sec and the computed peak flow is 89.9 ml/sec.

mm Hg.



$n = 4$

ml./sec.

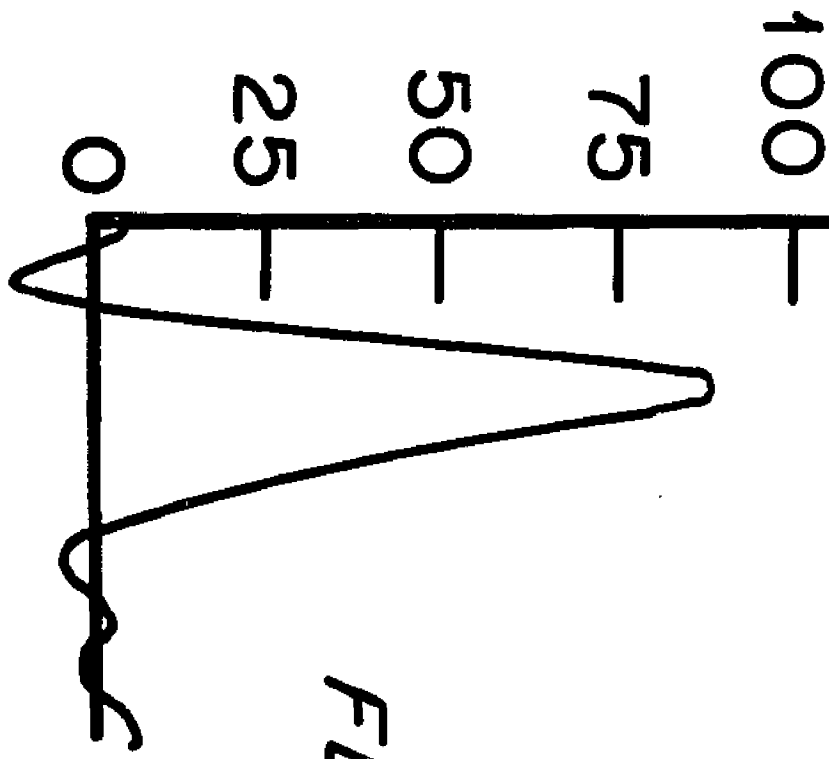


Figure 18

The resynthesized pressure curves and the computed  
flow curve for five harmonics

The solid curve is the measured pressure and the broken curve is the resynthesized pressure. The variance for  $P_1$  is 98.0 percent and the variance for  $P_2$  is 98.1 percent. The computed mean flow is 24.1 ml/sec and the computed peak flow is 100.5 ml/sec.

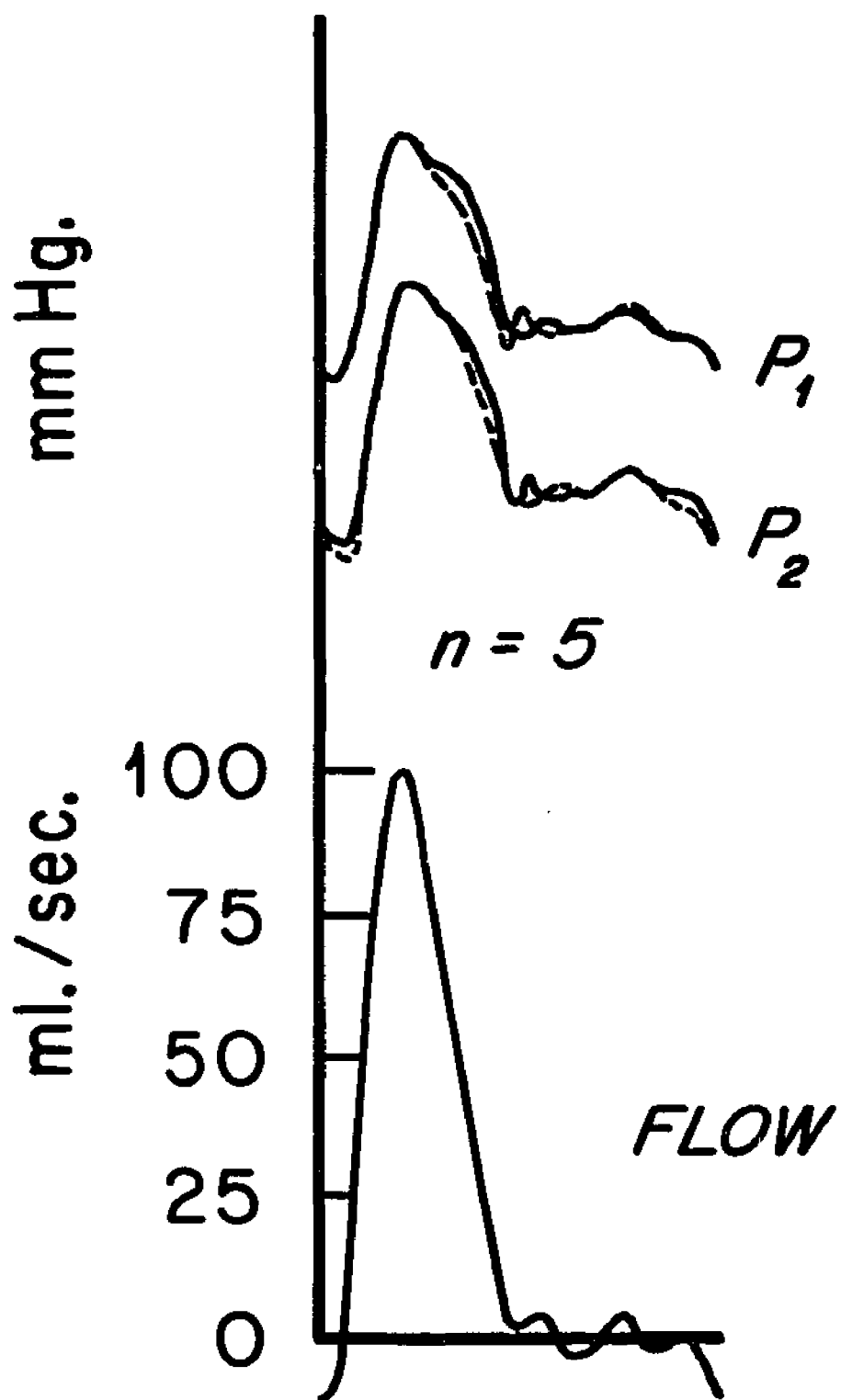
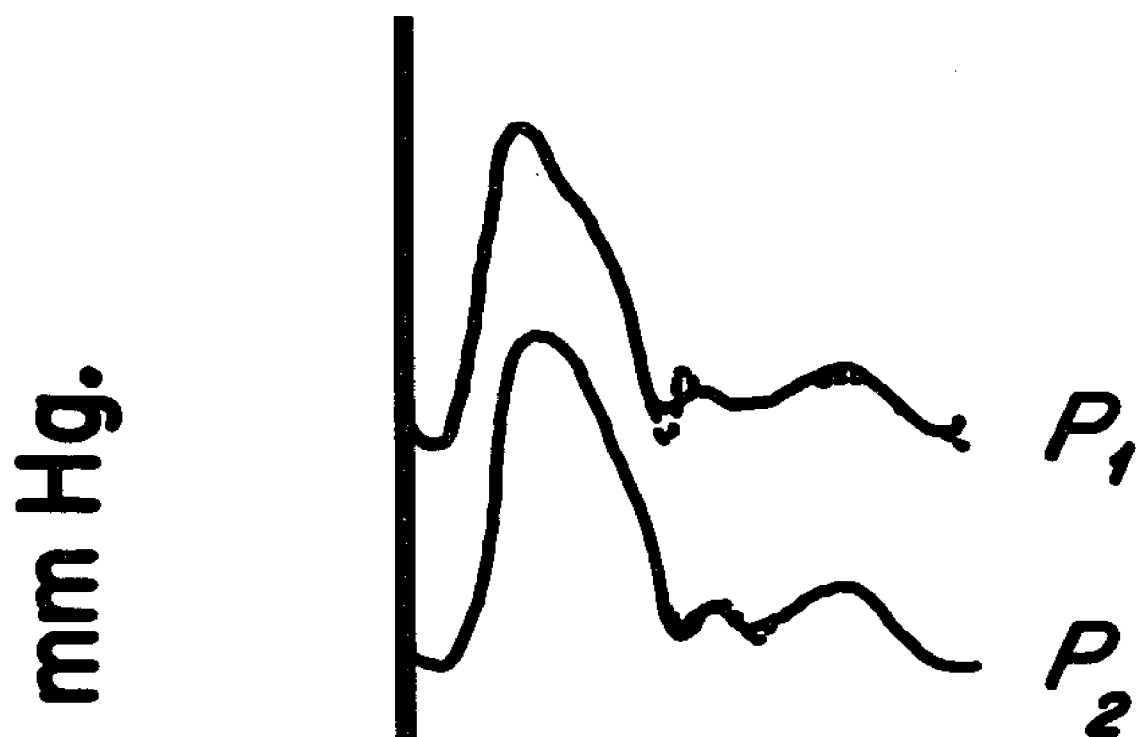


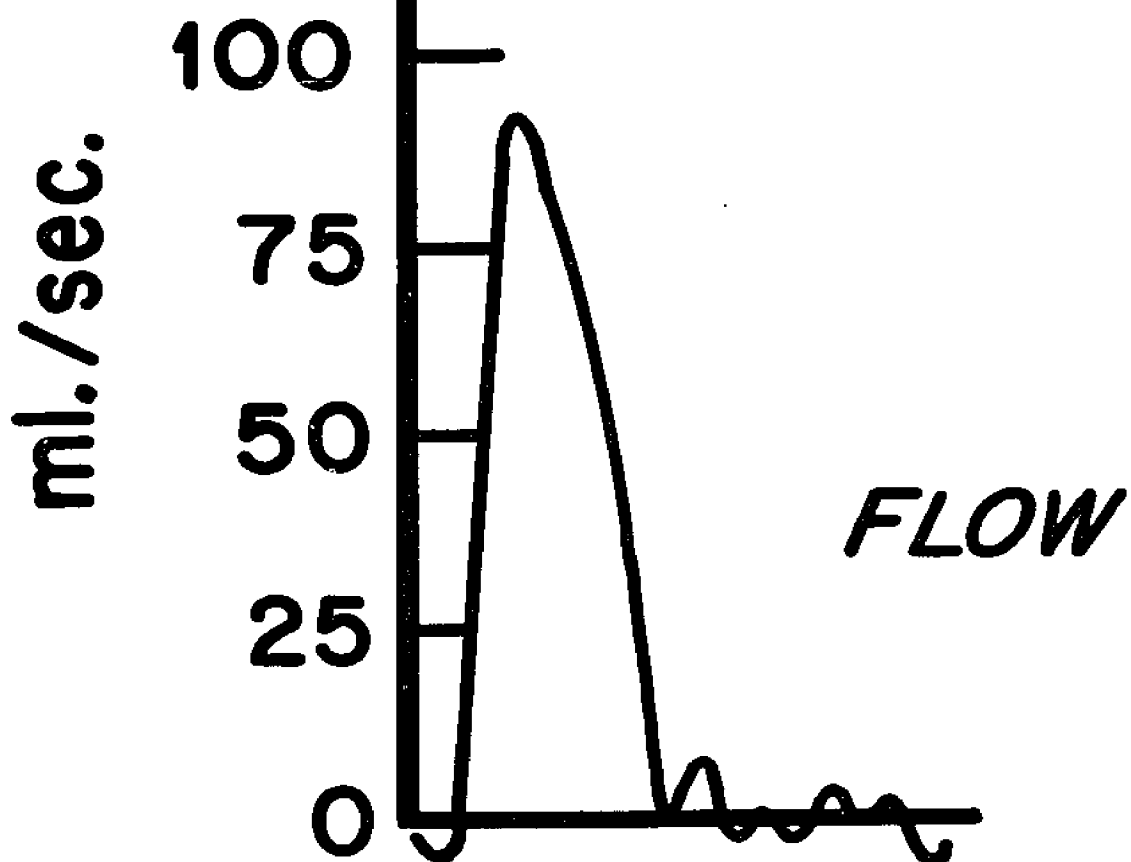
Figure 19

The resynthesized pressure curves and the computed  
flow curve for ten harmonics

The solid curve is the measured pressure and the broken curve is the resynthesized pressure. The variance for  $P_1$  is 99.3 percent and the variance for  $P_2$  is 99.5 percent. The computed mean flow is 20.3 ml/sec and the computed peak flow is 92.5 ml/sec.



$n = 10$



## EXPERIMENTAL PROCEDURES

In some of the experiments different interventions were introduced to produce changes in mean flow ( $\bar{Q}$ ), Peak Flow ( $\hat{Q}$ ), heart rate (HR), mean arterial pressure (MAP), input impedance (Z), and pulse wave velocity ( $c'$ ). These are summarized in Tables 6 and 11. When more than one intervention was applied in the same animal baseline conditions were established between them. At least 5 determinations of mean flow and peak flow were collected from each animal under control conditions and at least 10 determinations were made during or after each intervention.

(a) Dextran - Low molecular weight dextran (100-500 ml) was intravenously infused over 5 to 25 minute periods in 3 animals. This produced a maximal average increase in  $\bar{Q}$  of 85.5% from baseline values measured with the electromagnetic flowmeter. During the infusions the average HR fell slightly. There was an increase of 25% in the average MAP and an 88% increase in the average  $\hat{Q}$ .

(b) Hemorrhage - 50 ml of blood were withdrawn rapidly at intervals in 5 animals. This produced a maximal average decrease of 48.6% in  $\bar{Q}$ . During the withdrawals the average MAP fell 49 mmHg and the average  $\hat{Q}$  fell 42 ml/sec. HR did not vary appreciably in the individual animals.



Table 6

Changes in Mean Flow, Heart Rate, and Mean Arterial Pressure Produced by the Various Interventions

Intervention	No. of expts	No. of dets	Average Mean Flow (ml/sec)		Average Heart Rate (beats/min)		Average Mean Arte- rial Pressure (mm/Hg)	
			Base- line	@ maxi- mal effect	Base- line	@ maxi- mal effect	Base- line	@ maxi- mal effect
Pacing	2	38	28.8	25.9	150	177	78	73
Hemorrhage	5	114	21.8	14.6	146	140	96	47
RFAC	3	46	21.5	47.0	168	162	83	96
Vagal Stimulation	6	62	31.8	24.7	102	42	100	80
Dextran	3	58	22.2	41.1	162	150	90	115
Epinephrine	5	104	17.2	22.9	154	172	101	138
Nor-epinephrine	5	98	19.1	21.8	151	144	101	134
Isoproterenol	4	59	15.4	20.3	147	183	90	98
Metaraminol	5	75	22.7	25.2	136	137	87	114
Glucagon	1	25	21.4	25.0	168	174	120	107

RFAC - Recovery from Aortic Constriction  
dets - determinations

(c) Pacing - Electrodes were sutured to the right atrium of 2 animals and then connected to the Grass Model S4 Stimulator for pacing. Heart rates up to 186 beats/min were obtained. The average  $\bar{Q}$ ,  $\hat{Q}$ , and MAP fell slightly during the period of stimulation.

(d) Vagal stimulation - The distal end of the severed right vagus nerve was stimulated with the Grass Stimulator in 6 animals. Voltages ranging from 3 to 7 volts were used at a frequency of 100 Hz. The heart rates obtained with these voltages ranged from 102 to 42 beats/min. The average  $\bar{Q}$  fell from 31.8 to 24.7 ml/sec., while the average  $\hat{Q}$  rose from 145 to 160 ml/sec. During the period of stimulation MAP fell an average of 20 mmHg.

(e) Recovery from aortic constriction - The thoracic aorta was completely occluded in 3 animals momentarily and suddenly released. This intervention produced an average increase in  $\bar{Q}$  of 118%. The MAP rose an average of 13 mmHg and the average  $\hat{Q}$  rose from 143 to 235 ml/sec. The HR did not change appreciably during the period of recovery.

(f) Epinephrine - Constant infusions of an epinephrine (adrenalin chloride) solution (0.5-3.0  $\mu\text{g/kg/min}$ ) were administered over 1 - 5 min. intervals in 5 animals. This produced a maximal average increase of 34% in  $\bar{Q}$ . The HR increased an average of 18 beats/min, while the average MAP increased 37 mmHg and the average  $\hat{Q}$  increased from 91 to 141 ml/sec.

(g) Norepinephrine - Norepinephrine (1.0-2.5  $\mu\text{g/kg/min}$ ) was infused over 1 - 5 min. intervals in 5 animals. This produced a maximal average increase of 14.2% in  $\bar{Q}$ . The MAP rose an average of 33% while the  $\hat{Q}$  rose an average of 50%. The HR fell slightly during the infusion.

(h) Metaraminol - An infusion of metaraminol (3-10  $\mu\text{g/kg/min}$ ) was administered over 3 - 5 min. intervals in 5 animals. This produced a maximal average increase of 11% in  $\bar{Q}$ . HR and  $\hat{Q}$  rose slightly while MAP increased an average of 27%.

(i) Isoproterenol - Isoproterenol (0.3-1.0  $\mu\text{g/kg/min}$ ) was infused over 3 - 5 min. intervals in 4 animals. This produced a maximal average increase of 32% in  $\bar{Q}$ . The average HR increased from 147 to 183 beats/min. The MAP rose slightly while  $\hat{Q}$  increased an average of 31%.

(j) Glucagon - Injections ranging from 300 to 600  $\mu\text{g}$  of glucagon were given to one animal. This produced an average increase of 17% in  $\bar{Q}$ . HR rose slightly while the MAP fell slightly.

## RESULTS

A total of 720 determinations of mean flow and 573 determinations of peak flow were collected from 40 animals using the modified Womersley equation (equation 21). Thirty-five determinations of mean flow were collected from the first seven experiments (5 determinations from each) and compared to those simultaneously determined by the dye-dilution technique. The results from this group of animals are shown in the first row of Table 7; Figure 20 is a graphical representation of the results. A correlation coefficient of 0.95 was obtained. The regression line is described by  $y = 1.07x - 0.91$  ml/sec and the standard error of estimate is  $\pm 5.6$  ml/sec. Data were collected from four of the experiments while the chest was still closed. In these experiments the catheters were taped together with their tips 3 cm apart and inserted into the ascending aorta through the right common carotid artery. In the remaining three experiments of this group, the catheters were inserted through the femoral artery and manually positioned in the ascending aorta. The interval between the catheter tips was either 4 or 5 cm apart. Control data only were collected from these experiments.

In the remaining 33 experiments, 685 determinations of mean flow were collected using the pressure-gradient technique and compared to

Table 7

Statistical Analysis of the Computed Mean Flow Versus the Electromagnetic Flowmeter in the Individual Animals

Exp. No.	No. of Dets.	r	Slope	Inter-cept	Average Mean Flow				H.R. Range	MAP Range	$\bar{Q}$ Range	1.96 S.E.E.
					Com-puted	S.D.	EMF	S.D.				
1-7	35	0.95	1.07	-0.91	28.2	16.8	27.3*	14.9	108-180	95-140	10.3-55.0	11.1
8	15	0.84	1.05	-2.00	22.9	2.1	23.8	1.6	138-150	93-135	21.6-27.0	2.3
11	24	0.96	1.12	-0.57	20.9	4.2	19.1	3.6	162-186	90-130	13.0-24.0	2.4
12	15	0.84	0.92	2.09	18.5	3.3	17.8	3.0	156-186	90-135	12.4-20.6	3.7
13	15	0.92	1.02	-0.56	20.8	4.8	21.0	4.4	120-156	81-132	14.5-25.8	3.9
17	35	0.94	1.12	-1.85	20.6	7.5	20.0	6.3	44-150	70-125	13.1-34.0	5.1
18	35	0.94	1.06	-0.71	20.3	6.6	19.9	5.9	47-156	60-126	10.3-29.8	4.6
19	15	0.97	1.04	-3.75	32.9	14.9	35.1	13.9	47-102	64-100	24.8-54.5	7.1
20	28	0.90	1.10	-3.13	40.0	12.3	39.1	10.0	84-120	75-120	19.0-45.0	11.0
23	35	0.97	0.95	2.05	35.0	15.7	34.7	16.1	162-174	84-94	17.7-63.1	7.3
24	16	0.99	0.94	1.04	44.3	18.6	46.0	19.6	162-168	85-95	19.0-64.6	4.8
25	15	0.99	0.99	-0.66	46.8	18.7	47.8	18.7	168-180	80-105	21.7-64.6	4.3

Table 7 - continued

Exp. No.	No. of Dets.	r	Slope	Inter-cept	Com-puted	S.D.	EMF	S.D.	H.R. Range	MAP Range	$\bar{Q}$ Range	1.96 S.E.E.
27	15	0.92	0.97	1.07	24.2	4.9	23.8	4.6	138-156	75-105	18.5-32.4	3.9
28	15	0.89	0.99	0.60	27.5	5.9	27.2	5.3	144-162	100-130	19.4-33.4	5.7
29	15	0.66	0.51	9.25	20.6	3.0	22.5	4.0	150-156	73-135	14.7-28.9	4.7
32	39	0.97	1.05	-0.38	27.1	15.6	26.2	14.4	84-162	30-120	8.3-52.8	8.2
33	41	0.96	1.04	0.48	27.7	20.1	26.2	18.6	138-162	25-110	4.5-57.3	11.1
34	32	0.90	0.80	5.60	26.3	3.7	25.9	4.2	96-174	60-110	18.0-33.0	3.3
35	16	0.87	0.86	2.30	23.7	3.6	25.0	3.7	72-180	70-75	20.9-33.0	3.7
37	35	0.87	0.94	2.30	29.6	5.0	29.1	4.7	138-162	118-140	20.5-38.3	5.1
38	37	0.81	0.97	0.66	27.0	4.3	27.2	3.6	144-174	115-140	18.1-35.4	5.1
39	41	0.85	1.19	-5.35	23.9	6.2	24.5	4.4	132-180	70-150	16.2-30.9	6.7
40	80	0.87	0.98	0.24	13.7	4.6	13.8	4.1	162-180	90-140	10.9-24.7	4.5
@ Others	71	0.96	0.90	2.50	23.4	9.8	23.2	9.6	138-162	85-145	19.7-28.5	4.3
Total	720	0.97	1.00	0.19	25.5	12.6	25.3	12.2	42-186	25-150	4.5-64.6	6.3

Table 7 - continued

---

KEY

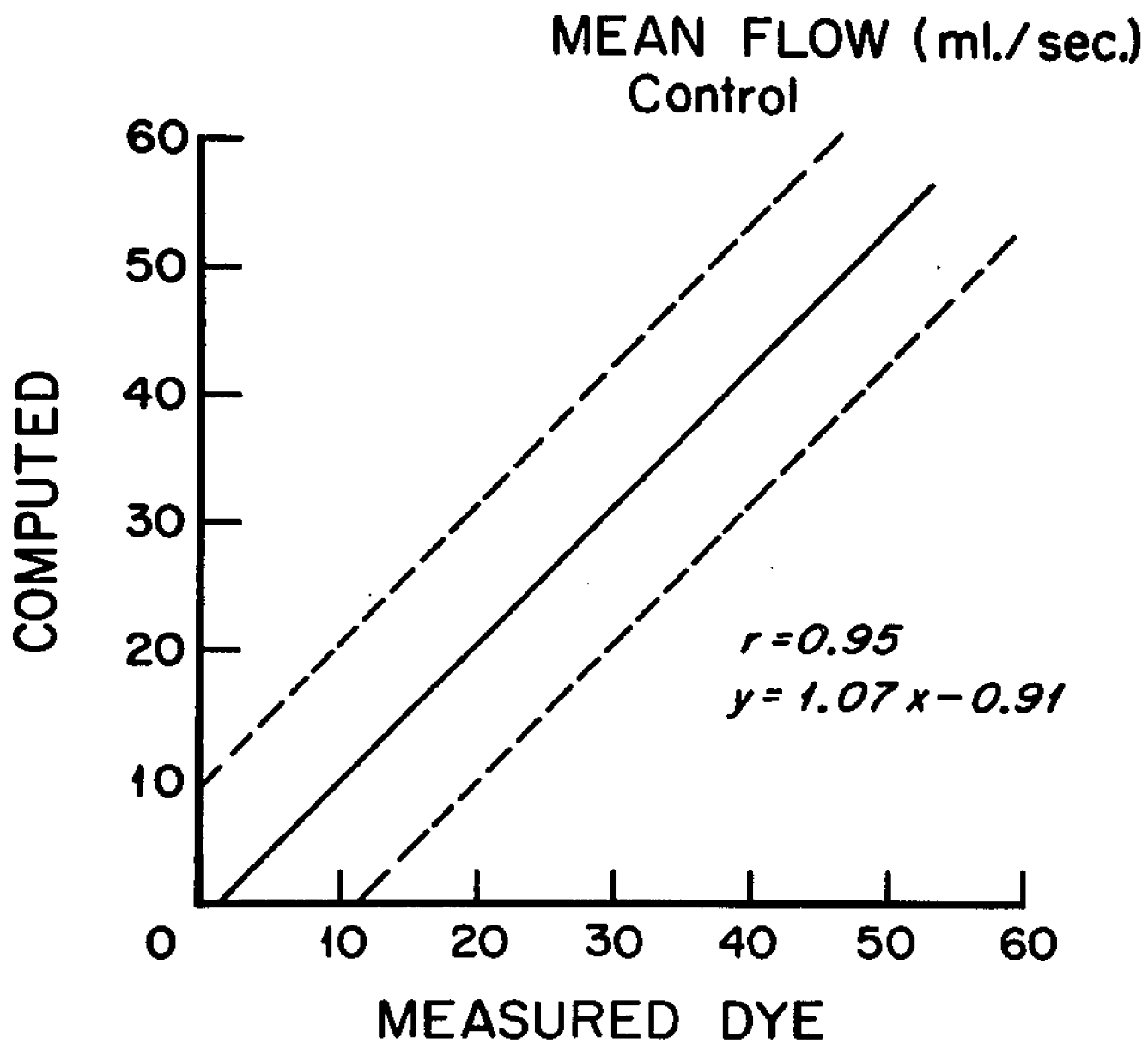
Dets.	=	Determinations
*	=	Mean flows were determined by the dye-dilution technique
@	=	Control data only were collected from these animals
r	=	Correlation coefficient
EMF	=	Electromagnetic flowmeter
H.R.	=	Heart rate (beats/min)
MAP	=	Mean arterial pressure (mmHg)
$\bar{Q}$	=	Mean flow (ml/sec)
S.E.E.	=	Standard error of estimate (ml/sec)
S.D.	=	Standard deviation (ml/sec)

Figure 20

A comparison of the mean flow as determined by the  
dye-dilution method with that computed from the  
pressure-gradient method

The broken lines represent 95% confidence limits ( $\pm 1.96$  S.E.E.)





those simultaneously measured with an electromagnetic flowmeter. The results from the individual animals are shown in Table 7. The number of interventions varied from one to three in each animal studied. As stated previously, when more than one intervention was introduced in a particular animal, baseline conditions were established between them. A wide range of variation in mean flow (4.5-64.6 ml/sec) and peak flow (32-266 ml/sec) as measured by the electromagnetic flowmeter was produced in the full series of animals studied, and was associated with changes in heart rate (42-186 beats/min) and mean arterial pressure (25-150 mmHg). Figure 21 is a graphical representation (scattergram) of all the determinations of mean flow (720) considered together. A correlation coefficient of 0.97 was obtained. The regression line is described by  $y = 1.00x + 0.19$  ml/sec and the standard error of estimate is  $\pm 3.15$  ml/sec ( $\pm 12\%$ ). The standard deviation is  $\pm 12.6$  for the computed mean flow and  $\pm 12.2$  for the measured mean flow. The slope (0.999) was not significantly different from 1.0 ( $p = 0.92$ ) and the intercept (0.19 ml/sec) was not significantly different from zero ( $p = 0.49$ ). Some scatter is seen in the data at high stroke outputs. As stated previously, the reason for this scatter will be considered in the Discussion. Table 8 is a computer print-out of the statistical data of all the mean flow comparisons. The correlation coefficient ranged from 0.81 to 0.99 in the individuals. The slope was not significantly different from 1.0 (the  $p$  value ranged from 0.1-0.7) and the intercept was not significantly different from zero (the  $p$  value ranged

Figure 21

A scattergram of all the computed mean flows (pressure-gradient method) versus the measured mean flows (dye-dilution and electromagnetic flowmeter)

The broken lines represent 95% confidence limits (see Table 7)

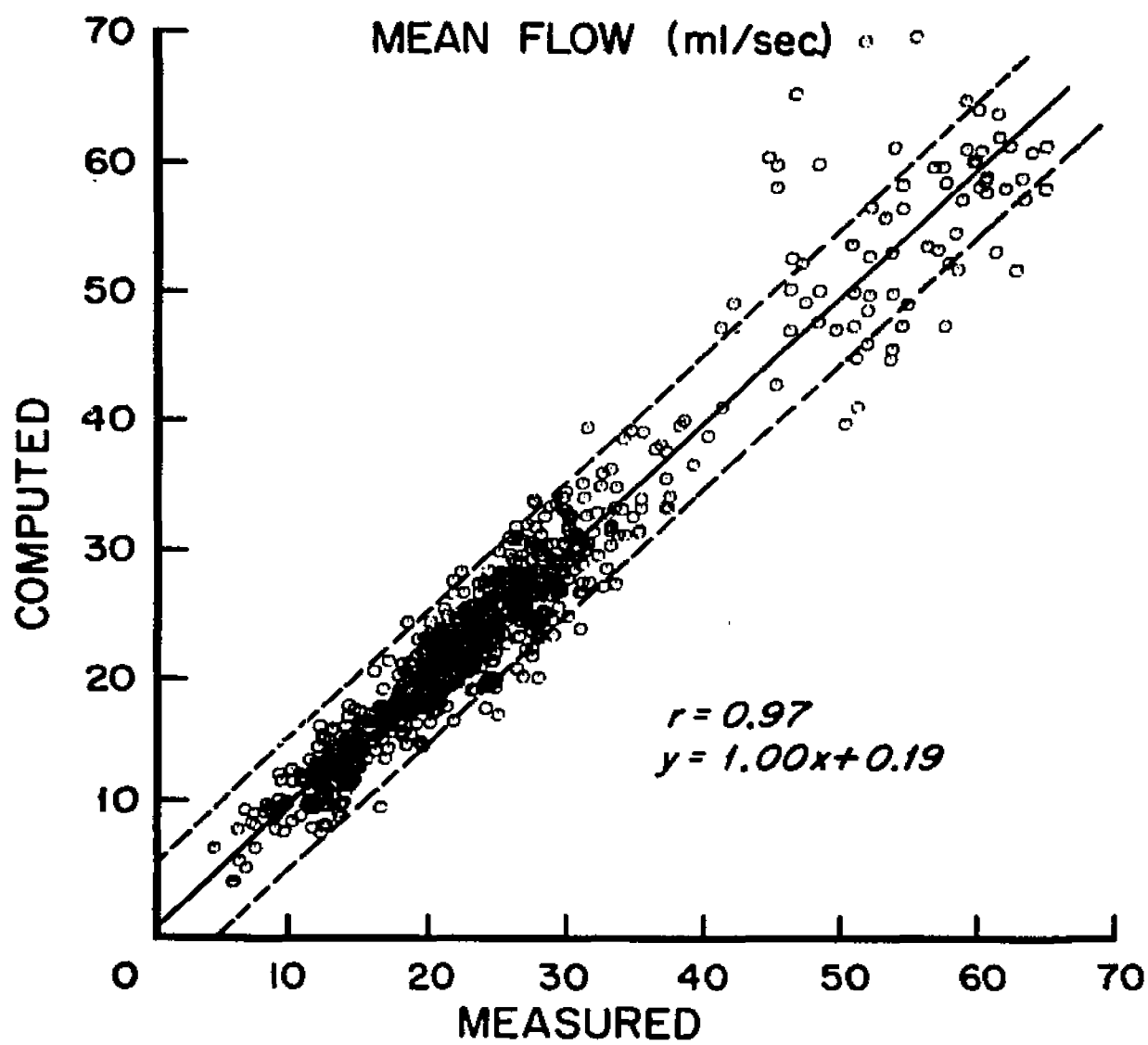


Table 8

Computer Print-Out of the Statistical Data of all the Mean Flow Comparisons

Variable		Mean	Standard Deviation	
X (measured)		25.32	12.161	
Y (computed)		25.49	12.571	

Coefficient	Estimate	Standard Deviation	T value	Null Hypothesis
A	25.49	0.120		
B	0.998982	0.009916	-0.102	Beta = 1
Intercept	0.19	0.278	0.696	Y(X=0)=0
Correlation	0.966			

#### Analysis of Variance

Source of Variance	Sums of Squares	Degrees of Freedom	Mean Squares	F
Due to Regression	106120.75	1	106130.75	10148.044
Residual	7508.31	718	10.45	
Total	113629.06	719		

from 0.1 to 0.5) except in animals 29 ( $p < 0.01$ ) and 34 ( $p < 0.01$ ). To look for possible sources of error over the frequency range, the computed flow moduli were compared to the measured flow moduli for all harmonic components below 20 Hz. Examples are illustrated from experiment 35: (a) under control conditions (Figure 22); (b) during vagal stimulation (Figure 23); (c) during the infusion of norepinephrine (Figure 24). The flow moduli comparisons were very close under control conditions and during vagal stimulation, but there is some discrepancy in the comparisons of harmonics one, two, and five during the infusion of norepinephrine. Figure 25 is an example of the computed flow curves under control conditions (A, B, C) and during the infusion of norepinephrine (D). The mean flow and peak flow comparisons in this particular experiment (experiment 8) were very good (see Tables 7 and 10), although in most of the experiments the peak flow comparisons were relatively poor except under control conditions (see Tables 10 and 11).

The comparison of the computed mean flow to the measured mean flow (experiment 18) during the introduction of several different interventions is shown in Figure 26. With few exceptions, this close comparison in the mean flow was seen in all of the animals studied.

When the various interventions were considered separately, certain differences became apparent (Table 9). For example, the correlation coefficients during the infusion of metaraminol and glucagon were relatively poor (0.82) and considerable scatter was

Figure 22

Comparison of the computed flow moduli to the measured flow moduli under control conditions

The average computed mean flow for these three runs was 22.3 ml/sec and the average measured mean flow was 23.5 ml/sec. The average computed peak flow was 105.6 ml/sec and the average measured peak flow was 108.5 ml/sec.

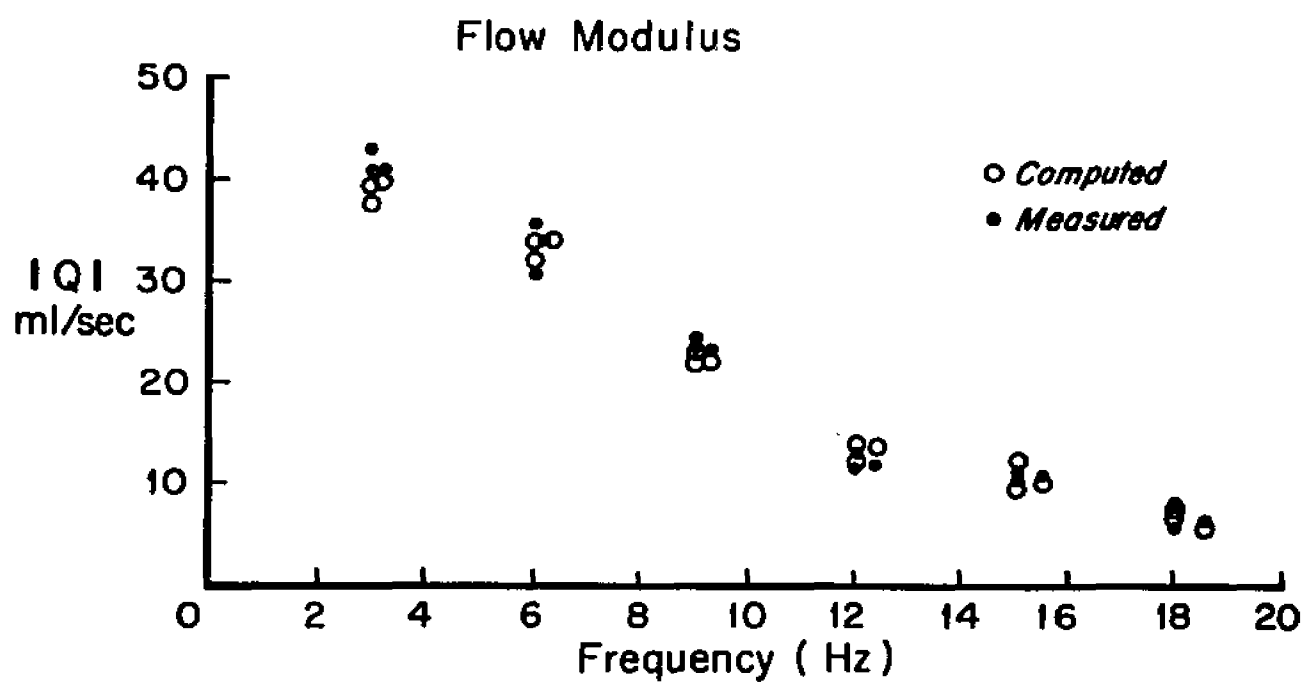




Figure 23

Comparison of the computed flow moduli to the measured flow moduli during vagal stimulation

The average computed mean flow for these two runs was 18.9 ml/sec and the average measured mean flow was 19.6 ml/sec. The average computed peak flow was 121.7 ml/sec and the average measured peak flow was 145.6 ml/sec

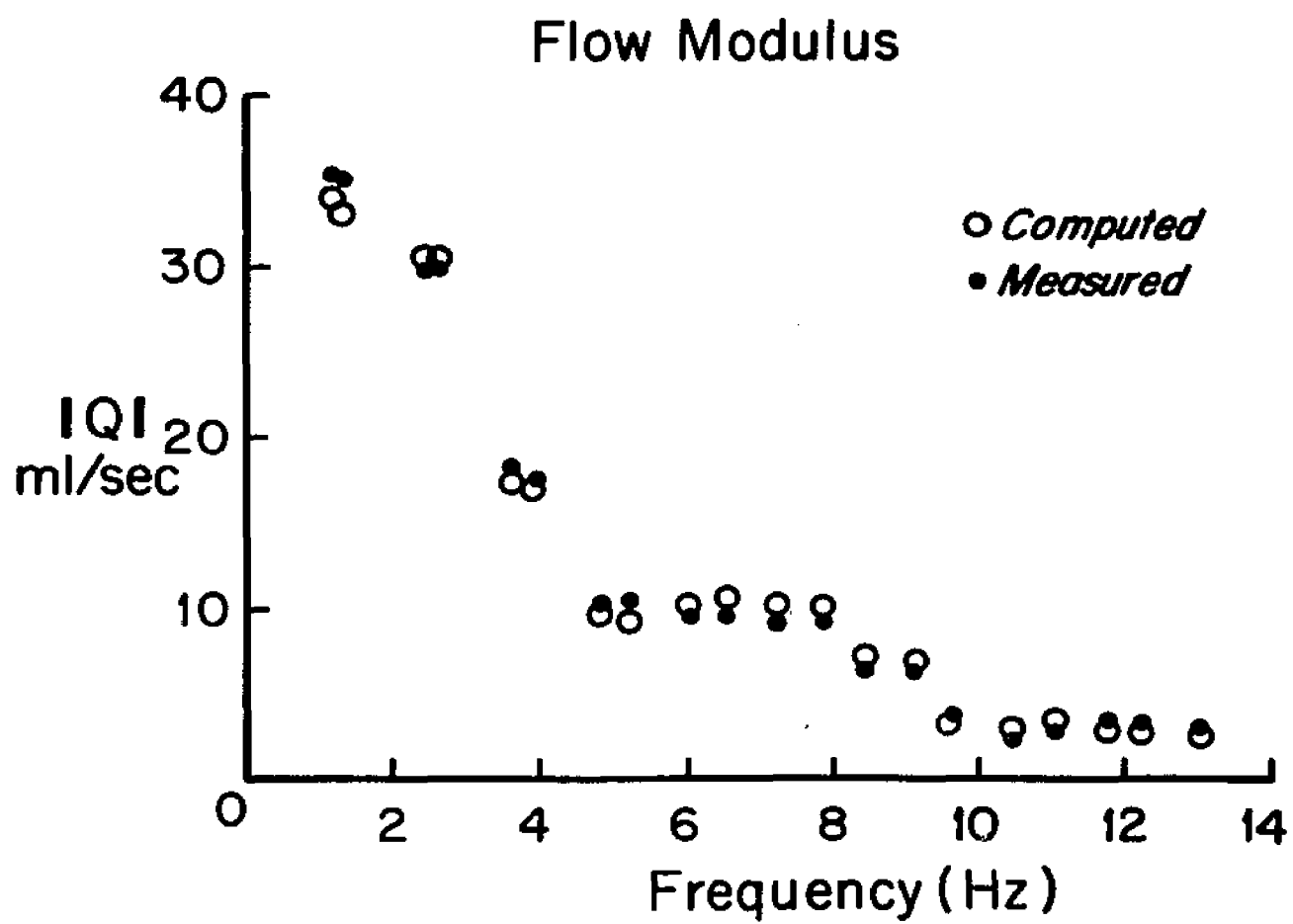
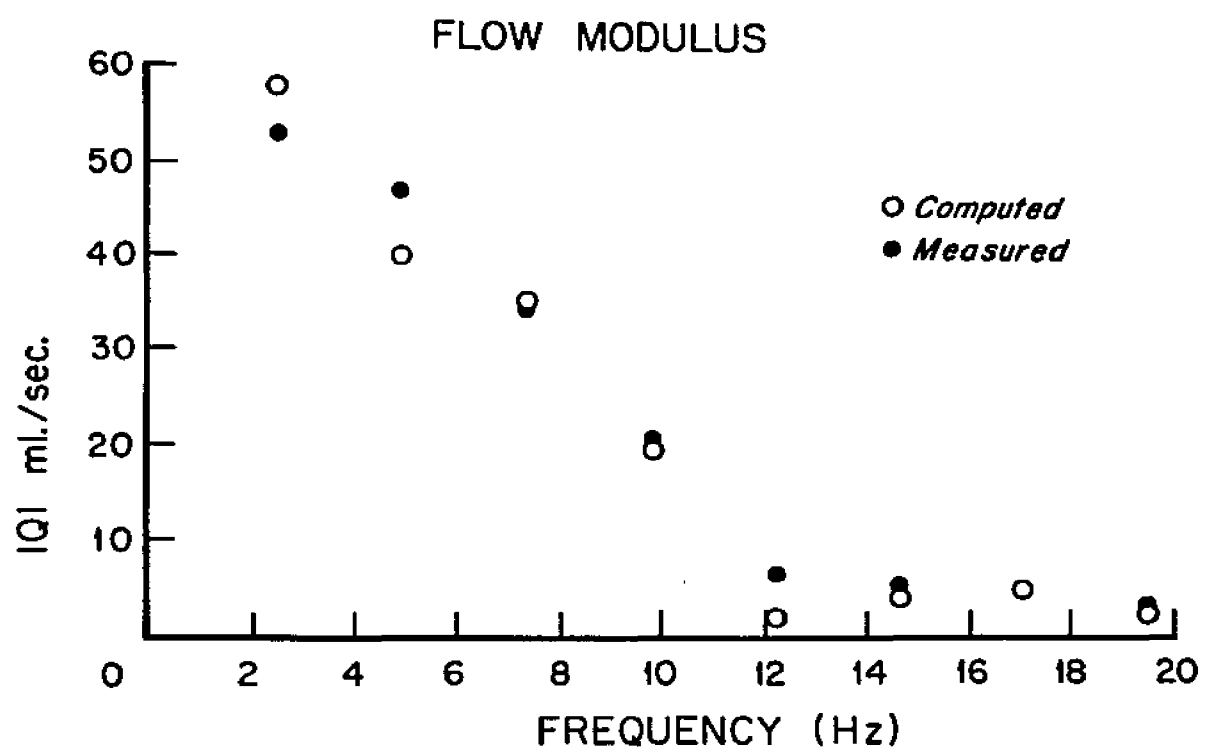


Figure 24

Comparison of the computed flow moduli to the measured flow moduli during the infusion of norepinephrine

The computed mean flow was 35.6 ml/sec and the measured mean flow was 33.5 ml/sec. The average computed peak flow was 115.7 ml/sec and the measured peak flow was 121.6 ml/sec.



## Figure 25

Pulsatile flow curves computed using the pressure-  
gradient method

Curves A, B, and C were computed under control conditions and  
Curve D was computed during the infusion of norepinephrine (see  
text).

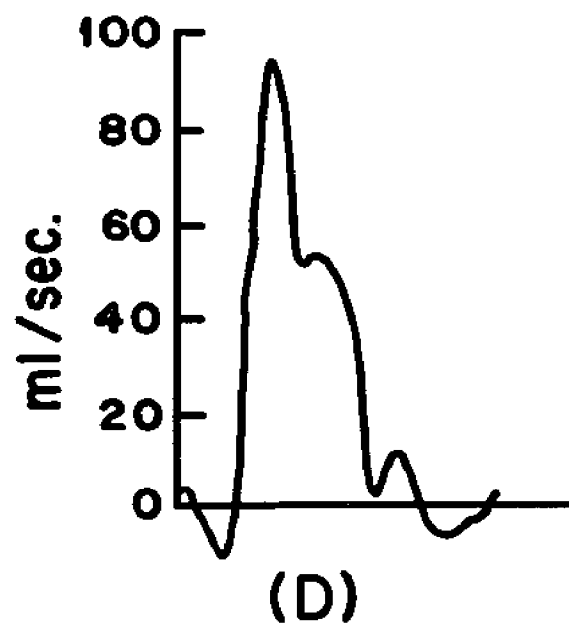
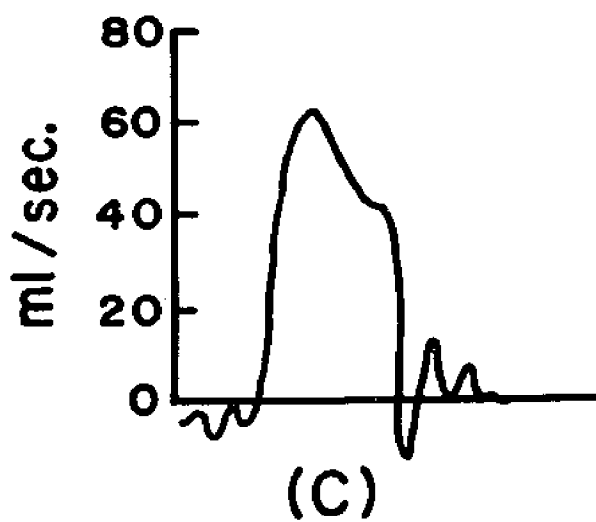
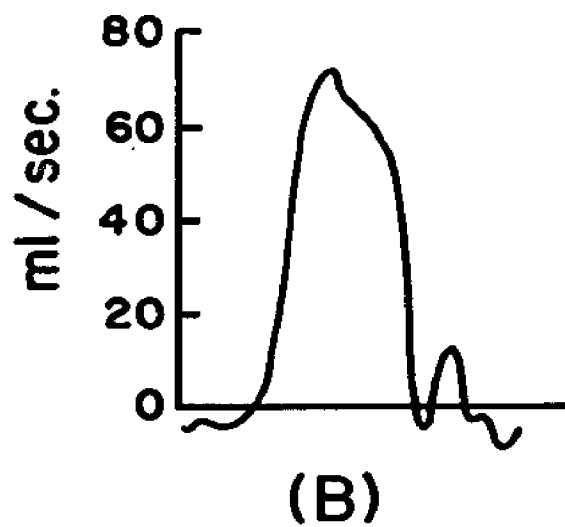
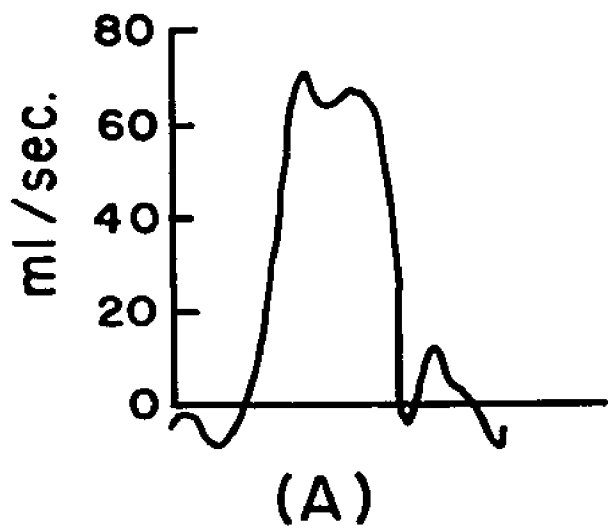


Figure 26

Comparison of the computed mean flow to the measured  
mean flow during the introduction of several different  
interventions.

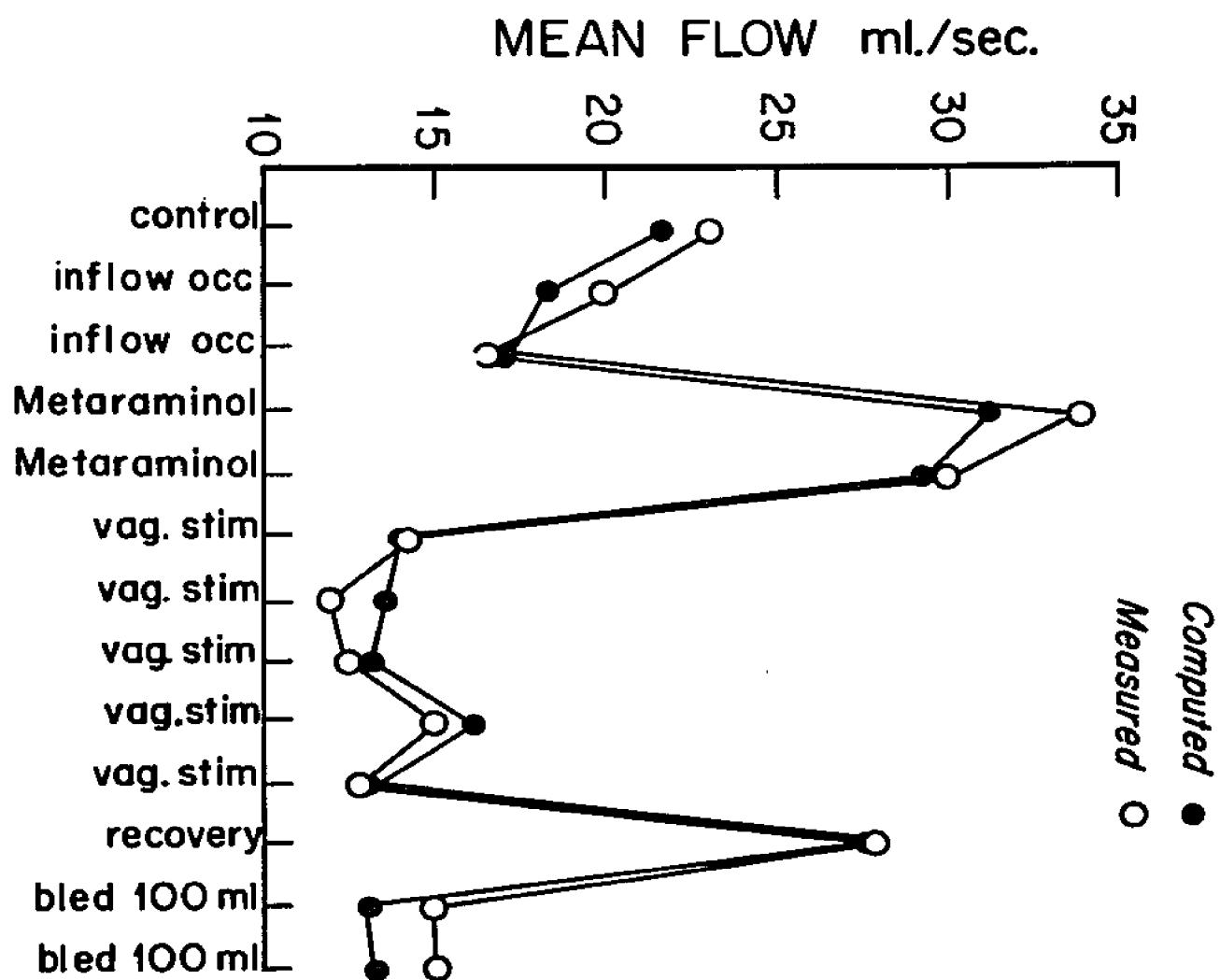




Table 9

Statistical Analysis of the Computed Mean Flow Versus the Electromagnetic Flowmeter with the 10 Interventions

Intervention	r	Slope	Intercept ml/sec	<u>Average Mean Flow(ml/sec)</u>				1.96 S.E.E. ml/sec
				Com- puted	S.D.	EMF	S.D.	
Pacing	0.89	0.85	3.33	25.4	3.9	25.9	4.1	3.6
Hemorrhage	0.93	1.03	-0.45	14.7	6.3	14.6	5.6	4.8
RFAC	0.98	0.97	0.20	45.9	18.1	47.0	18.3	6.3
Vagal Stimulation	0.96	0.96	0.79	24.5	9.7	24.7	9.7	5.5
Dextran	0.88	1.02	1.21	43.1	13.6	41.1	11.8	13.0
Epinephrine	0.93	0.98	0.76	23.1	6.6	22.9	6.3	5.1
Nor-epinephrine	0.95	0.92	1.53	21.7	6.4	21.8	6.6	4.1
Isoproterenol	0.94	1.10	-1.21	21.1	5.9	20.3	5.0	4.2
Metaraminol	0.82	0.94	1.92	25.5	5.1	25.2	4.4	6.0
Glucagon	0.82	0.84	4.70	25.7	4.7	25.0	4.6	5.4

r = Correlation Coefficient  
 EMF = Electromagnetic Flowmeter  
 S.E.E. = Standard Error of Estimate

RFAC = Recovery from Aortic Constriction  
 S.D. = Standard Deviation

seen in the data during the infusion of dextran (Figure 27) (1.96 S.E.E. = 13.0 ml/sec). The average mean flow comparisons were still good during the introduction of these interventions. The possible reasons for these discrepancies will be considered in the Discussion. After hemorrhage (i.e. at low stroke outputs) the mean flow comparisons were very good (Figure 28) ( $r = 0.93$ ,  $y = 1.03x - 0.45$  ml/sec and 1.96 S.E.E. =  $\pm 4.8$  ml/sec). Excellent correlation ( $r = 0.96$ ) in mean flow comparisons was also seen during vagal stimulation (Figure 29) (pulse frequency 0.7 to 1.5 Hz). The mean flow computed using the pressure-gradient method was excellent when the peripheral resistance was decreased with isoproterenol ( $r = 0.94$ ) (Figure 30) and when it was increased with norepinephrine ( $r = 0.95$ ) (Figure 31).

Five hundred and seventy-three determinations of peak flow were collected from 30 animals and compared to those simultaneously measured with an electromagnetic flowmeter. The results from the individuals are shown in Table 10. The correlation coefficient was excellent (0.92 to 0.99) in all the animals studied except the ones in which the vagus nerve was stimulated or metaraminol was infused. During these two interventions the correlation coefficient ranged from 0.35 to 0.81 (see Discussion). Although the correlation coefficient was good in ten of the animals, the other statistical data (slope and intercept) were very poor ( $p < 0.05$ ) except in animals 32, 33, and 37. In these three animals, the slope was not significantly different from 1.0 (the  $p$  value ranged from 0.1 to 0.2) and the intercept was not significantly different from zero (the  $p$  value ranged from 0.1 to 0.8).

Figure 27

Comparison of the computed mean flow to the measured  
mean flow during the infusion of dextran

Broken lines represent 95% confidence limits

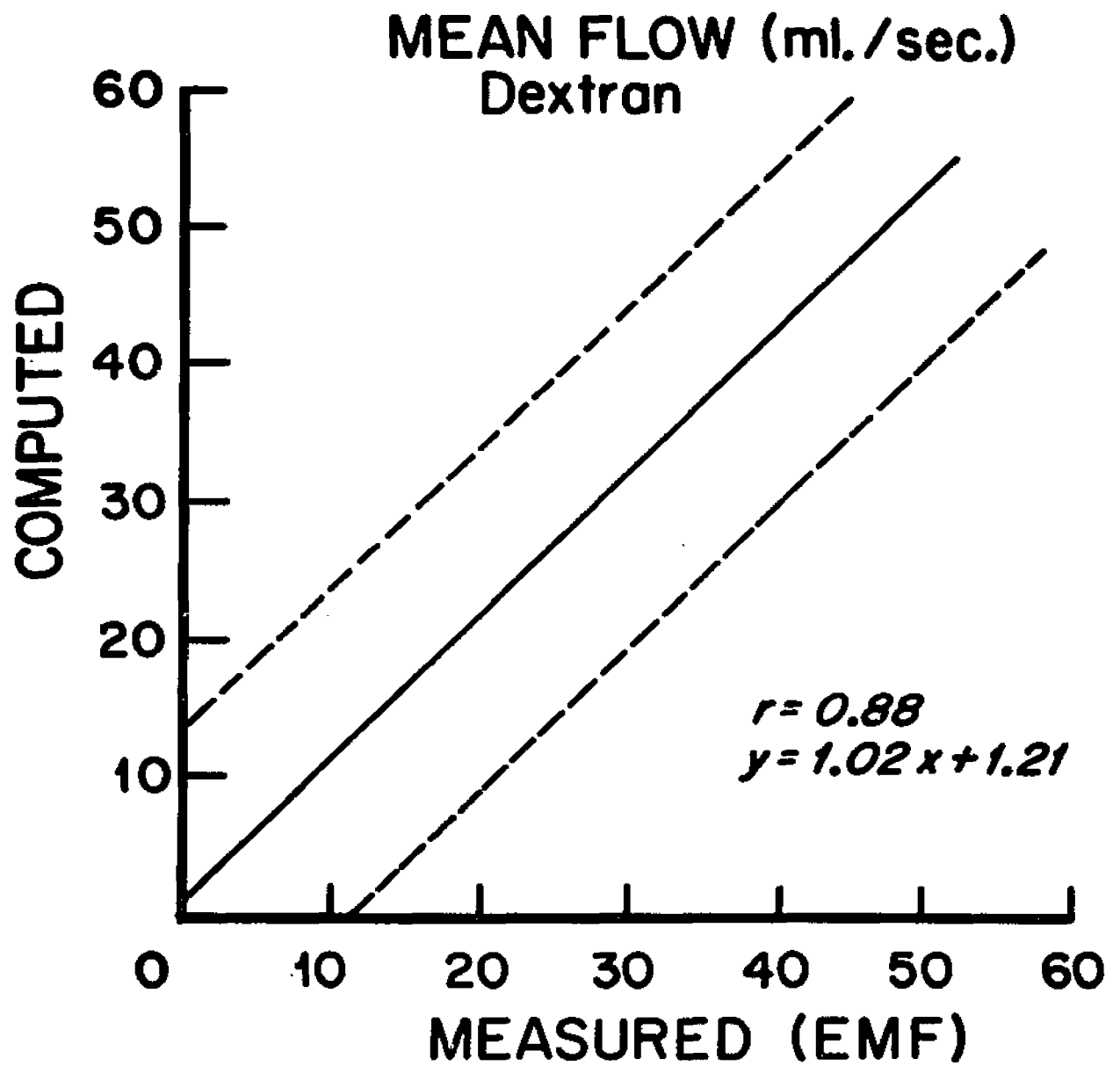


Figure 28

Comparison of the computed mean flow to the measured  
mean flow after hemorrhage

Broken lines represent 95% confidence limits

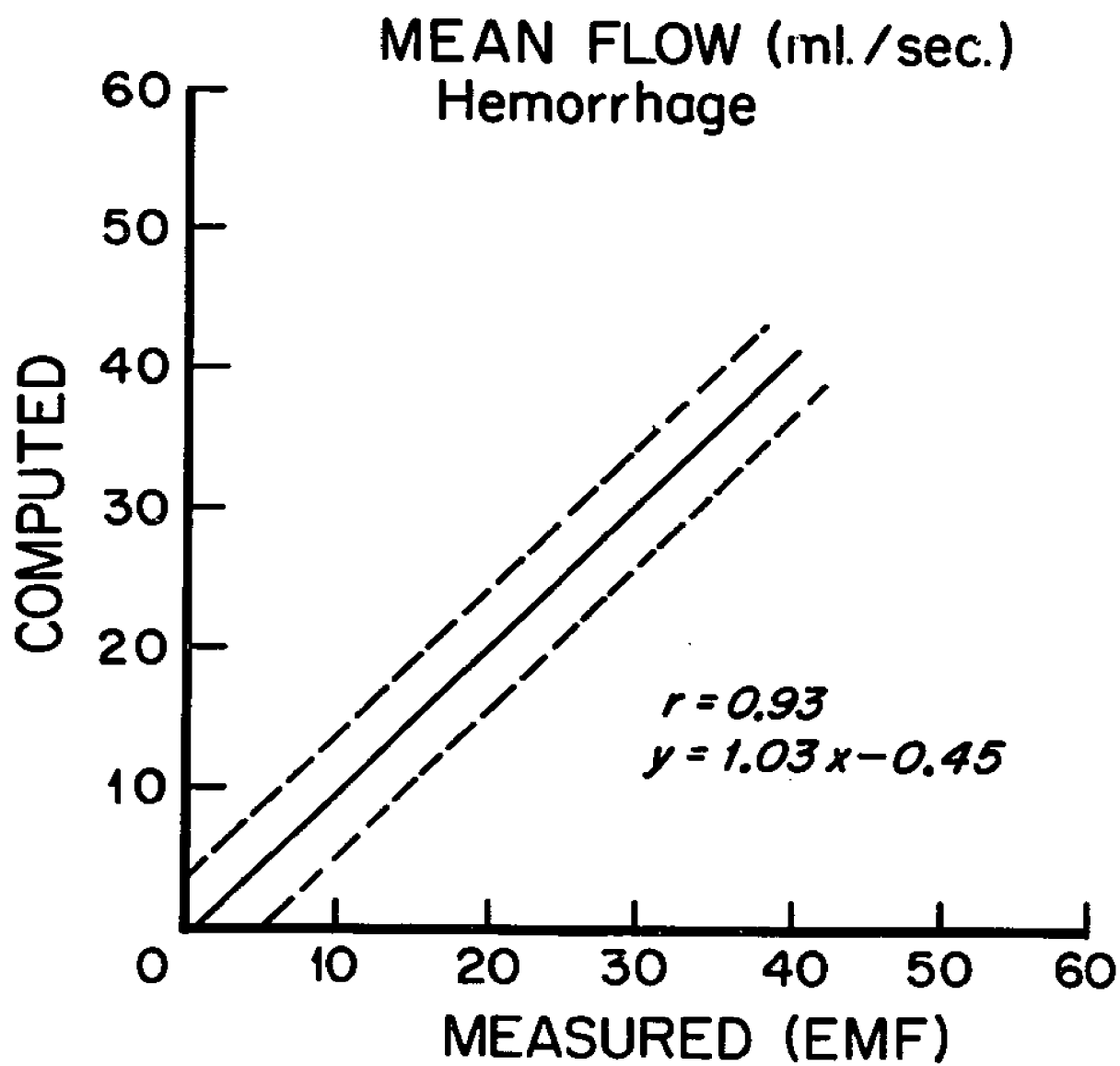


Figure 29

Comparison of the computed mean flow to the measured  
mean flow during vagal stimulation

The pulse frequency ranged from 0.7 to 1.5 Hz. Broken lines  
represent 95% confidence limits.

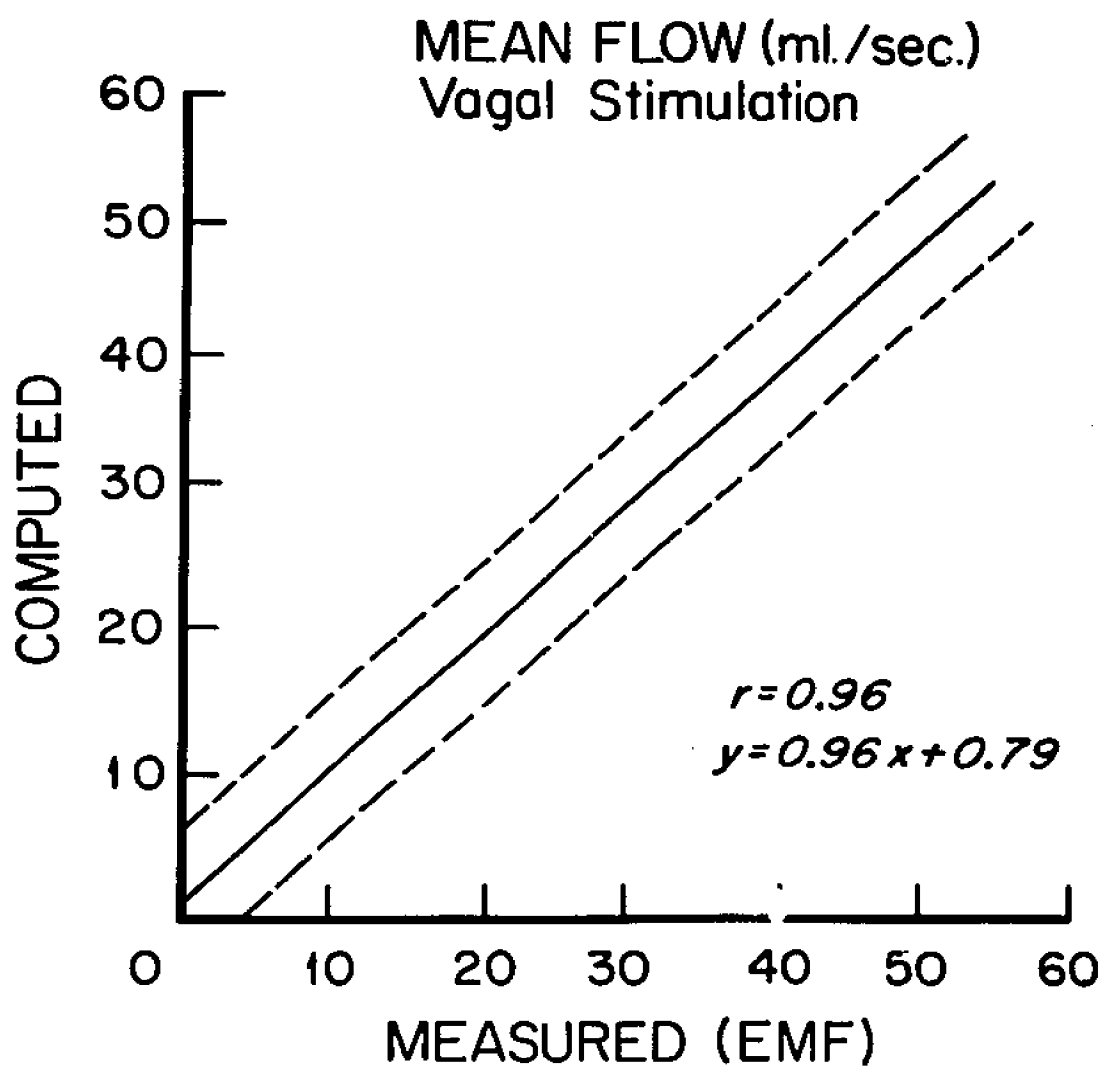




Figure 30

Comparison of the computed mean flow to the measured  
mean flow during the infusion of isoproterenol

Broken lines represent 95% confidence limits

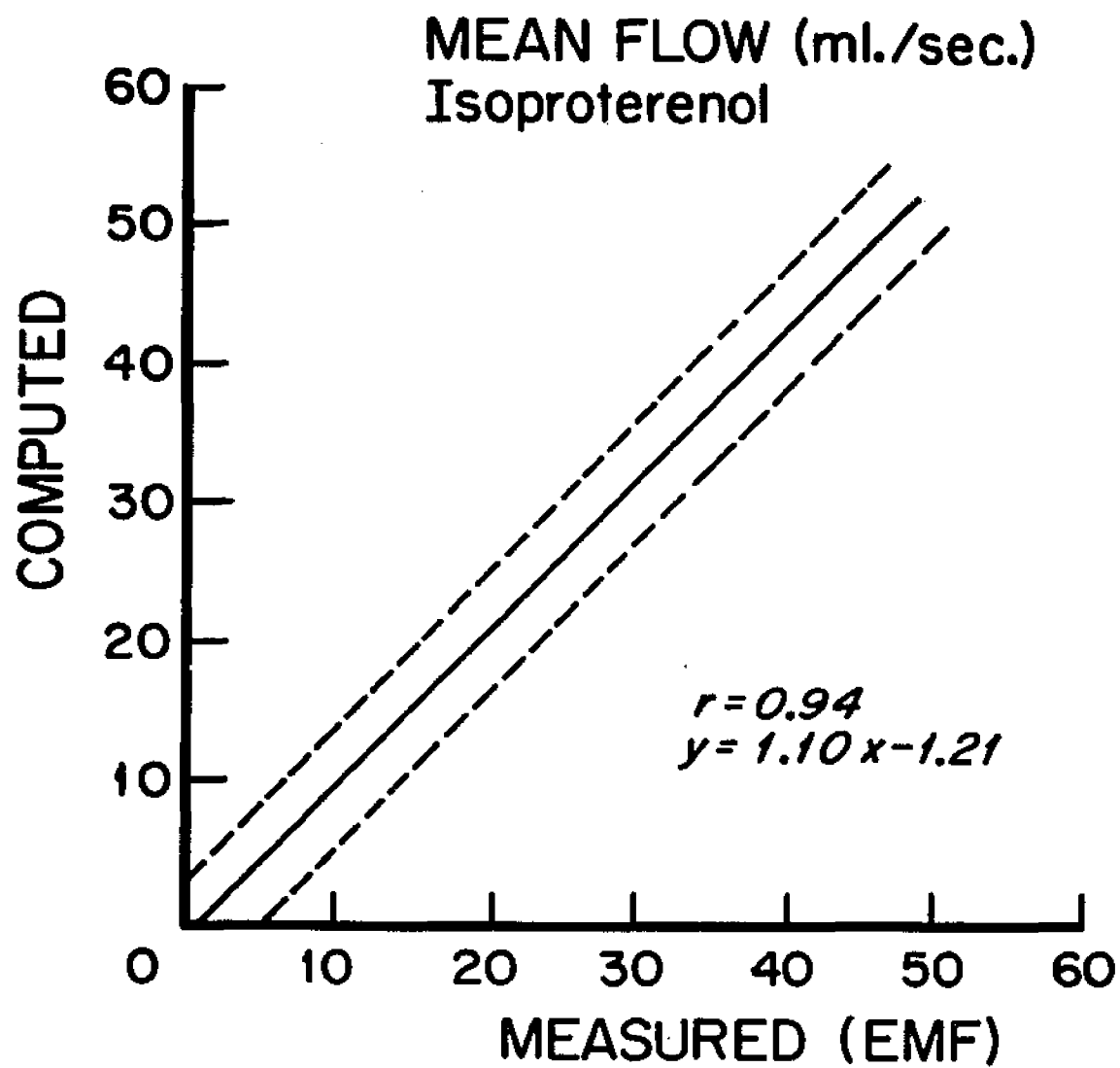


Figure 31

Comparison of computed mean flow to the measured  
mean flow during the infusion of norepinephrine

Broken lines represent 95% confidence limits

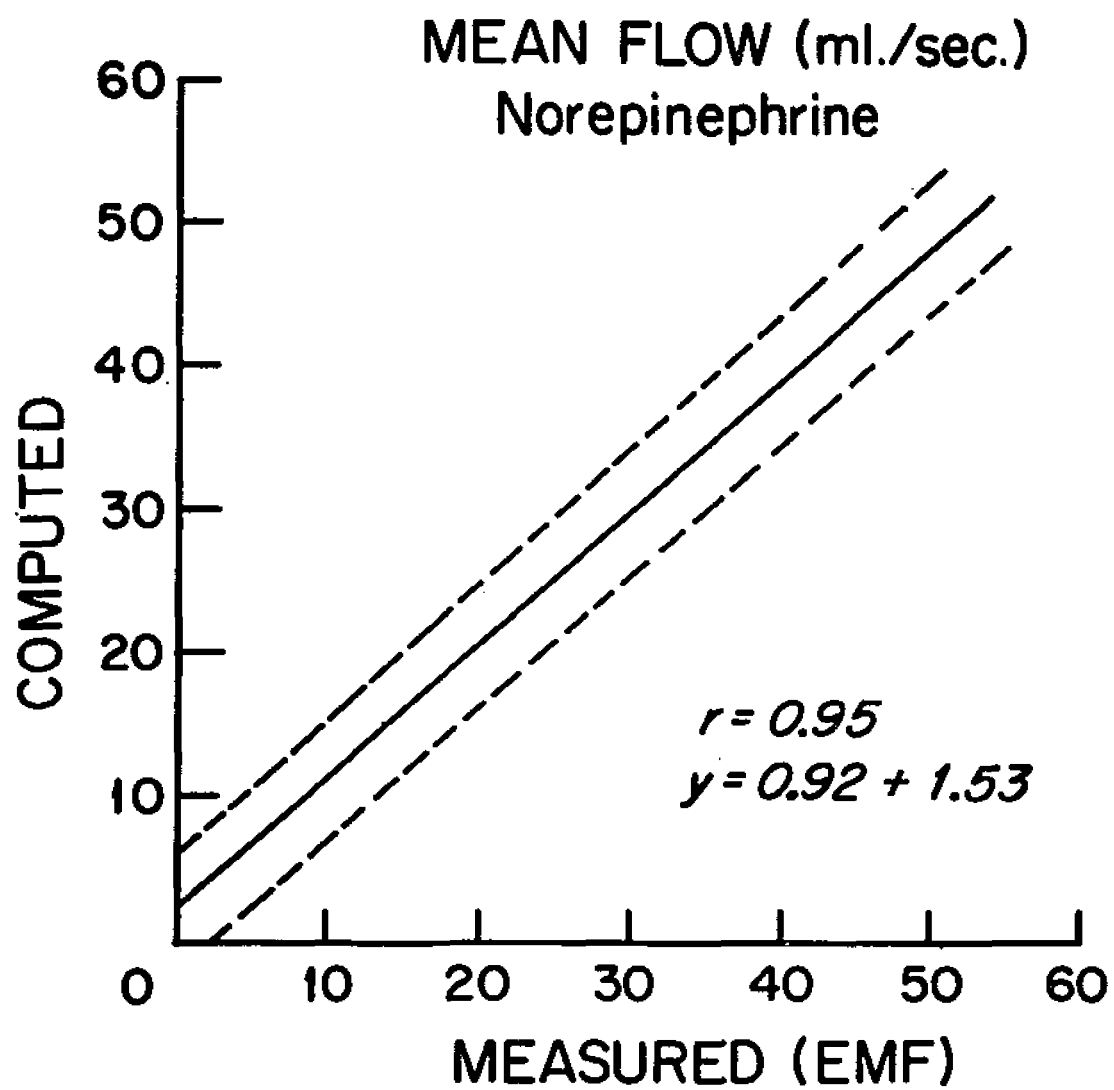


Table 10

Statistical Analysis of the Computed Peak Flow Versus the Electromagnetic Flowmeter in the Individual Animals

Expt. No.	No. of Dets.	r	Slope	Intercept	Average Peak Flow				$\hat{Q}$ Range	1.96 S.E.E.	Intervention
					Computed	S.D.	EMF	S.D.			
8	15	0.96	1.13	-13.3	80.1	4.1	83.1	3.5	76-88	12.4	Nor-epinephrine
11	24	0.98	0.74	20.9	104.0	20.2	112.8	26.8	55-142	9.7	Epinephrine and Isoproterenol
12	15	0.96	0.77	17.2	86.0	15.4	89.8	19.5	55-123	8.4	Isoproterenol
17	34	0.47	0.39	31.3	70.2	19.0	100.7	23.1	59-136	34.0	VS, Hemorrhage, and Metaraminol
18	35	0.69	0.74	-8.6	68.2	20.6	104.1	19.3	73-139	30.3	VS, Hemorrhage, and Metaraminol
19	15	0.76	-1.71	622.8	189.0	23.6	253.4	10.4	237-266	32.1	VS
20	15	0.35	1.44	-150.1	195.3	29.6	240.1	7.2	228-250	57.5	VS
23	15	0.99	0.64	46.6	178.6	28.8	206.7	44.5	120-250	9.4	RFAC
24	20	0.98	0.59	52.4	163.5	30.2	187.1	49.8	122-243	12.1	RFAC
25	15	0.95	0.53	64.4	171.9	26.0	204.3	46.9	135-260	16.9	RFAC
27	15	0.76	1.21	-9.3	108.5	14.4	97.6	9.1	80-108	19.4	Metaraminol

Table 10 - continued

Expt. No.	No. of Dets.	r	Slope	Intercept	Average Peak Flow				$\hat{Q}$ Range	1.96 S.E.E.	Interventions
					Computed	S.D.	EMF	S.D.			
28	15	0.69	0.56	50.1	105.7	9.2	98.5	11.2	80-112	13.7	Metaraminol
29	15	0.74	0.50	41.1	94.1	12.3	106.2	18.3	63-125	17.0	Metaraminol
32	41	0.97	0.94	1.8	112.7	54.7	118.3	56.8	43-125	25.5	Hemorrhage and Dextran
33	42	0.97	0.96	5.8	116.2	68.9	115.0	69.8	32-203	32.8	Hemorrhage and Dextran
34	32	0.76	0.55	37.9	110.2	13.9	131.6	14.3	107-181	18.4	Pacing and VS
35	16	0.81	0.50	41.9	103.6	11.1	122.4	17.8	106-160	13.4	Pacing, VS, and Nor-epinephrine
37	35	0.94	0.93	-3.5	128.5	26.3	141.9	26.5	102-192	18.7	Epinephrine and Nor-epinephrine
38	37	0.92	0.80	10.2	130.2	26.0	144.5	29.8	100-218	20.5	Epinephrine and Nor-epinephrine
Others*122		0.97	0.91	5.4	106.1	39.4	110.2	42.0	85-140	18.0	Control
Total	573	0.91	0.85	13.2	112.8	44.7	128.1	52.9	32-266	37.5	

\* - Control data only were collected from these animals;  $\hat{Q}$  - Peak flow (ml/sec);

r - Correlation coefficient; S.E.E. - Standard error of estimate; VS - Vagal stimulation;

EMF - Electromagnetic flowmeter; S.D. - Standard deviation; RFAC - Recovery from aortic constriction

Table 11

## Statistical Analysis of Computed Peak Flow Versus Electromagnetic Flowmeter with the 10 Interventions

Interventions	No.of Expts	No.of Dets.	r	Slope	Inter- cept (ml/sec)	Average Peak Flow (ml/sec)		Average Peak Flow (ml/sec)				1.96 S.E.E. (ml/sec)
						Base- line	@ maxi- mal effect	Com- puted	S.D.	EMF	S.D.	
Pacing	2	38	0.78	0.55	38.3	134	114	105.5	8.5	122.2	13.5	12.1
Hemorrhage	4	73	0.78	0.75	12.2	104	62	68.4	23.0	75.1	23.9	29.1
RFAC	3	50	0.97	0.59	53.9	143	235	170.6	28.7	198.1	47.3	13.8
Vagal Stimulation	6	98	0.90	0.77	1.2	145	160	119.4	55.4	153.7	65.2	47.6
Dextran	3	42	0.92	0.98	-1.3	107	201	162.9	48.9	167.3	46.0	38.3
Epinephrine	4	77	0.79	0.64	26.1	91	141	107.5	21.6	126.3	26.6	26.6
Nor-epinephrine	4	69	0.97	0.83	6.3	95	142	112.2	35.2	127.8	41.0	18.5
Isoproterenol	4	44	0.81	0.96	4.3	80	105	96.4	24.3	96.3	20.6	28.8
Metaraminol	5	73	0.76	0.68	30.2	82	116	97.4	22.4	107.3	23.6	25.9

r = Correlation coefficient  
 EMF = Electromagnetic flowmeter  
 S.D. = Standard deviation

S.E.E. = Standard error of estimate  
 RFAC = Recovery from aortic constriction  
 Dets. = Determinations

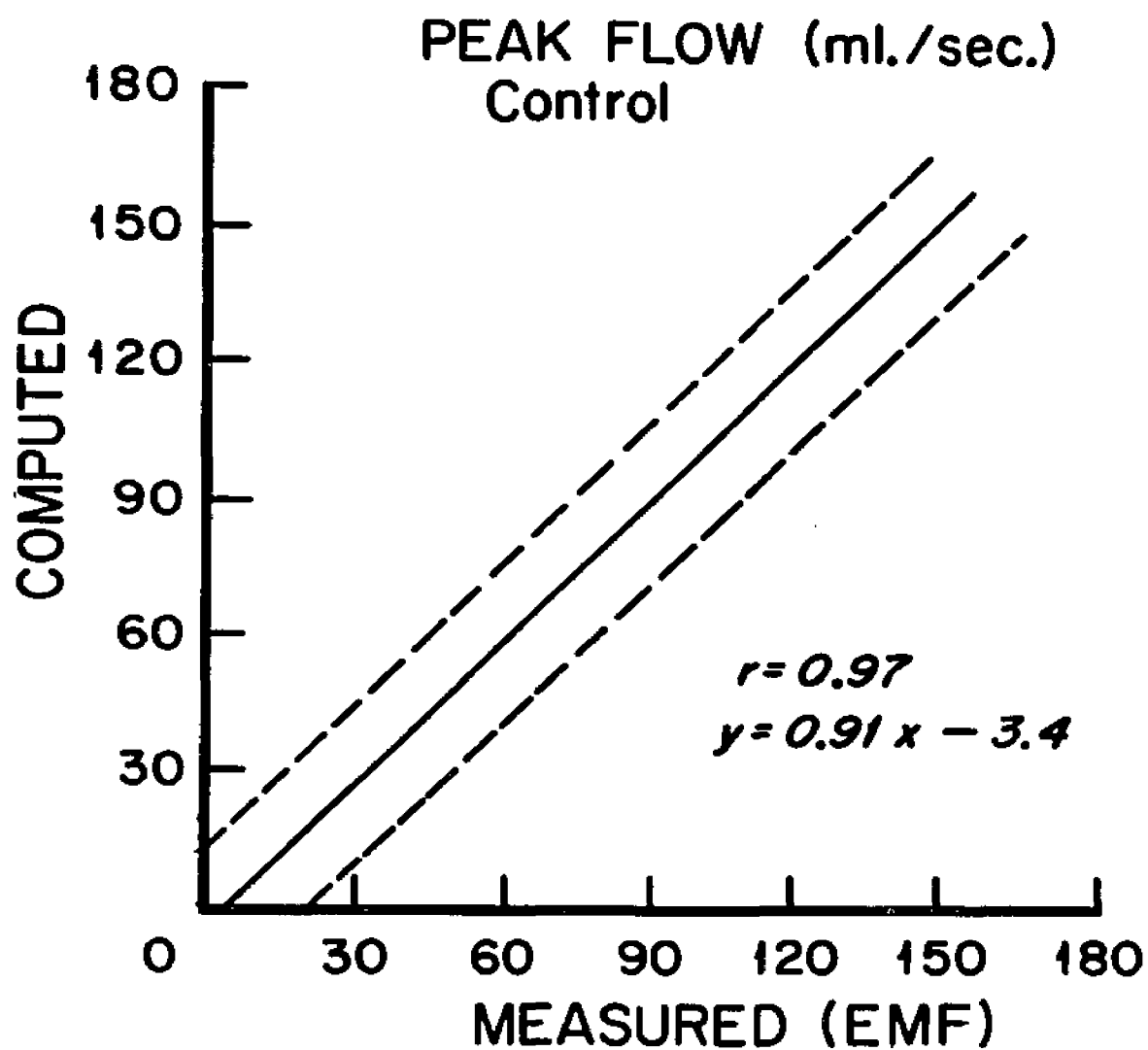
Control data only were collected from 11 of the animals. The statistical data from these animals were acceptable ( $p > 0.05$ ) ( $r = 0.97$ ,  $y = 0.91x + 5.4$  ml/sec and  $1.96 \text{ S.E.E.} = \pm 18.0$  ml/sec) (Figure 32). At very slow pulse frequencies (0.7–1.5 Hz) the computed peak flow was consistently lower than the measured peak flow (Figure 33). This is probably due to an error in the computed phase and will be considered in the Discussion. Figure 34 is a graphical representation of the peak flow comparisons with the vagal stimulation determinations omitted. The correlation coefficient is 0.92 and the regression line is described by  $y = 0.84x + 6.6$  ml/sec. The slope is not significantly different from 1.0 ( $p > 0.05$ ) and the intercept is not significantly different from zero ( $p > 0.05$ ). When the vagal stimulation determinations are included the correlation coefficient becomes 0.91 and the regression line becomes  $y = 0.85x + 13.2$  ml/sec (Figure 35). This slope is significantly different from one ( $p < 0.05$ ) and the intercept is significantly different from zero ( $p < 0.05$ ). Table 12 is a computer print-out of the statistical data of all the peak flow comparisons.



Figure 32

Comparison of the computed peak flow to the measured  
peak flow under control conditions

Broken lines represent 95% confidence limits



**Figure 33**

**Comparison of the computed peak flow to the measured  
peak flow during vagal stimulation**

**The pulse frequency ranged from 0.7 to 1.5 Hz. Broken lines  
represent 95% confidence limits.**

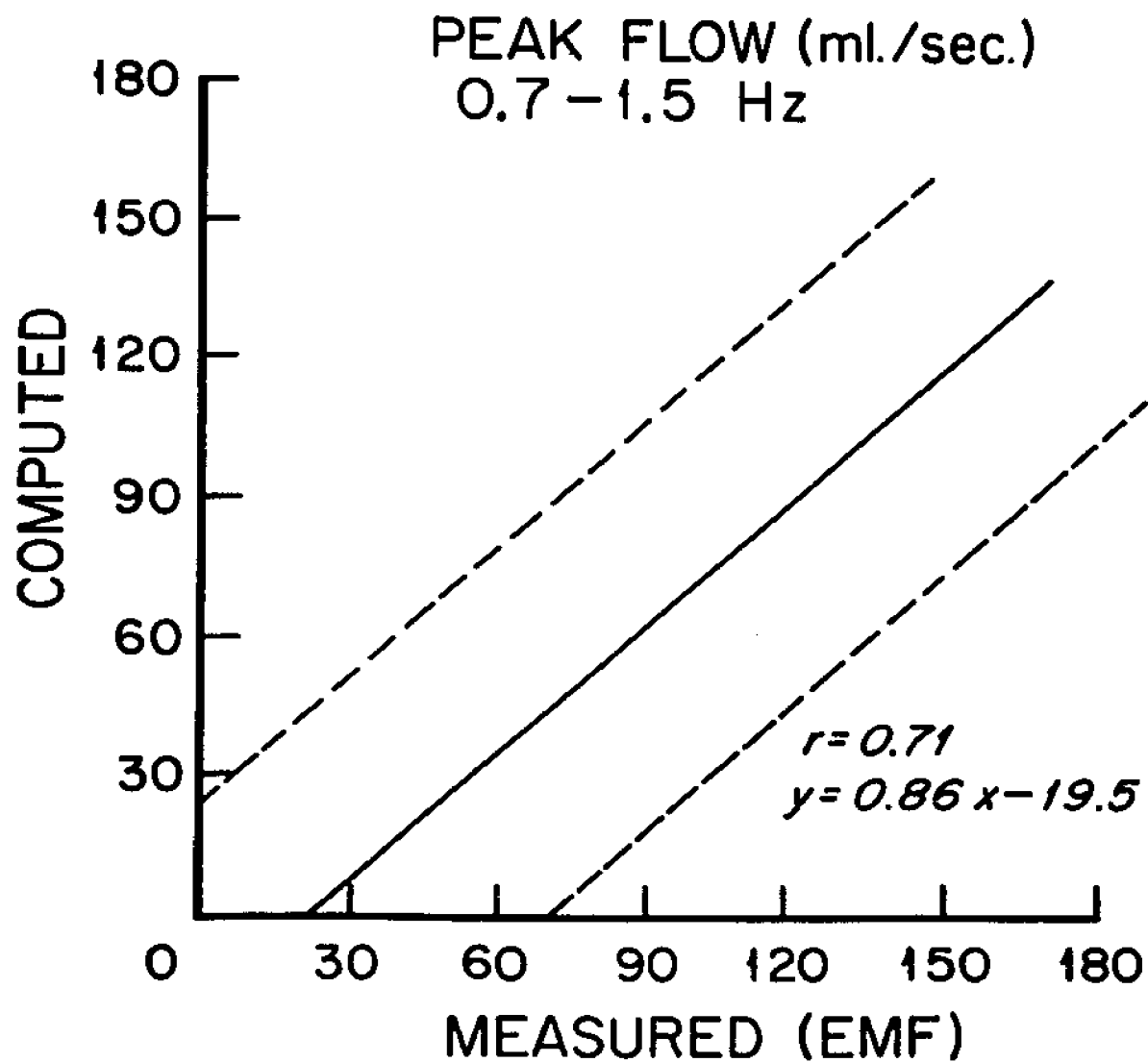


Figure 34

A comparison of the computed peak flow to the measured  
peak flow with the vagal stimulation determinations  
omitted

Broken lines represent 95% confidence limits

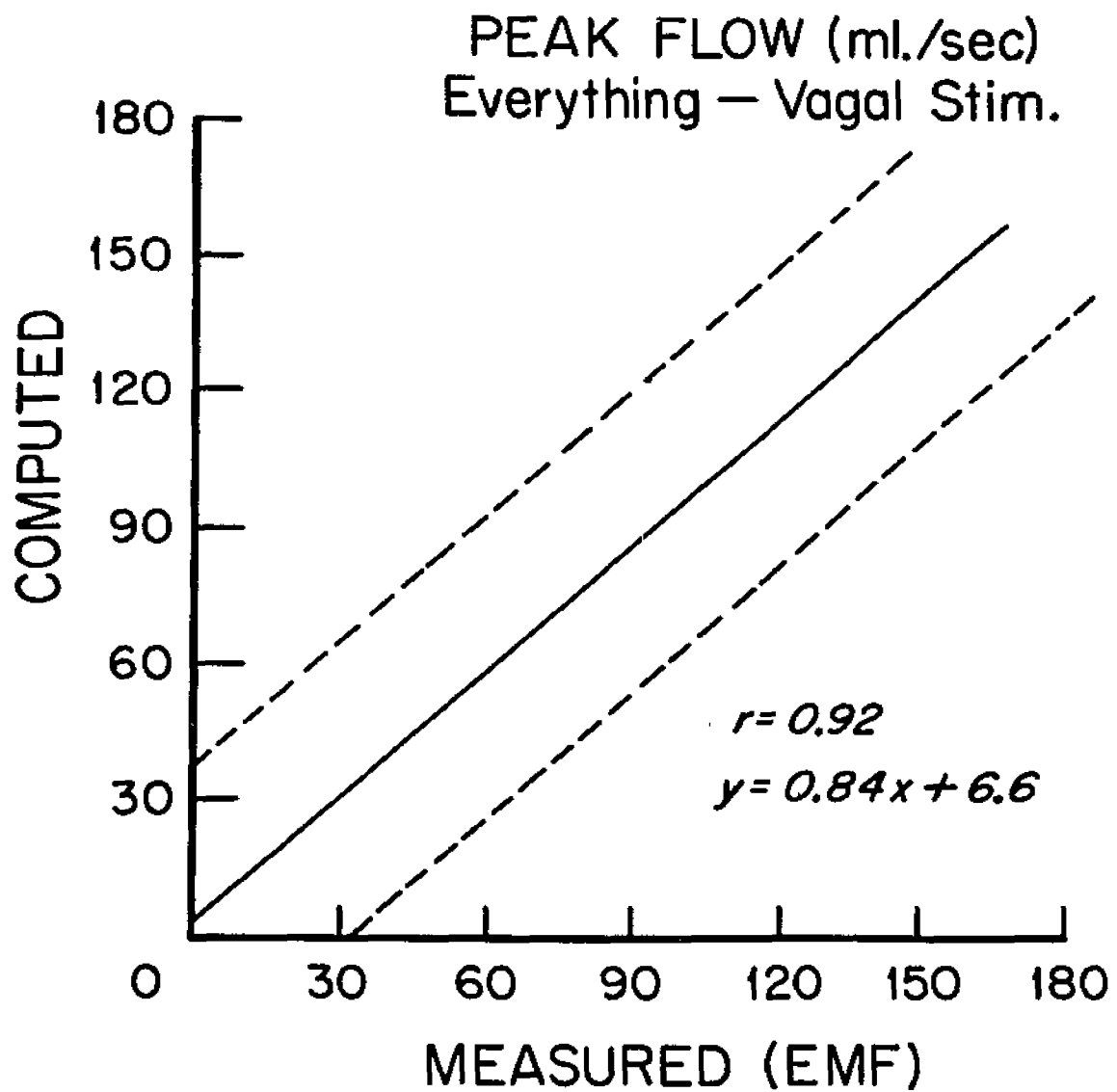


Figure 35

A scattergram of all the computed peak flows (pressure-gradient method) versus the measured peak flows (electromagnetic flowmeter)

Broken lines represent 95% confidence limits

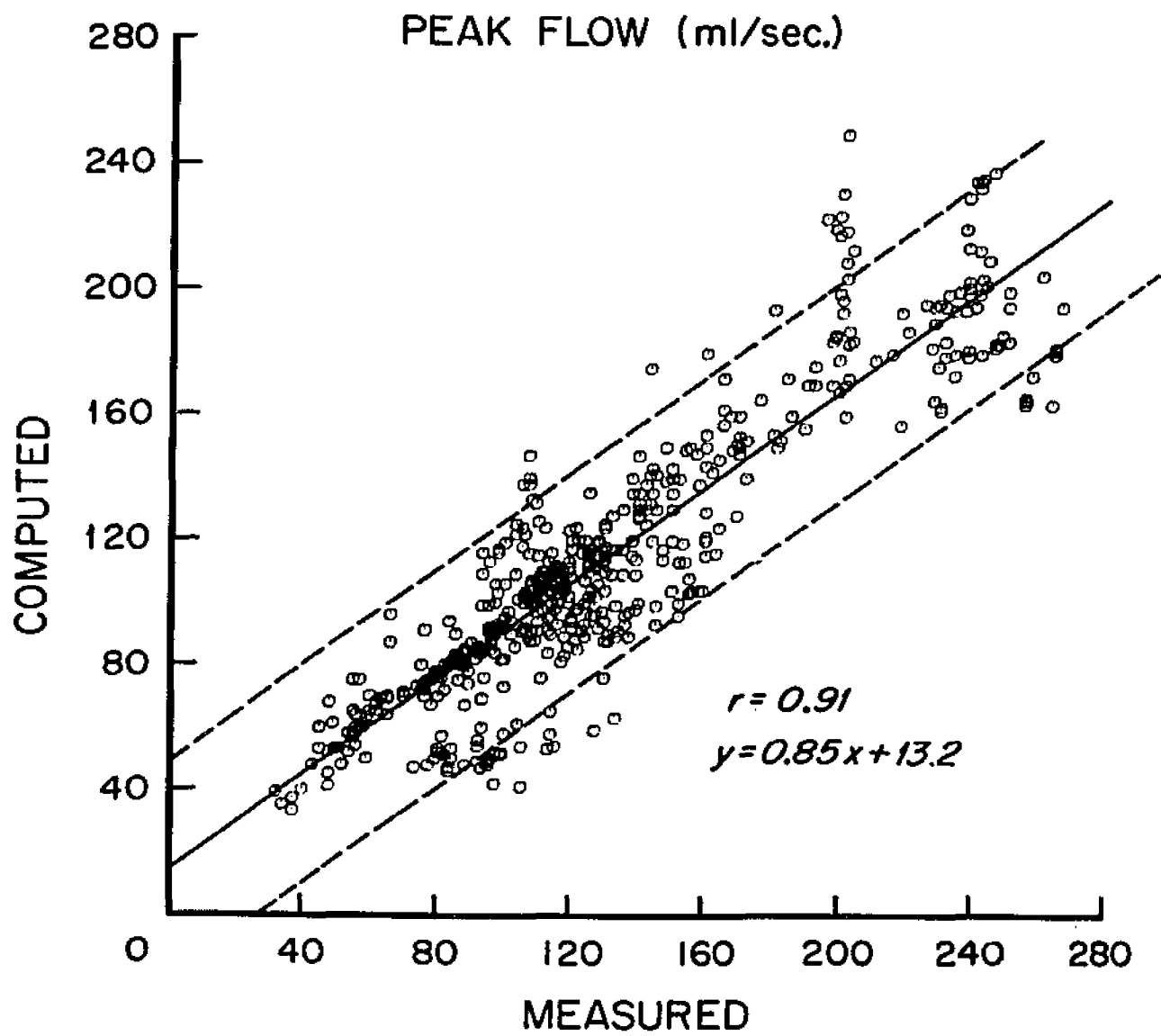




Table 12

Computer Print-Out of the Statistical Data of all the Peak Flow Comparisons

Variable		Mean	Standard Deviation	
X (measured)		128.12	52.891	
Y (computed)		112.82	44.787	

Coefficient	Estimate	Standard Deviation	T value	Null Hypothesis
A	112.82	0.782		
B	0.769313	0.014806	-15.580	Beta = 1
Intercept	13.20	2.052	6.946	$Y(X=0)=0$
Correlation	0.908			

#### Analysis of Variance

Source of Variance	Sums of Squares	Degrees of Freedom	Mean Squares	F
Due to Regression	947068.54	1	747068.54	2699.777
Residual	200304.00	571	350.79	
Total	1147372.54	572		

## DISCUSSION

Objectives of the research. Present results compared to other methods.

The primary objective of this investigation has been to develop a method that would predict the ventricular output continuously in a patient with a minimum of trauma; the transcutaneous intra-arterial insertion of catheters for pressure recordings and the estimate of aortic radius is all that would be necessary for the calculation of the flow from the pressure-gradient. This procedure is independent of other flow methods for calibration and is therefore still valid in the face of possibly profound circulatory changes, for example, the mean blood pressure and the pulse frequency. In this investigation, 720 determinations of mean flow (range 4.5 - 64.6 ml/sec) were collected under control conditions and during the introduction of several different interventions (see Tables 6 and 9) (MAP range 25 - 150 mmHg; HR range 42 - 186 beats/min) and compared to those simultaneously determined by the dye-dilution technique or measured with an electromagnetic flowmeter. The overall correlation coefficient for the mean flow comparisons was 0.97, the regression line was  $y = 1.00x + 0.19$  ml/sec and the standard error of estimate was  $\pm 12\%$  (see Figure 21). These results are better than any that have previously been reported for

a pressure-based method (see below).

A secondary objective has been to record the instantaneous flow pattern in the vessel rather than aim only to derive stroke volume. Other simple methods have been reported that do this reasonably well, though there is some question of their reliability over a wide range of circulatory conditions. A record of the actual flow pattern would enable one to derive additional information on the power output of the heart. This parameter is much more likely to indicate changes in the functional state of the cardiac muscle than measurement of stroke volume alone would. The prediction of the flow pattern in this investigation (see Tables 10 and 11) was not as successful as the mean flow results; for the overall peak flow comparisons  $r = 0.91$ ,  $y = 0.85x + 13.2$  ml/sec, S.E.E. =  $\pm 17\%$  (Figure 35). They were, however, almost as good as the results from other pressure-gradient methods which have been reported (e.g. Greenfield et al., 1962, and Greenfield and Fry, 1965 - see below).

For the measurement of beat-by-beat heart output, most workers have used the Fry simplification (Fry et al., 1956; Fry et al., 1957, and Fry, 1959) of the pressure-gradient equation of Womersley or, more commonly, the substitution of his formulation for the pressure-gradient using the time-derivative of the pressure. The first paper to introduce this latter and to avoid the use of a second pressure channel by using a calibration constant determined by comparison with another method (in this case dye-dilution) was that of Jones et al. (1959). In a series of 8 dogs, the cardiac

output was varied by changing the left atrial pressure with a reservoir of adjustable height. Also, in 6 dogs, the cardiovascular status was further varied by infusions of first epinephrine and then methoxamine, although they did not quote doses used, nor the number of values derived from these interventions. The range of output varied up to three or four times the minimum in individual dogs; ranges of mean arterial pressure and heart rate were not reported though they were stated to vary widely. The overall correlation coefficient was 0.97 ( $N = 67$ ) with a regression line of  $y = 1.1x - 0.75$  ml/sec; the range of correlation coefficients in the individual dogs was 0.85 – 0.99. The standard error of estimate was not reported. These are the best values previously reported for a pressure-based method for measurement of cardiac output or stroke volume. In view of their methods for altering cardiac output, we can compare their results with the correlation coefficients for similar interventions in the present study, for example, controls (0.96), dextran infusion (0.88), hemorrhage (0.93), epinephrine infusion (0.93), and possibly the predominant changes in rate induced by pacing (0.89) and vagal stimulation (0.96)(see Table 9).

A later paper by Jones and Griffin (1962) compared stroke volume measured by the same technique with the flow measured with an electromagnetic flowmeter. They altered the cardiovascular system by hemorrhage, transfusion, and the administration of methoxamine and nitroglycerine. The statistical results were:  $r = 0.93$ ,  $y = 0.90x + 9.2$  ml/sec; S.D. =  $\pm 13.2$  ( $N = 350$ , 5 dogs).

The correlation coefficient and the slope of the regression line are considerably less than those obtained in the entire series of our study.

Another more recent comparison of this method against dye-dilution is that of Boyett et al. (1966). Changes in output were produced by hemorrhage and amyl nitrite. In 5 dogs, the overall correlation coefficient for cardiac output was 0.92 ( $N = 61$ ) (range 0.74 - 0.97) and the regression line was  $y = 1.029x - 0.9$  ml/sec. The 95% confidence limits were shown, but not enumerated, and appear to be much larger than our own (Figure 21). Again, our statistical data for hemorrhage,  $r = 0.93$  ( $N = 114$ ),  $y = 1.03x - 0.45$  ml/sec, are better than those reported by Boyett (see Table 9).

Another method for estimating stroke volume from a single pressure recording in the dog was recently reported by Kouchoukos et al. (1970). The stroke volume was derived from the systolic area of the central aortic pressure and was tested in 12 dogs. The formula used was  $S.V. = K \cdot P_{sa} (1 + T_s/T_d)$  where  $P_{sa}$  is the area under the systolic part of the curve above end-diastolic pressure,  $T_s$  and  $T_d$  are the durations of systole and diastole respectively, and  $K$  is an arbitrary constant derived from measurement of an initial stroke volume by the electromagnetic flowmeter in each dog and used thereafter without change, in that dog. In the 12 dogs, 541 simultaneous determinations of stroke volume by the pressure contour and electromagnetic flowmeter methods were compared under normal and altered circulatory conditions employing 12 different

interventions. The total range of stroke volume was 2.4 - 28.1 ml, of heart rate 35 - 207 beats/min, and of the mean arterial pressure 24 - 166 mmHg. The overall correlation coefficient was 0.93 with a regression line  $y = 1.04x + 0.21$  ml (standard error of estimate  $\pm 17\%$ ). They obtained excellent correlation coefficients (0.93 - 0.99) with all interventions except the infusion of isoproterenol (0.70, S.E.E. =  $\pm 17\%$ , N = 38), metaraminol (0.77, S.E.E. =  $\pm 13\%$ , N = 56), and norepinephrine (0.79, S.E.E. =  $\pm 13\%$ , N = 21) showing that the method becomes very unreliable with vasoactive drugs. These results are not as good as those obtained by us using the more complex pressure-gradient method (see Table 9).

Peak flows were determined in the descending thoracic aorta by Greenfield et al. (1962) and Greenfield and Fry (1965) using the pressure-gradient and time-derivative (with an assumed constant wave velocity) techniques introduced by Fry. Their results were compared to those simultaneously measured with an electromagnetic flowmeter. The study of Greenfield et al. (1962) included 10 dogs (N = 25 for each dog). Both flow and pressure were varied by infusing the dog with isoproterenol and methoxamine, and by producing anoxia and acute hemorrhage. The correlation coefficient ranged from 0.91 to 0.98 in individual dogs and the regression line from  $y = 0.84x + 9.6$  ml/sec to  $y = 1.64x - 17.6$  ml/sec (S.E.E. range  $\pm 2.4$  to  $\pm 9.0\%$ ).

In the other study (i.e. Greenfield and Fry, 1965) 130 determinations of peak flow were collected from 6 dogs. During the

study, both blood flow and pressure were varied widely by infusions of blood, isoproterenol, methoxamine and by acute hemorrhage. They obtained a correlation coefficient which ranged from 0.91 to 0.98 and a regression line which ranged from  $y = 0.80x + 11.6$  ml/sec to  $y = 1.43x - 9.1$  ml/sec (S.E.E. range  $\pm 6.2$  to  $\pm 17.0\%$ ). The standard error of estimate (S.E.E.) is one of the most important statistical variables that can be measured because it gives an indication of the amount of scatter in the data. The correlation coefficient and the regression line can be very good and yet the data may have a great deal of scatter (i.e. a large S.E.E.). This variable is excluded from many scientific publications.

The three methods mentioned above have been successfully used in patients (e.g. Jones et al., 1966; Kouchoukos et al., 1969, and Barnett et al., 1961) but the results from these studies will not be compared to our results since ours were obtained from dogs.

The comparative methods for measurement of stroke volume and cardiac output were checked in our own laboratory in order to see what errors are inevitable. In experiments which have not been separately reported in five dogs, Kerr and Kouchoukos found a correlation between duplicate simultaneous dye-dilution (cardiogreen) measurements, i.e. calculated from samples withdrawn from different sites following a single injection, that gave  $r = 0.99$ ,  $y = 0.94x + 88.0$  ml/min with S.E.E. =  $\pm 7\%$  ( $N = 60$ ). They then found that dye-dilution cardiac output compared with the electromagnetic flowmeter in five dogs gave  $r = 0.98$ ,  $y = 0.92x + 182$  ml/min with S.E.E. =

$\pm 10\%$  ( $N = 31$ ). In these experiments the cardiac output by dye-dilution ranged from 0.5 - 5.0 liters/min. Variations in stroke volume in steady state conditions are rarely below  $\pm 8 - 10\%$  (S.E.E.) (McDonald, personal communication). The overall series comparing the pressure-gradient method (mean flow) with the electromagnetic flowmeter has a variability ( $\pm 12\%$ ) which is slightly higher than this (Table 7) but clinically a change in stroke volume of less than 15-20% might not be regarded as significant. The reliability of the other method with which comparison is made is impossible to assess because standard errors are rarely quoted, or else given in terms which cannot with any certainty be converted to 95% confidence limits.

Even though the results presented here are very good, it is necessary to try to assess the possible causes of error to see how the accuracy might be improved.

Effect of no flow probe and a small interval (3 cm) between the two pressure taps.

When the computed mean flow (pressure-gradient method) was compared to the measured mean flow (dye-dilution method), considerable scatter was seen in the data (S.E.E. =  $\pm 19.9\%$ ) (see Figure 20 and Table 7). There are two possible causes for this discrepancy.

(a) The two pressure curves from this group of experiments were hand digitized and punched on IBM cards for analysis. It is possible that during digitization some of the ordinate values were misread,



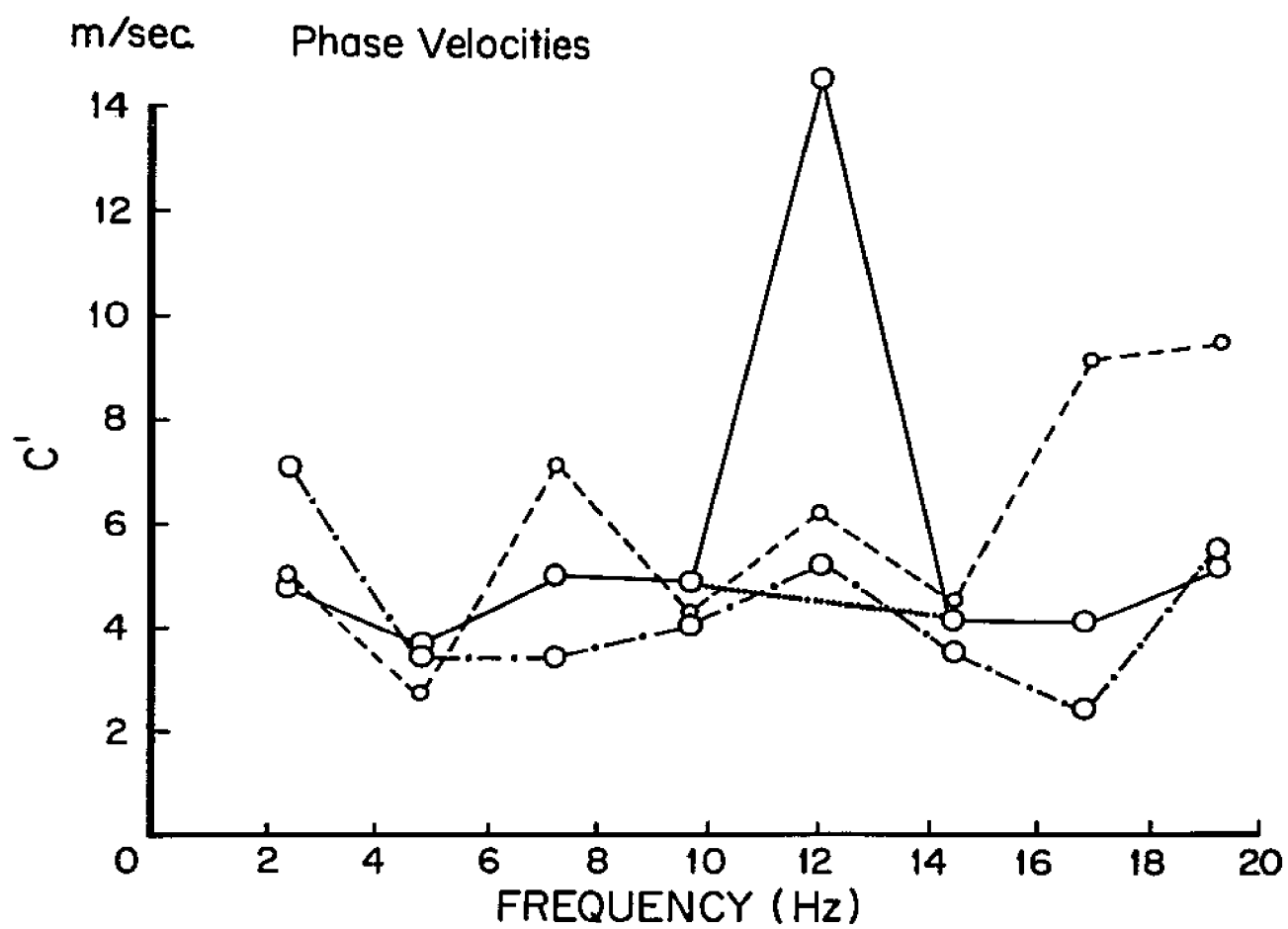
thereby introducing errors in the computed mean flows. (b) In four of the experiments of this group, the interval between the two pressure taps was 3 cm. When an interval this small is used, the phase shift ( $\Delta\phi$ ) between the lower frequency harmonic components of the pressures is very small and its measurement may be beyond the resolution of the A-D converters. This would cause considerable scatter in the apparent phase-velocities (see Figure 36); in fact, some of the phase-velocities from this group were negative. This would produce errors in the computed flow moduli and subsequently in the computed mean flow. Three different intervals (3, 4, and 5 cm) were tried in this group of experiments to determine which would produce the least amount of scatter in the apparent phase-velocities and still predict the flow accurately. The least amount of scatter in the phase-velocities was seen when an interval of 5 cm was used (see Figures 2 and 3) even though it probably straddles the brachiocephalic junction. This suggests that reflections at this junction are minimal. Also, there was no significant difference in the phase-velocities when the chest was opened as compared to the velocities when the chest was closed (Nichols and McDonald, 1970).

#### Effect of the flow probe on the pressure contour and the phase-velocity.

Greenfield et al. (1962) noted that the placement of the electromagnetic flow probe on the descending thoracic aorta tended to alter slightly both the contours of pressure pulse and flow

Figure 36

Apparent phase velocities from 3 runs measured in the  
ascending aorta, using an interval of 3 cm between the  
two pressure taps

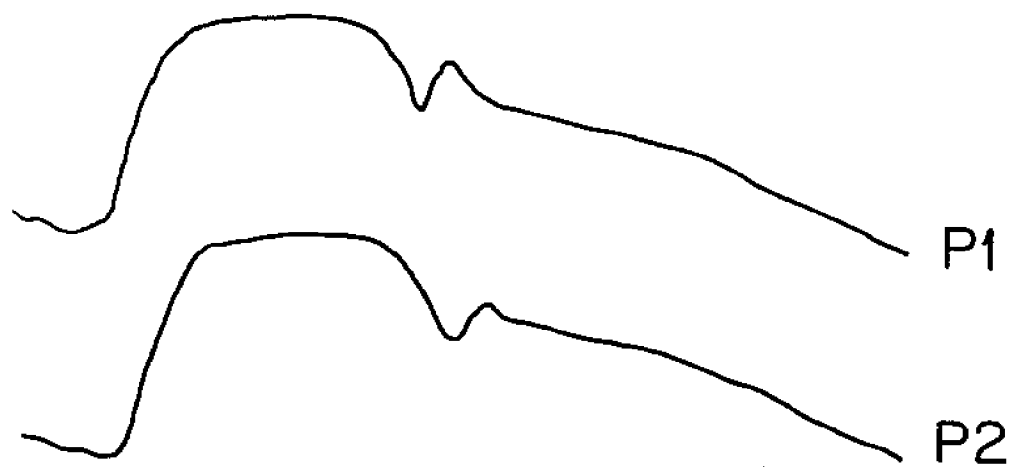


profile 5 cm downstream. They go on to say that this was true even though care was taken in selecting the probe size so that the vessel would not be narrowed more than enough to ensure adequate electrode contact with the vessel wall. If the pressure and flow curves are distorted as a result of splinting the blood vessel by the flow probe, then the average apparent phase velocity will increase and the predicted mean flow will decrease. The change in the average apparent phase-velocity before and after the placement of the electromagnetic flow probe on the ascending aorta was studied in this investigation and has been reported separately (Nichols and McDonald, 1970). We found that the phase-velocity was not significantly altered by the placement of the probe on the vessel. Very little change was seen in the pressure contours ( $P_1$  and  $P_2$ ) before (Figure 37) and after (Figure 38) placement of the flow probe. The effect of the probe on the two pressure curves and the computed flow curve was studied in more detail by examining their moduli and phase. The placement of the probe did not significantly alter the moduli (Figures 39 and 40) or the phase (Figures 41 and 42) of the pressure curves or the moduli of the computed flow curve (Figure 43). The accuracy of the in vivo flow measurement with the electromagnetic flowmeter was checked by Kerr and Kouchoukos in five dogs of the group studied here. They found that dye-dilution cardiac output compared with the electromagnetic flowmeter gave  $r = 0.98$ ,  $y = 0.92x + 3$  ml/sec, with S.E.E. =  $\pm 10\%$  ( $N = 31$ ). These results have not yet been published separately but are mentioned

Figure 37

The two pressures ( $P_1$  and  $P_2$ ) recorded in the ascending aorta before placement of the flow probe

The interval between the two pressure taps was 5 cm.

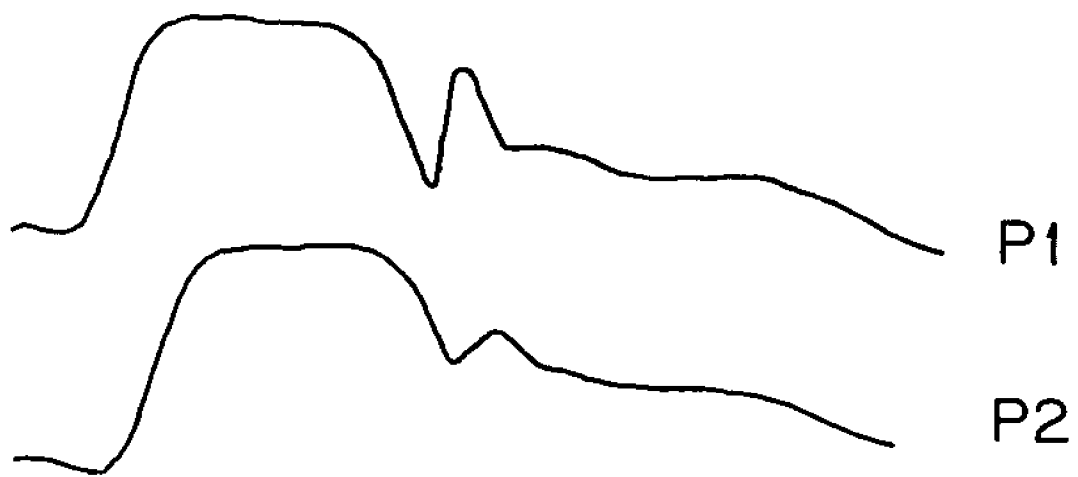


BEFORE PLACEMENT OF FLOW PROBE

Figure 38

The two pressures ( $P_1$  and  $P_2$ ) recorded in the ascending aorta after placement of the flow probe.

The interval between the two pressure taps was 5 cm.



AFTER PLACEMENT OF FLOW PROBE



## Figure 39

Moduli of pressure number 1 recorded in the ascending aorta before and after placement of the flow probe

These moduli were computed from the Fourier series expansion of the pressure curve ( $P_1$ ) in Figures 37 and 38.

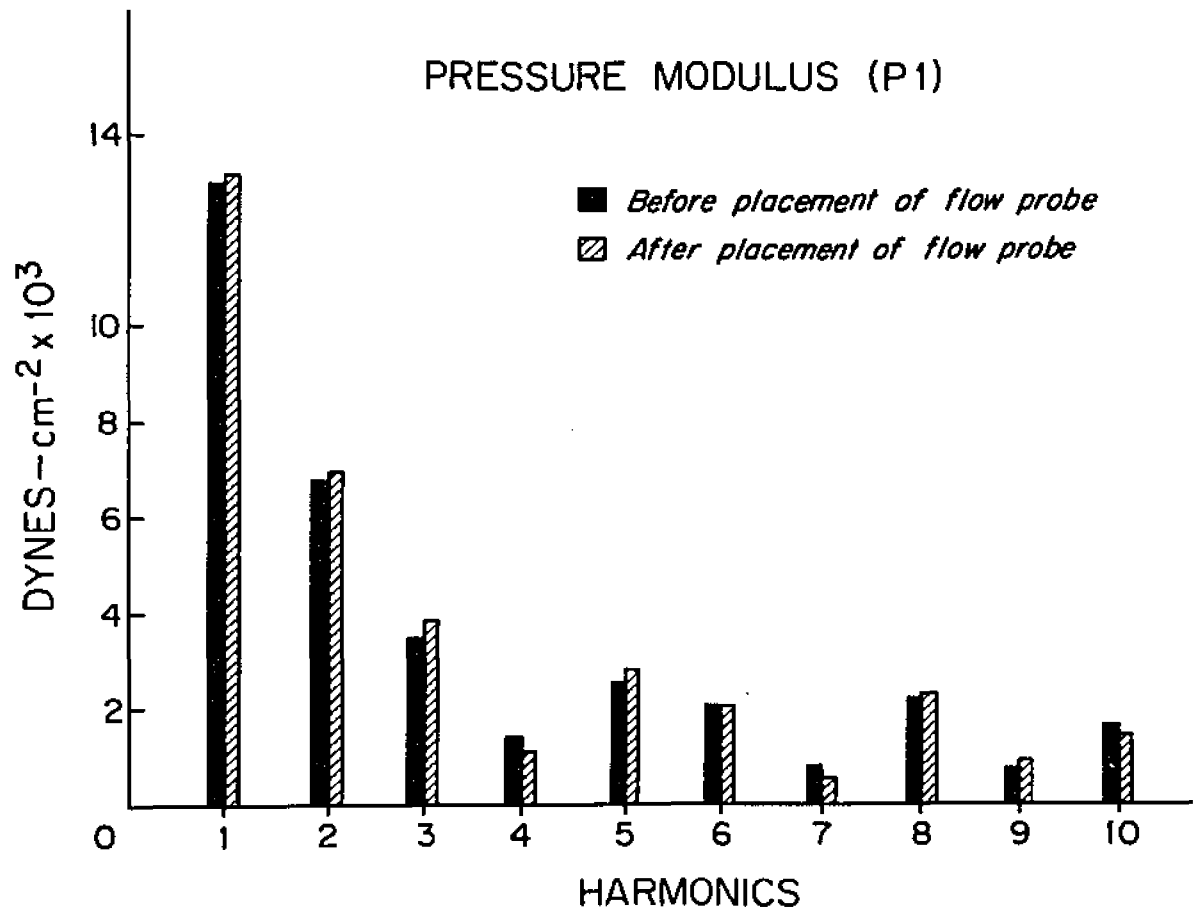
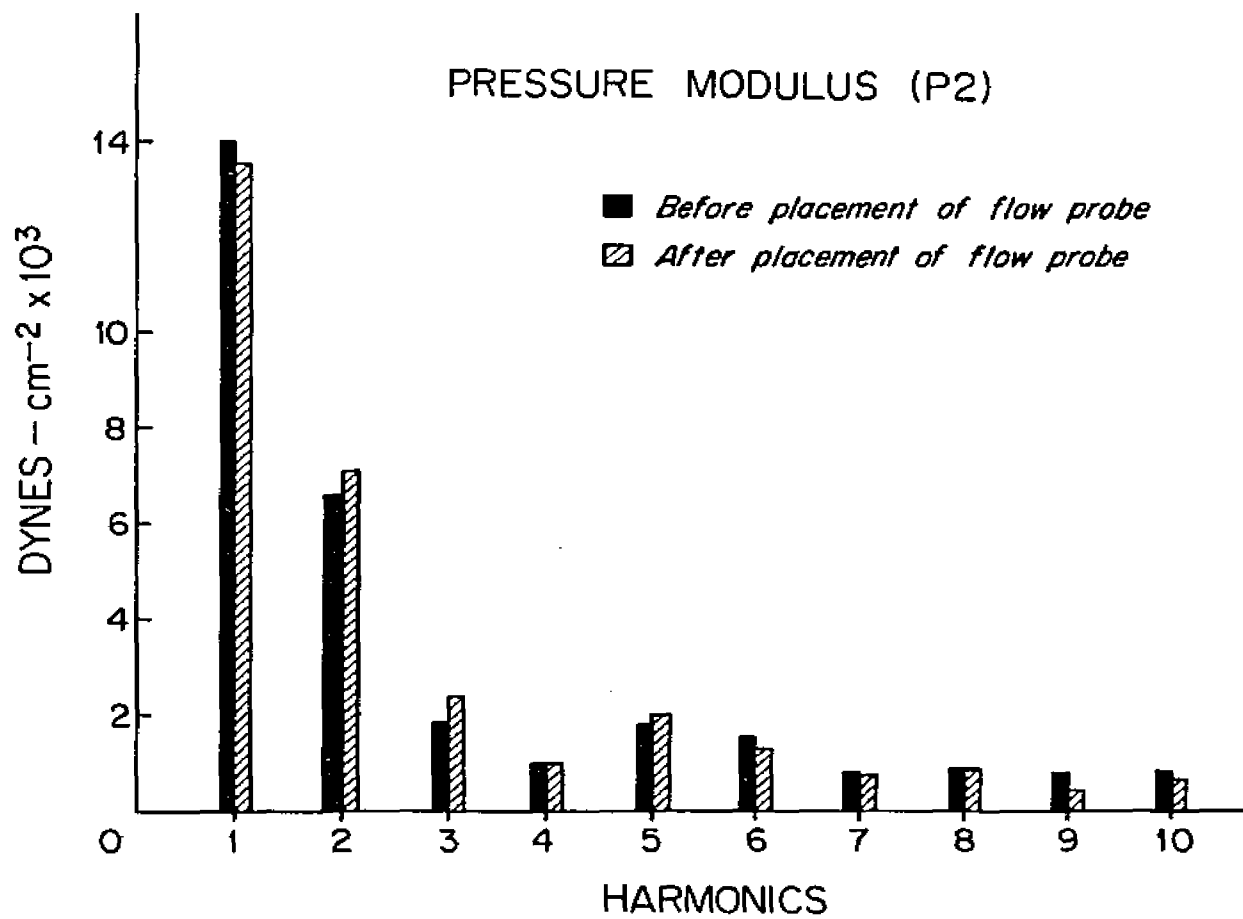


Figure 40

Moduli of pressure number 2 recorded in the ascending aorta before and after placement of the flow probe

These moduli were computed from the Fourier series expansion of the pressure curves ( $P_2$ ) in Figures 37 and 38.



## Figure 41

Phase angles of pressure number 1 recorded in the  
ascending aorta before and after placement of the  
flow probe

These phase angles were computed from the Fourier series expansion  
of the pressure curves ( $P_1$ ) in Figures 37 and 38.

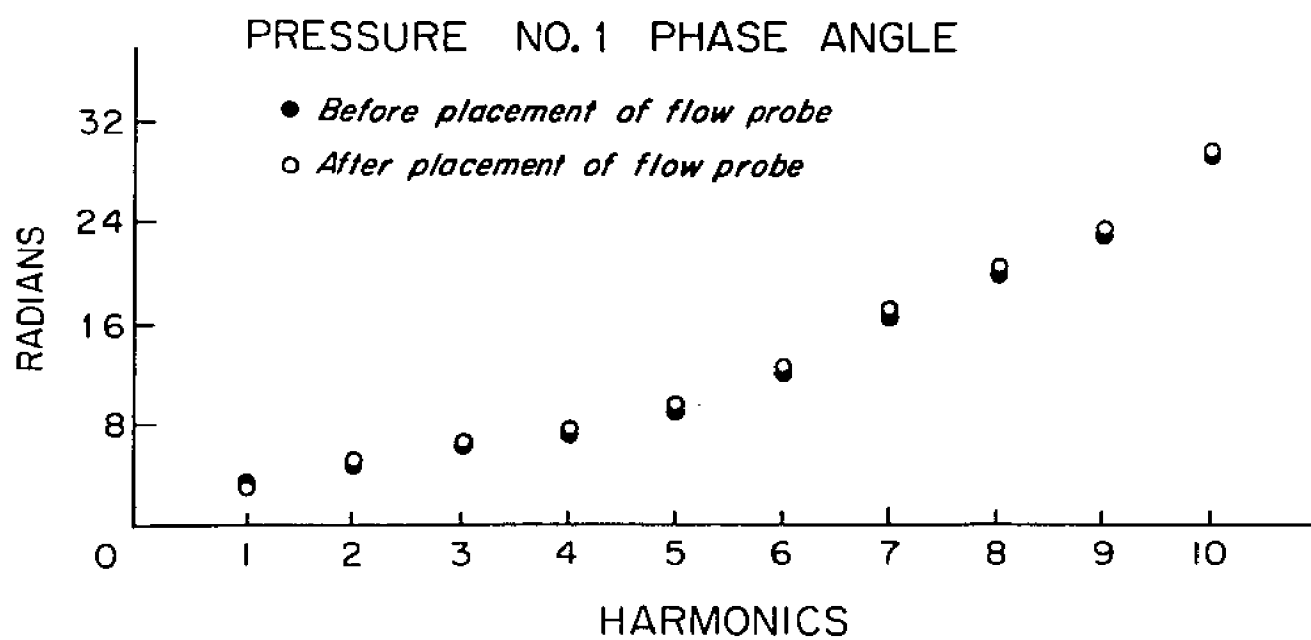
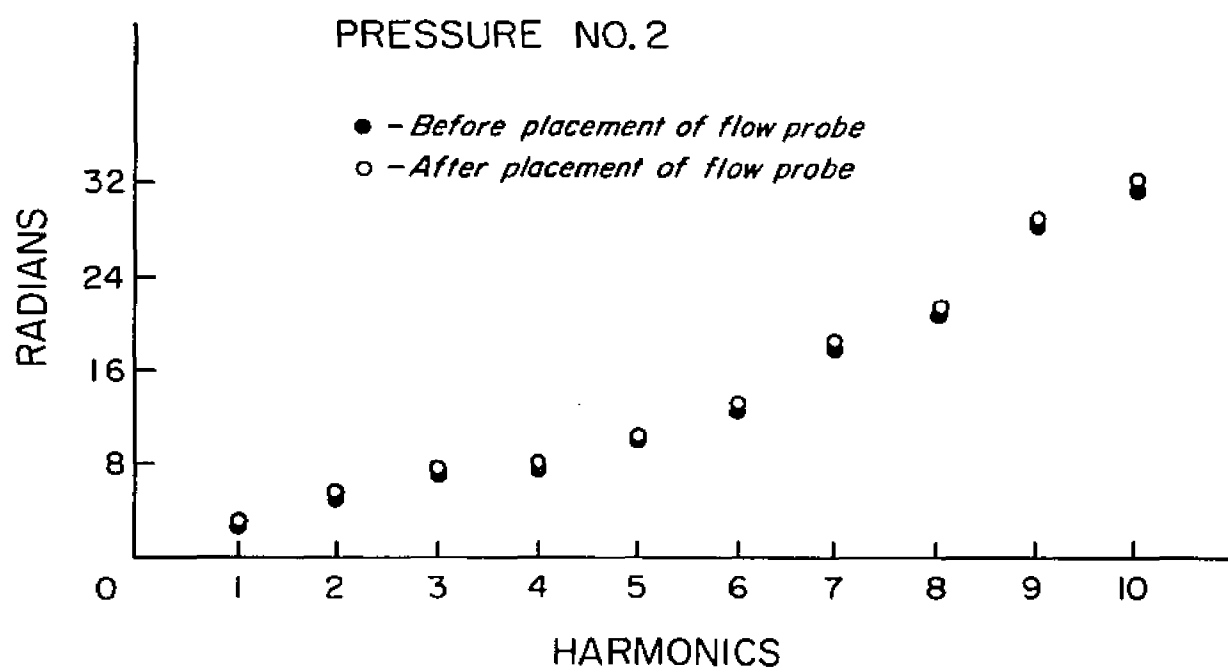


Figure 42

Phase angles of pressure number 2 recorded in the  
ascending aorta before and after placement of the  
flow probe

These phase angles were computed from the Fourier series expansion  
of the pressure curves ( $P_2$ ) in Figures 37 and 38.



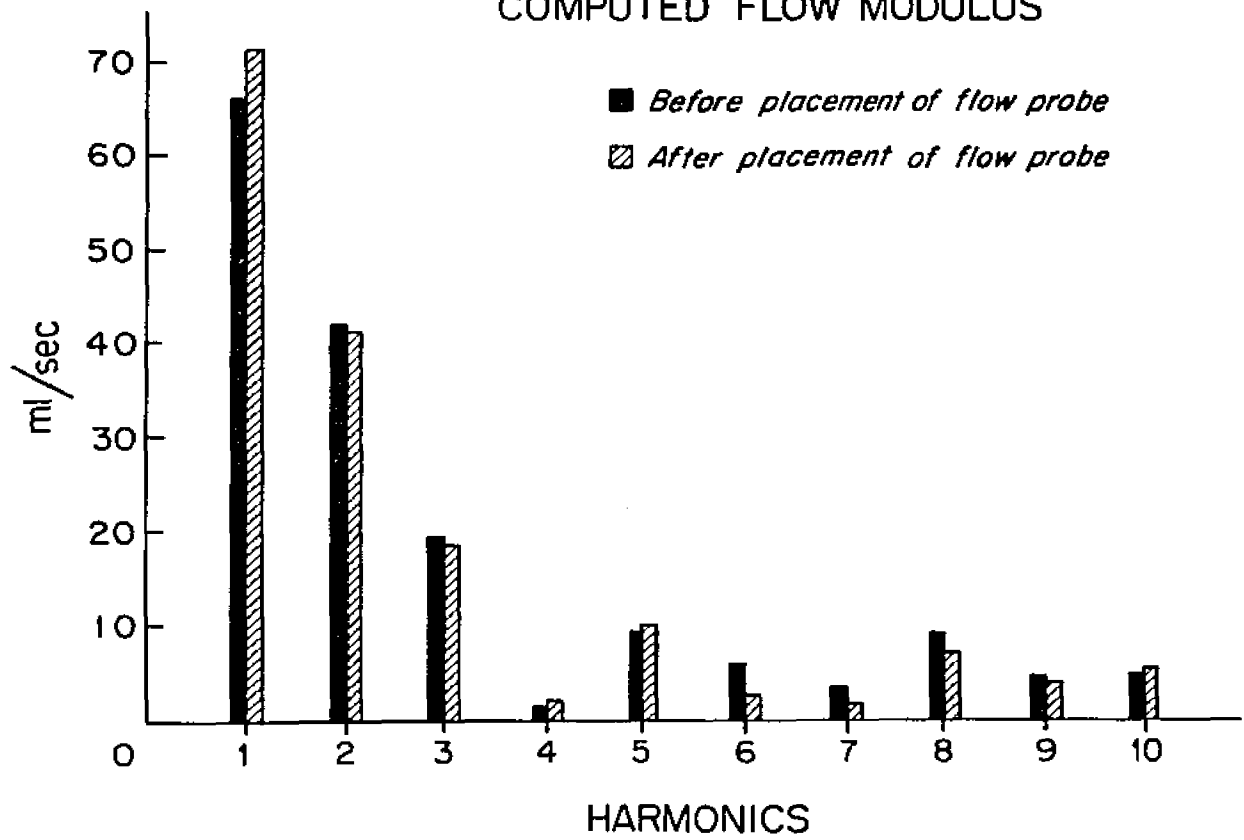


## Figure 43

Computed flow moduli before and after placement of  
the flow probe

These moduli were computed from the pressures recorded in Figures 37 and 38 using the pressure-gradient technique. The computed mean flow was 22.7 ml/sec before placement of probe and 23.0 ml/sec after placement of the probe. The measured mean flow was 23.2 ml/sec.

# COMPUTED FLOW MODULUS



in the publication by Kouckoukos et al. (1970).

Accuracy of the Fourier Series fit to the pressure and flow curves.

The accuracy of fit of the Fourier series to the pressure and flow curves was estimated by comparing the variance of the curve to the sum of the squares of the moduli of the harmonic components (equations 29 and 30). The variance of a curve is a measure of its energy content and it can be seen from Table 5 and Figures 10, 11, 12, 13, and 19 that 10 harmonic terms always give a good measure of the curve and that the first two components account for at least 70 percent (Table 5 and Figures 10, 11, and 12). The Fourier series was extended to 20 harmonics and the sampling rate was changed from 100 samples per second to 200 samples per second in one experiment. It was found that this did not increase the accuracy of the fit significantly as expressed by the sum of variance (from 99.8 to 99.9%) (Table 5 and Figure 12); it only increased the computing time. The dominance of the first two harmonics is also marked in the detailed analyses of Randall (1958) where a long series of waves have been analysed by a digital computer. Porjé (1946) also found that over 90 percent of the variance, of three harmonics that he measured, was determined by the first two components. For a low pulse-frequency a greater number of harmonics is needed to obtain the same accuracy as in a pulse-wave with a higher fundamental frequency (see Table 5 and Figures 10 and 11).

Individual faulty experiments.

Post-mortem observations in experiments 29 and 34 revealed that the tip of the catheter used to measure pressure no.1 had hit the aortic valve and doubled back making the interval smaller between the two pressure taps (approximately 2.5 cm). This would account for the poor slopes and intercepts in the mean flow comparisons of these two experiments (see Table 7).

Possible causes of scatter in the computed mean flow at high stroke outputs.

There are two possible causes for the scatter in the data at large stroke outputs (see Figures 21 and 27 and Table 9). (1) At large stroke outputs there is a possibility that turbulent flow may occur for a very short time (10 to 15 msec) just after peak velocity is reached (McDonald, 1960). If this does occur, then the pressure-gradient technique no longer predicts the flow accurately. (2) Also at large flow velocities the kinetic energy component is large as compared to the kinetic energy component at low flow velocities (Berne and Levy, 1967) and since the pressures in most of these experiments were measured end-on the pressure-gradient technique may tend to over-estimate the flow. This cause may be questionable since the catheters usually lie obliquely to the axis of the vessel and the results from "open" or "side" end catheters should be the same. In the presence of vortices shed

from the aortic valves the precise definition of end- or side-pressure is very difficult to make.

Possible causes of errors in the computed mean flow during the infusion of metaraminol and glucagon.

As mentioned earlier under Methods, the correlation coefficients during the infusion of metaraminol and glucagon were relatively poor (0.82) even though the mean flow comparisons were good (see Table 9). The reason for these discrepancies may be explained as follows: as mentioned earlier, the data collected from experiment 29 were very poor because of the small interval between the two pressure taps and these data are included in the metaraminol group. Glucagon was administered in only one animal (N = 25). In this particular animal, all the computed mean flows (including the controls) were lower than those measured with the electromagnetic flowmeter. Apparently the flow probe was too tight on the ascending aorta causing abnormally high phase velocities which would in turn cause an under-estimation of the actual flow.

Possible causes of errors in the computed peak flow.

The time derivative method predicts the mean flows very well but often introduces some distortions in the wave form resulting in an under-estimation of the peak flow. The peak flow comparisons were very good under control conditions (see Figure 32) but when

certain interventions were introduced (especially vagal stimulation) the computed peak flows were approximately 25 percent lower than those measured with the electromagnetic flowmeter (see Figure 33 and Tables 10 and 11). This was attributed to the fact that while the time derivative method predicts the modulus of the flow fairly accurately (see Figures 22, 23, and 24), it cannot derive the phase and so distortions in the synthesized flow curve appear. In essence, when we are relating flow to pressure, we are attempting to measure the fluid impedance which is a complex quantity, i.e. is expressed in terms of modulus and phase. As we are taking the velocity as wholly real this only enables us to measure the modulus of the impedance. It has been shown above (Figures 22, 23, and 24) that modulus is well predicted. The phase, however, remains that of the longitudinal impedance ( $\epsilon$ ) whereas the input impedance has a markedly negative value at low frequencies (Figure 44).

Figure 45 shows a flow curve synthesized from the computed moduli and the computed phase (solid curve) during vagal stimulation (pulse frequency 1.5 Hz). This curve was then compared to the flow curve synthesized from the computed moduli and the measured phase (i.e. the phase derived from the Fourier series expansion of the flow curve measured with the electromagnetic flowmeter) (broken curve). Some distortion is still seen in the curve during diastole, but the peak flow has improved to the point where it almost completely matches the measured peak flow (Figure 46). The phase correction did not change the computed mean flow. The discrepancies

Figure 44

Modulus and phase of the input impedance in the dog  
ascending aorta under control conditions and during  
vagal stimulation

When the phase is negative, the flow leads the pressure and  
when it is positive, the pressure leads the flow.

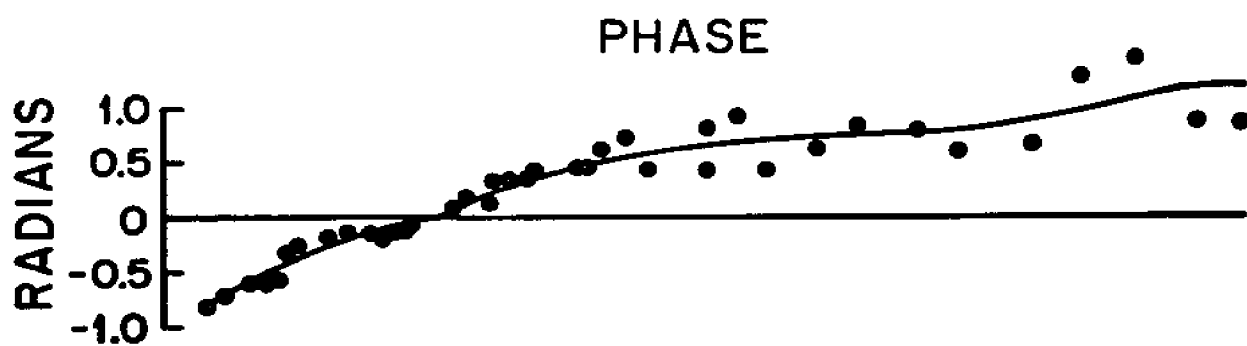
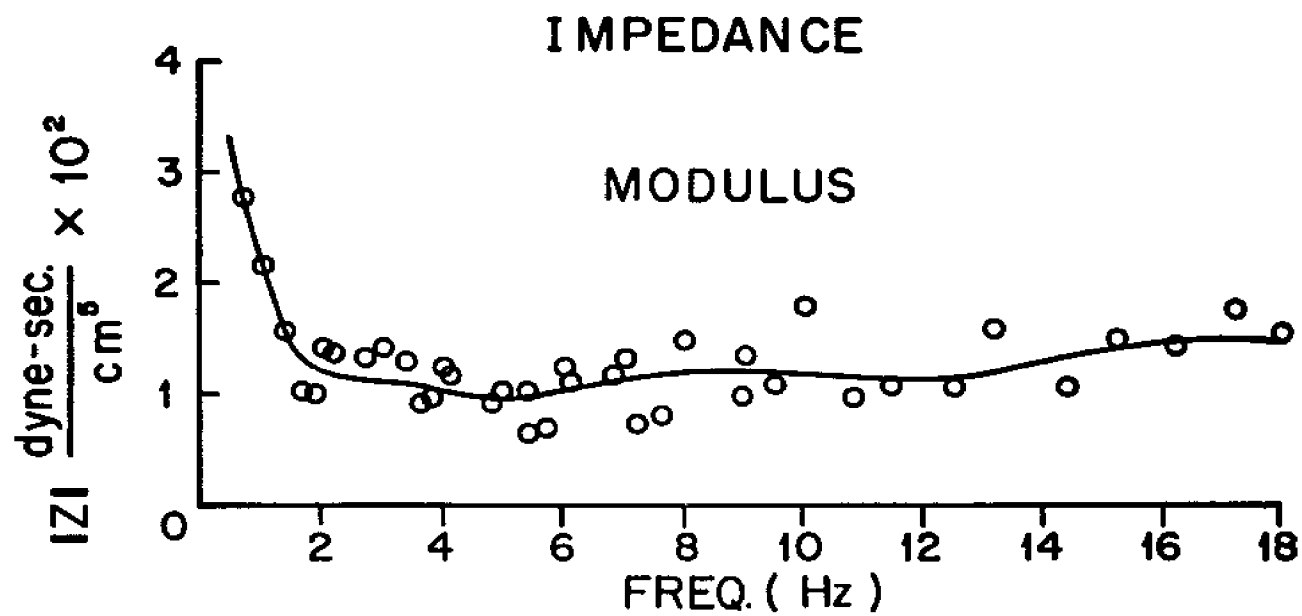




Figure 45

A flow curve computed using the pressure-gradient technique during vagal stimulation before and after a phase correction

The solid curve was synthesized from the computed moduli and the computed phase and the broken curve was synthesized from the computed moduli and the phase derived from the Fourier series expansion of the flow measured with the electromagnetic flowmeter. The broken line represents the computed mean flow.

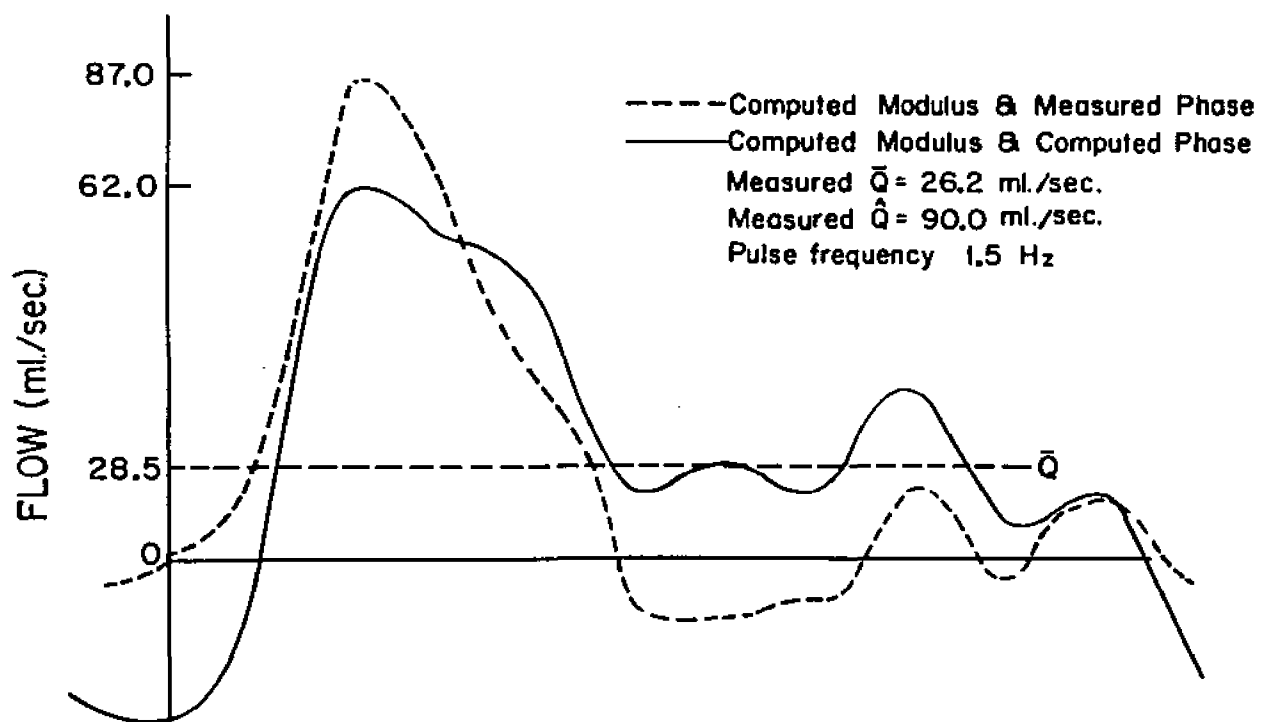
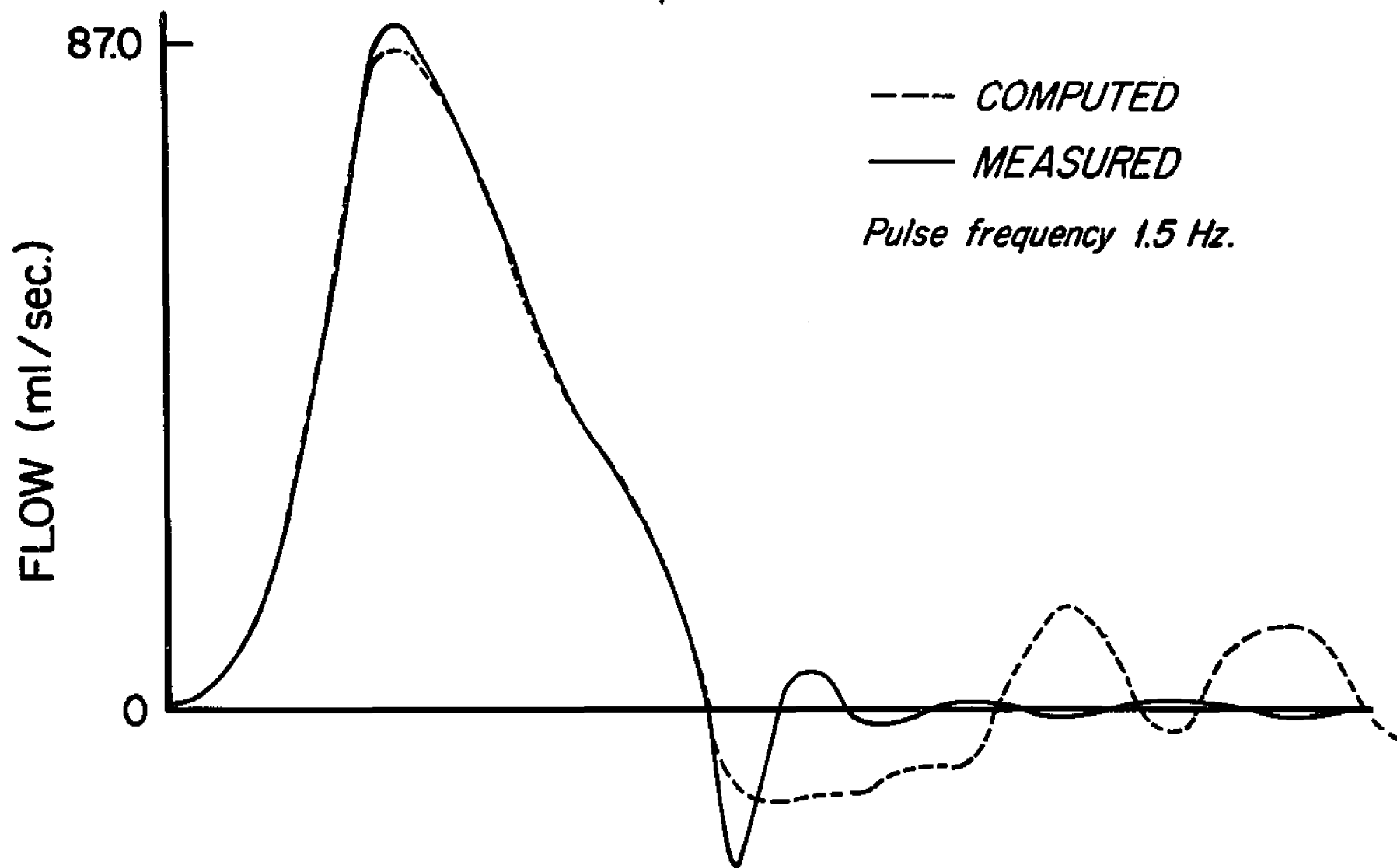


Figure 46

The computed flow curve after a phase correction  
compared to the flow curve measured with the electro-  
magnetic flowmeter

The computed flow curve is the same one as seen in Figure 45.



in diastole are almost certainly due to measurement errors in the higher harmonics because of their small amplitude.

Validity of the Womersley equations when applied to the arterial system.

In a method studied primarily for its practical applications the causes of experimental error, discussed above, may be regarded as the most important. Nevertheless, it is also necessary to discuss the theoretical implications of the hydrodynamic analysis.

The validity of any mathematical derivation of flow from the pressure must be based upon certain basic assumptions. The validity of the Womersley equations when applied to the arterial system has been discussed in detail by McDonald and Taylor (1959), McDonald (1960), and Fry and Greenfield (1964). The physical assumptions made by Womersley were:

(1) That the flow is laminar. For oscillating flow in a large artery (i.e. for values of  $\alpha$  found in the ascending aorta of the dog) the velocity profile is almost flat across most of the lumen (Hale et al., 1955), and the inertial component is large compared with the viscous component. In this study the velocity profiles were calculated using the velocity equation derived by Womersley (1955a) (see equation 46). The predictions of the velocity profile made by Womersley have recently been verified experimentally by Schultz et al. (1969) in dogs and in humans. To measure the velocity profile, they used a hot film probe which could be moved across the

lumen of the ascending aorta. At high flow rates in large arteries there is a possibility that a transient breakdown of laminar flow may occur just after peak velocity is reached but does not persist for more than 10 or 15 msec. This may be one reason why considerable scatter is seen in the data at large stroke outputs (see Figures 21 and 27 and Table 9).

(2) That blood is an incompressible, Newtonian fluid. A fluid is said to be Newtonian if the ratio of the applied stress to the rate of shearing is constant (Whitmore, 1968). At high shear rates such as those found in the aorta the above ratio (the viscosity) is relatively constant and does not present a problem in the derivation of flow from the pressure.

(3) That the radius of the tube does not vary, for example, with changes of pressure. Womersley investigated oscillatory flows in a rigid tube (1955a), in a free elastic tube (1955c) and in a constrained elastic tube (1957). He found very little difference in the computed flow curves from these three different models. This investigation showed no significant difference in the computed flows before and after the placement of a flow probe.

(4) That flow may be expressed as a sum of the harmonic components derived from the corresponding individual harmonic terms of the pressure-gradient (i.e. the system if linear). With an elastic tube this is not strictly true and there is some interaction between the harmonic components of the flow. It has been shown by Attinger et al. (1966), Dick et al. (1968), Nichols and McDonald

(1969), and Nichols and McDonald (1970) that these interactions are very small and the system deviates very little from linearity.

(5) That the liquid does not slip at the walls. This was the assumption that  $V = 0$  when  $r = R$  which was made in evaluating the constant of integration in equation (42). This condition is held to be universally true for liquids and has been discussed in detail by Goldstein (1938a).

(6) That the tube is long compared with the region being studied. This is the "inlet length" problem and has been discussed in detail by Goldstein (1938b) and McDonald (1960). It was pointed out by them that within the inlet length the bulk of the fluid in the center of a tube will move as a mass, affected very little by the force of viscosity, and will have a flat velocity profile. McDonald (1960) also pointed out that the inlet length is probably short with oscillating flow.

## SUMMARY

A method for computing the phasic flow pattern from the pressure-gradient in the ascending aorta of 39 dogs and one pig has been presented. Since the pressure-gradient is very difficult to measure accurately within the limits of the ascending aorta, it was derived from the relation

$$\frac{dP}{dt} = \frac{dt}{dz} \cdot \frac{dP}{dt} = \frac{1}{c'} \frac{dP}{dt}$$

where  $dP/dt$  is the time derivative of the leading pressure ( $P_1$ ) and  $c'$  is the apparent phase velocity derived from the measured phase shift ( $\Delta\phi$ ) between the two pressures ( $P_1$  and  $P_2$ ) for each harmonic component ( $N = 10$ ). This velocity is not only dependent upon the elastic properties of the vessel wall but is modified by the presence of reflected waves, especially at slow heart rates (below approximately 120 beats/min).

Mean flows ( $N = 720$ ) and peak flows ( $N = 573$ ) were collected and compared with those obtained from dye-dilution and an electromagnetic flowmeter. Both flow (mean flow range 4.5 - 64.6 ml/sec; peak flow range 32 - 266 ml/sec) and pressure (MAP 25 - 150 mmHg) were varied by infusion of dextran, epinephrine, norepinephrine, isoproterenol, metaraminol and glucagon, and by producing acute hemorrhage and recovery from aortic constriction. The heart rate



(42 - 186 beats/min) was varied by vagal stimulation and electronic pacing. Under the conditions of this experiment, correlation of mean flow measured by dye-dilution and the electromagnetic flowmeter with that obtained by the pressure time derivative method (for the overall series  $r = 0.97$ ,  $y = 1.00x + 0.19$  ml/sec and S.E.E. =  $\pm 12\%$ ) is better than any that has previously been reported for a pressure-based method. There are two possible reasons why our results were better.

(1) The pressure-gradient in the dog ascending aorta oscillates between approximately  $\pm 3$  mmHg and in order to measure it accurately the calibration matching of the two pressure manometers must be extremely accurate. A small error in the measurement of the pressure-gradient will cause the computed flow to be in error.

(2) If the time derivative is used to derive the pressure-gradient then the pulse wave velocity must be determined for each harmonic (i.e. the phase-velocity) and cannot be considered constant unless the heart rate is above approximately 120 beats/min. Even above 120 beats/min the phase velocity is not completely constant because there is still a small amount of interaction with reflected waves. The reason the results are as good as they are from the studies that assume a constant wave velocity is that all the dogs studied had a heart rate above 110 beats/min.

The predicted flow moduli from this method compared very well with those derived from the Fourier series expansion of the measured flow curve.

This method did not predict the peak flow (for the overall series  $r = 0.91$ ,  $y = 0.85x + 13.2$  ml/sec, S.E.E.  $\pm 17\%$ ) as successfully as it did the mean flow but the results were at least almost as good as those previously reported. We found that the accuracy of the peak flow predictions could be increased by making a correction in the computed phase angle of the flow.

## APPENDIX

### 1. Derivation of the Flow Equation

The equation of motion of a liquid through a straight tube of uniform circular section was derived using the method introduced by Lamb in 1879. It proceeds as follows: take a thin cylindrical shell, of thickness,  $\delta r$ , inner radius,  $r$ , and length,  $L$ , oriented symmetrically on the axis,  $z$ , of the tube. The viscous force retarding the motion of the cylindrical shell is

$$\frac{-d}{dr} \left[ \mu \frac{dV}{dr} \cdot 2\pi r L \right] \delta r \dots \dots \dots (31)$$

where  $\mu$  is the coefficient of viscosity,  $\frac{dV}{dr}$  is the velocity gradient, and  $\mu \frac{dV}{dr}$  is the tangential stress across a plane perpendicular to  $r$ . Since the flow is steady the above force must be balanced by the normal pressures on the plane ends of the shell. Since  $\frac{dV}{dz} = 0$ , the difference of the two normal pressures is

$$(P_1 - P_2) 2\pi r \delta r \dots \dots \dots (32)$$

where  $P_1$  and  $P_2$  are the respective pressures at either end of the length,  $L$ . Equating equations (31) and (32) gives

$$\frac{d}{dr} \left[ r \frac{dv}{dr} \right] = - \frac{(P_1 - P_2)}{\mu L} r \quad \dots \dots \dots (33)$$

carrying out the indicated differentiation and dividing through by  $r$  we get

$$\frac{d^2 v}{dr^2} + \frac{1}{r} \frac{dv}{dr} + \frac{(P_1 - P_2)}{\mu L} = 0 \quad \dots \dots \dots (34)$$

This is the equation of motion for steady flow, i.e.  $\frac{P_1 - P_2}{L} =$  constant and  $\frac{dv}{dt} = 0$ . If the pressure-gradient varies in a simple harmonic manner, i.e.

$$\frac{(P_1 - P_2)}{L} = \tilde{A} e^{i\omega t} \quad \dots \dots \dots (35)$$

then equation (34) becomes

$$\frac{\partial^2 v}{\partial r^2} + \frac{1}{r} \frac{\partial v}{\partial r} - \frac{1}{v} \frac{\partial v}{\partial t} = \frac{\tilde{A} e^{i\omega t}}{\mu} \quad \dots \dots \dots (36)$$

where

$\tilde{A} = M (\cos \phi - i \sin \phi)$ ,  $M$  is the modulus of the complex conjugate,  $\tilde{A}$ , and  $\phi$  is its amplitude.  $e^{i\omega t} = \cos \omega t + i \sin \omega t$ .  $v = \frac{\mu}{\rho}$  is the kinematic viscosity and  $\rho$  is the density of the liquid.

If we let

$$v = u e^{i\omega t}$$

where  $u$  is a function of  $r$  alone, and  $y = \frac{r}{R}$  ( $R$  = radius of tube)  
then

$$\frac{\partial V}{\partial y} = \frac{du}{dy} e^{i\omega t}, \quad \frac{\partial^2 V}{\partial y^2} = \frac{d^2 u}{dy^2} e^{i\omega t}$$

and

$$\frac{\partial V}{\partial t} = i\omega u e^{i\omega t}$$

Substituting these values into equation (36) gives

$$e^{i\omega t} \frac{d^2 u}{R^2 dy^2} + \frac{e^{i\omega t}}{Ry} \frac{du}{dy} - \frac{1}{v} i\omega u e^{i\omega t} = \frac{-\tilde{A}}{\mu} e^{i\omega t} \quad \dots \dots \dots (37)$$

If we multiply both sides of equation (37) by  $R^2/e^{i\omega t}$  and replace  
 $-i$  by  $i^3$  we get

$$\frac{d^2 u}{dy^2} + \frac{1}{y} \frac{du}{dy} + i^3 \alpha^2 u = \frac{-\tilde{A}R^2}{\mu} \quad \dots \dots \dots (38)$$

where  $\alpha^2 = R^2 \frac{\omega}{v}$

The general solution (Spiegel, 1958) of equation (38) is of  
the form

$$u = u_c + u_p$$

where  $u_c$  is the complementary solution and satisfies equation (38)  
if  $\frac{-\tilde{A}R^2}{\mu} = 0$  and  $u_p = \frac{-\tilde{A}R^2}{\mu i^3 \alpha^2}$  is the particular solution.

To find  $u_c$  we let

$$\frac{du^2}{dy^2} + \frac{1}{y} \frac{du}{dy} + i^3 \alpha^2 u = 0 \quad \dots \dots \dots (39)$$

The solution to equation (39) is

$$u_c = C_1 J_0 (\alpha y i^{3/2}) + C_2 Y_0 (\alpha y i^{3/2}) \quad \dots \dots \dots (40)$$

where  $C_1$  and  $C_2$  are arbitrary constants and  $J_0$  and  $Y_0$  are Bessel functions of order zero of the first and second kind respectively (Pipes, 1958) when

$$r = 0, \quad y = 0, \quad \text{and} \quad Y_0(0) = \infty$$

Therefore,  $C_2 = 0$ , so

$$u_c = C_1 J_0 (\alpha y i^{3/2}) \quad \dots \dots \dots (41)$$

and we have for the general solution of (38)

$$u = u_c + u_p = C_1 J_0 (\alpha y i^{3/2}) - \frac{\tilde{A} R^2}{\mu i^3 \alpha^2} \quad \dots \dots \dots (42)$$

when  $r = R$ ,  $u = 0$ , and  $y = 1$ .

Therefore, we have

$$0 = C_1 J_0 (\alpha i^{3/2}) - \frac{\tilde{A} R^2}{\mu i^3 \alpha^2} \quad \dots \dots \dots (43)$$

or

$$C_1 = \frac{\tilde{A}R^2}{\mu i^3 \alpha^2 J_0(\alpha i^{3/2})} \dots \dots \dots (44)$$

If we substitute the value for  $C_1$  into equation (42) we get

$$u = \frac{-\tilde{A}R^2}{i^3 \alpha^2} + \frac{\tilde{A}R^2}{\mu i^3 \alpha^2} \frac{J_0(\alpha y i^{3/2})}{J_0(\alpha i^{3/2})} \dots \dots \dots (45)$$

Since  $V = u e^{i\omega t}$  and  $-i = i^3$  we have

$$V = \frac{\tilde{A}R^2}{\mu i \alpha^2} \left[ 1 - \frac{J_0(\alpha y i^{3/2})}{J_0(\alpha i^{3/2})} \right] e^{i\omega t} \dots \dots \dots (46)$$

which is the equation used to compute velocity profiles (McDonald, 1960).

A formula essentially the same as the real part of (46) when  $A$  is real was derived by Lambossy (1952).

To obtain the volume flow ( $Q = \text{ml/sec}$ ) we proceed as follows:

The volume of flow, i.e. the quantity of liquid passing through any cross-section per unit time, is given by (Johnson and Klokemeister, 1962)

$$Q = 2\pi \int_0^R V r dr \dots \dots \dots (47)$$

If we substitute equation (46) into (47) we get

$$Q = \frac{2\pi\tilde{\nu}AR^2e^{i\omega t}}{\mu i\alpha^2} \left[ \int_0^R r dr - \frac{1}{J_0(\alpha i^{3/2})} \int_0^R r J_0\left(\frac{\alpha r i}{R}\right)^{3/2} dr \right] \dots (48)$$

From the properties of Bessel functions (Wiley, 1960)

$$\int_a^b x J_0(x) dx = x J_1(x)$$

Therefore, we have

$$Q = \frac{\pi\tilde{\nu}AR^4}{\mu i\alpha^2} \left[ 1 - \frac{2J_1(\alpha i^{3/2})}{\alpha i^{3/2} J_0(\alpha i^{3/2})} \right] e^{i\omega t} \dots (49)$$

Tables of  $J_0(y i^{3/2})$  are available in the form (McLachlan, 1941)

$$J_0(y i^{3/2}) = M_0(y) e^{i\theta_0(y)}$$

where  $M_0$  and  $\theta_0$  both vary with  $y$ , and by using these we are led to the modulus and phase of the motion. We write

$$J_0(\alpha i^{3/2}) = M_0 e^{i\theta_0} \text{ and } J_1(\alpha i^{3/2}) = M_1 e^{i\theta_1}$$

Then if the real part of  $Ae^{i\omega t}$  is  $M \cos(\omega t - \phi)$  then the corresponding flow is

$$Q = \frac{\pi\tilde{\nu}AR^4M}{\mu\alpha^2} \left[ \sin(\omega t - \phi) - \frac{2M_1}{\alpha M_0} \sin(\omega t - \phi - \delta_{10}) \right] \dots (50)$$



where

$$\delta_{10} = \theta_0 - \theta_1 + 135^\circ$$

Tables of  $M_1$  and  $\theta_1$  are given by McLachlan (1941).

If we let  $\frac{\alpha M_0}{2M} = K$  and define

$$M'_{10} = \frac{1}{K} \left[ \sin^2 \delta_{10} + (K - \cos \delta_{10})^2 \right]^{1/2}$$

and

$$\tan \epsilon_{10} = \frac{\sin \delta_{10}}{K - \cos \delta_{10}}$$

then equation (50) may be written as

$$Q = \frac{\pi R^4 M M'_{10}}{\mu \alpha^2} \sin (\omega t - \phi + \epsilon_{10})$$

This is essentially the same derivation as that of Womersley (1954, 1955), McDonald (1960), and McDonald and Taylor (1959) except that their derivations were a bit more abbreviated than the one presented here.

## 2. A Review of Fourier Series

Let  $f(t)$  be a periodic function, i.e.  $f(t+cT) = f(t)$  where  $T$  is the period and  $c$  is any integer, defined in the interval

$-\frac{T}{2} \leq t \leq \frac{T}{2}$ . If  $f(t)$  has a finite number of points of ordinary discontinuity and a finite number of maxima and minima in the interval  $-\frac{T}{2} \leq t \leq \frac{T}{2}$ , then it can be represented by the series (Sokolnikoff, 1939, and Pipes, 1958).

$$\frac{A_0}{2} + \sum_{n=1}^{\infty} (A_n \cos n\omega t + B_n \sin n\omega t) \dots \dots \dots (52)$$

The coefficient  $\frac{A_0}{2}$  represents the mean value of the function. The magnitude of the coefficients of the higher harmonics usually decreases with frequency so that a given function can be well approximated by only the first few terms of the series. Therefore, the function  $f(t)$  can be represented by a finite number of terms, i.e.

$$\frac{A_0}{2} + \sum_{n=1}^k (A_n \cos n\omega t + B_n \sin n\omega t) \dots \dots \dots (53)$$

where the coefficients  $A_n$  and  $B_n$  are to be selected so as to render the integral

$$I_n = \int_{-T/2}^{T/2} \left[ f(t) - \frac{A_0}{2} - \sum_{n=1}^k (A_n \cos n\omega t + B_n \sin n\omega t) \right]^2 dt \dots (54)$$

a minimum.

Calculating the partial derivatives gives

$$\frac{\partial I_n}{\partial A_0} = \int_{-T/2}^{T/2} \left[ f(t) - \frac{A_0}{2} - \sum_{n=1}^k (A_n \cos n\omega t + B_n \sin n\omega t) \right] dt \dots (55)$$

$$\frac{\partial I_n}{\partial A_n} = -2 \int_{-T/2}^{T/2} \left[ f(t) - \frac{A_0}{2} - \sum_{n=1}^k (A_n \cos n\omega t + B_n \sin n\omega t) \right] \cos n\omega t \, dt, \quad (56)$$

$$\frac{\partial I_n}{\partial B_n} = -2 \int_{-T/2}^{T/2} \left[ f(t) - \frac{A_0}{2} - \sum_{n=1}^k (A_n \cos n\omega t + B_n \sin n\omega t) \right] \sin n\omega t \, dt, \quad (57)$$

But it is known that

$$\int_{-T/2}^{T/2} \cos^2 n\omega t \, dt = T/2, \quad \text{if } n \neq 0; \dots \dots \dots (58)$$

$$\int_{-T/2}^{T/2} \sin n\omega t \cos n\omega t \, dt = 0; \dots \dots \dots (59)$$

$$\int_{-T/2}^{T/2} \sin^2 n\omega t \, dt = T/2, \quad \text{if } n \neq 0; \dots \dots \dots (60)$$

$$\int_{-T/2}^{T/2} \cos n\omega t \, dt = 0; \dots \dots \dots (61)$$

$$\int_{-T/2}^{T/2} \sin n\omega t \, dt = 0; \dots \dots \dots (62)$$

so that carrying out the integrations indicated in (55), (56), and (57) gives

$$\frac{\partial I_n}{\partial A_0} = - \int_{-T/2}^{T/2} f(t) dt + \frac{T}{2} A_0; \quad . . . . . (63)$$

$$\frac{\partial I_n}{\partial A_n} = -2 \int_{-T/2}^{T/2} f(t) \cos n\omega t dt + T A_n; \quad . . . . . (64)$$

$$\frac{\partial I_n}{\partial B_n} = -2 \int_{-T/2}^{T/2} f(t) \sin n\omega t dt + T B_n \quad . . . . . (65)$$

The necessary condition for a minimum of  $I_n$  requires that these derivatives vanish, and this leads to the following values for the coefficients:

$$A_0 = \frac{2}{T} \int_{-T/2}^{T/2} f(t) dt; \quad . . . . . (66)$$

$$A_n = \frac{2}{T} \int_{-T/2}^{T/2} f(t) \cos n\omega t dt; \quad . . . . . (67)$$

$$B_n = \frac{2}{T} \int_{-T/2}^{T/2} f(t) \sin n\omega t dt \quad . . . . . (68)$$

By using the trigonometric identity

$$M_n \cos (n\omega t - \phi_n) = M_n \cos \phi_n \cos n\omega t + M_n \sin \phi_n \sin n\omega t \quad . . . (69)$$

it is possible to combine the sine and cosine series in equation (53)

through letting

$$A_n = M_n \cos \phi_n; \dots \dots \dots (70)$$

and

$$B_n = M_n \sin \phi_n \dots \dots \dots (71)$$

where

$$M_n = \left[ A_n^2 + B_n^2 \right]^{1/2} \dots \dots \dots (72)$$

and

$$\phi_n = \tan^{-1} \frac{B_n}{A_n} \dots \dots \dots (73)$$

The Fourier series can then be written as a sum of cosine terms alone, i.e.

$$f(t) = M_0 + \sum_{n=1}^k M_n \cos (n\omega t - \phi_n) \dots \dots \dots (74)$$

The coefficient  $M_n$  and the angle  $\phi_n$  are, respectively, the modulus and phase angle of the  $n$ th harmonic.  $M_0$  represents the mean value of the function.

By using the Euler identities for sine and cosine, equation (53) can be written as

$$f(t) = \sum_{n=-\infty}^{\infty} \beta_n e^{in\omega t} \dots \dots \dots (75)$$

where

$$\beta_n = \frac{1}{T} \int_{-T/2}^{T/2} f(t) e^{-in\omega t} dt, \dots \dots \dots (76)$$

For a derivation of the complex exponential form see Guillemin (1949).

### 3. The velocity of wave propagation in an elastic tube.

An elastic tube filled with a liquid will propagate a wave. In the case of the circulatory system, the wave is created by the ejection of blood from the heart at a certain velocity which is largely determined by the elastic properties of the vessel wall. Physical conditions such as the viscosity of the blood, the damping of the pulsatile flow and the presence of reflected waves, also change the velocity of wave propagation.

The study of the velocity of wave propagation in an elastic tube is closely related to the physics of sound and was first studied by Newton about 1687. Its application to the physiology of the arterial pulse was first due to Thomas Young (1808, 1809) and is the subject of a historical review by Lambossy (1950).

Newton's equation can be written as

$$c_o = \left[ \frac{E_b}{\rho} \right]^{1/2} \dots \dots \dots (77)$$

where  $\rho$  is the density of the fluid in gm/cm<sup>3</sup> and  $E_b$  is the bulk modulus in dynes/cm<sup>2</sup>. By definition

$$E_b = \frac{\Delta P}{\frac{\Delta V}{V}} \dots \dots \dots (78)$$

where  $P$  is the pressure in dynes/cm<sup>2</sup> and  $V$  is the volume in cm<sup>3</sup>.

If we substitute equation (78) into equation (77) we get

$$C_o = \left[ \frac{V}{\rho} \frac{\Delta P}{\Delta V} \right]^{1/2} \dots \dots \dots (79)$$

which is the same equation derived by Bramwell and Hill (1922) using a different approach.

If the tension is given by  $T = PR$  ( $R$  = radius in cm) then equation (79) becomes

$$C_o = \left[ R \frac{\Delta T - P \Delta R}{2\rho \Delta R} \right]^{1/2} \dots \dots \dots (80)$$

It can be shown (Lambossy, 1950) that

$$V \frac{dP}{dV} = \frac{Eh}{2R} \dots \dots \dots (81)$$

where  $E$  is the elastic modulus in dynes/cm<sup>2</sup> and  $h$  is the wall thickness in centimeters. By substituting equation (81) into equation (79) we get the well-known Moens-Korteweg equation, i.e.

$$C_o = \left[ \frac{Eh}{2\rho R} \right]^{1/2} \dots \dots \dots (82)$$

This simple equation for the velocity of propagation of a pressure pulse is due to Moens (McDonald, 1960) who established it from experimental evidence. The formula derived by Moens had an arbitrary constant ( $K = 0.9$ ) before the parenthesis. The same formula was derived theoretically for a tube of perfectly elastic material at about the same time, and apparently independently, by Korteweg and Resal (McDonald, 1960) without the constant  $K$ .

It can be seen from this equation that the velocity of wave propagation will increase when the elastic modulus of the wall increases and since  $E$  is directly (exponentially) related to the distending pressure the wave velocity is also directly (exponentially) related to the pressure (Bramwell and Hill, 1922; Anliker, 1968).

Equation (82) is only true for a thin-walled vessel, i.e. with  $h$  small compared with  $R$ . It assumes that the fluid is incompressible i.e. that its bulk modulus is high compared with  $E$ , and that it has no viscosity. Also, this velocity is not modified by the presence of reflected waves.

4. The method of calculating an oscillatory flow from the time derivative of the pressure.

The actual calculation of the Fourier terms of a given curve is best given by an example.

If a function is represented by a set of discrete points, i.e.  $F_r = F(r\Delta t)$ ,  $r = 0, 1, \dots, N-1$ , then the coefficients  $A_n$  and  $B_n$  can be calculated numerically as follows (Hamming, 1962):

$$A_n = \frac{2}{N\Delta t} \sum_{r=0}^{N-1} F(r\Delta t) \cos \left[ n \cdot \frac{2\pi}{N\Delta t} \cdot r\Delta t \right] \Delta t \dots \dots \dots (83)$$

$$= \frac{2}{N} \sum_{r=0}^{N-1} F_r \cos \frac{2\pi nr}{N}, \quad n = 0, 1, \dots, M$$

where  $n = \frac{T}{\Delta t}$  is the number of ordinates and  $\Delta t$  is the time interval between consecutive ordinates. Similarly,



$$B_n = \frac{2}{N} \sum_{r=0}^{N-1} F_r \sin \frac{2nr}{N}, \quad n = 1, 2, \dots, M \quad \dots \quad (84)$$

If the two pressures are sampled 24 times throughout the cycle and if each cycle is  $360^\circ$ , then each interval represents  $15^\circ$ .

Therefore, we have from equations (83) and (84) and Table 13

$$\frac{A_0}{2} = \frac{1}{24} \sum_{r=0}^{23} P_r = 91.9 \text{ mmHg},$$

(which is the mean pressure)

$$A_n = \frac{1}{12} \sum_{r=0}^{23} P_r \cos (nr \times 15^\circ),$$

and

$$B_n = \frac{1}{12} \sum_{r=0}^{23} P_r \sin (nr \times 15^\circ).$$

If, for example,  $f = 2.04 \text{ Hz}$ ,  $R = 0.6 \text{ cm}$ ,  $\Delta z = 3.0 \text{ cm}$ ,  $\rho = 1.055 \text{ gm/cm}^3$ , and  $\mu = 0.04 \text{ Poise}$ , then for the first harmonic (i.e.  $n = 1$ ) we have the following (see Appendix 1 and Tables 13, 14, 15, and 16):

$$\alpha_1 = R \left[ \frac{2\pi f \rho}{\mu} \right]^{1/2} = 11.03,$$

$$A_1 = \frac{1}{12} \sum_{r=0}^{23} P_r \cos (r \times 15^\circ) = \frac{-85.14}{12} = -7.10,$$

$$B_1 = \frac{1}{12} \sum_{r=0}^{23} P_r \sin (r \times 15^\circ) = \frac{17.64}{12} = 1.47,$$

$$M_1 = \left[ A_1^2 + B_1^2 \right]^{1/2} = 7.25 \text{ mmHg},$$

Table 13  
 Ordinate Values for the Two Pressures\*

r	$\phi$ degrees	P <sub>1</sub> mmHg	P <sub>2</sub> mmHg
0	0	86.2	82.3
1	15	84.7	80.3
2	30	83.9	80.3
3	45	83.6	79.9
4	60	83.4	79.9
5	75	82.2	77.6
6	90	87.9	79.5
7	105	100.6	91.1
8	120	108.6	102.2
9	135	107.3	104.1
10	150	102.6	101.1
11	165	99.7	98.1
12	180	98.0	95.2
13	195	94.1	92.2
14	210	90.6	90.0
15	225	91.1	89.7
16	240	92.0	89.5
17	255	91.4	88.2
18	270	90.5	87.6
19	285	90.3	88.1
20	300	90.5	88.1
21	315	90.0	86.3
22	330	89.2	84.7
23	345	88.4	84.4

\* These two pressure curves are given in Figure 9

Table 14

Oscillatory Components of Pressure No. 1 for the First Harmonic

r	$\phi$ degrees	$P_1 \cos \theta$ mmHg	$P_1 \sin \theta$ mmHg
0	0	86.1	00.0
1	15	81.8	21.9
2	30	72.6	41.9
3	45	59.1	59.1
4	60	41.7	72.2
5	75	21.2	79.3
6	90	00.0	87.9
7	105	-26.0	97.2
8	120	-54.3	94.0
9	135	-75.8	75.8
10	150	-88.8	51.2
11	165	-96.2	25.8
12	180	-97.9	00.0
13	195	-90.9	-24.3
14	210	-78.4	-45.3
15	225	-64.4	-64.4
16	240	-46.0	-79.7
17	255	-23.6	-88.3
18	270	00.0	-90.4
19	285	23.3	-87.2
20	300	45.2	-78.3
21	315	63.6	-63.6
22	330	77.2	-44.5
23	345	85.3	-22.8

$$\theta = r \times 15^\circ$$

Table 15  
Fourier Components of Pressure No. 1

Harmonic No.	A	B	M (mmHg)	Tan $\phi$	$\phi$ (Radians)
0	91.940				
1	-7.095	1.468	7.25	-0.206	2.93
2	0.317	-5.930	5.94	-18.707	4.78
3	2.640	1.400	2.98	0.530	0.48
4	-1.187	1.050	1.58	-0.885	2.43
5	-1.210	-1.027	1.58	0.850	3.86
6	1.170	-0.333	1.21	-0.285	6.04

Table 16  
Fourier Components of Pressure No. 2

Harmonic No.	A	B	M (mmHg)	Tan $\phi$	$\phi$ (Radians)
0	88.350				
1	-7.966	-0.134	7.97	0.017	3.17
2	1.445	-5.180	6.08	-3.584	5.00
3	1.830	2.260	2.91	1.235	0.90
4	-1.964	0.620	2.10	-0.316	2.84
5	-0.210	-1.547	1.56	7.560	4.59
6	1.810	-0.225	1.20	-0.191	6.10

$$\phi_{1(1)} = \tan^{-1} \frac{B_n}{A_n} = \frac{1.47}{-7.10} = 2.93 \text{ radians},$$

$$\Delta\phi_1 = (\phi_2 - \phi_1)_1 = 0.24 \text{ radians},$$

$$M'_{10(1)} = 1 - \frac{\sqrt{2}}{\alpha_1^2} + \frac{1}{\alpha_1^2} = 0.86,$$

$$\epsilon_{10(1)} = \frac{\sqrt{2}}{\alpha_1} + \frac{1}{\alpha_1^2} + \frac{19}{24\sqrt{2}\alpha_1^3} = .14 \text{ radians},$$

Now,

$$Q_n = \frac{R^2 \Delta\phi_n}{2nf\rho\Delta x} M_n M'_{10} \sin(nr \times 15^\circ + 90^\circ = \phi_n + \epsilon'_{10(n)})$$

where  $M_n$  and  $\phi_n$  are the modulus and phase angle of pressure no. 1. The modulus of the pressure is in mmHg. Therefore, we must change this to dynes/cm<sup>2</sup> in order for the flow to be in ml/sec (1 mmHg = 1333 dynes/cm<sup>2</sup>). Therefore,

$$\begin{aligned} Q_1 &= \frac{(1333) (0.36) (0.24) (7.25) (0.86)}{(2) (2.04) (1.055) (3.0)} \sin(nr \times 15^\circ - 70^\circ) \\ &= 55.61 \sin(nr \times 15^\circ - 70^\circ) \end{aligned}$$

A value for  $Q$  must be determined for each  $r$  from 0 to 23 for each harmonic (see Tables 17, 18, and 19, and Figures 47 and 48).

## 5. The Computer Program.

The computer program was written in machine language and Fortran II. In addition to giving the computed and measured flow, the program also gives the peak and average power (see Figure 49).

Table 17  
Fourier Components of the Computed Flow Curve

Harmonic No.	$\alpha$	$M'_{10}$	$\epsilon'_{10}$	$\Delta\phi$ (radians)	$M_Q$ (ml/sec)	$\phi_Q$ (radians)
1	11.03	0.862	0.14	0.24	55.61	-1.22
2	15.19	0.913	0.10	0.22	22.37	3.19
3	18.60	0.930	0.08	0.41	17.14	1.16
4	21.50	0.935	0.07	0.41	7.06	-0.77
5	24.02	0.940	0.06	0.73	9.99	-2.21
6	26.31	0.945	0.05	0.06	0.74	1.91

Table 18

Oscillatory Components of the Flow for the First Harmonic

$r$	$r \times 15^\circ$	$\phi_{Q_1}$ (degrees)	$\sin\phi_{Q_1}$	$M_{Q_1} \sin\phi_{Q_1}$ (ml/sec)
0	0	-70.00	-0.94	-52.3
1	15	-55.00	-0.82	-45.6
2	30	-40.00	-0.64	-35.6
3	45	-25.00	-0.42	-23.6
4	60	-10.00	-0.17	-09.5
5	75	05.00	0.09	05.0
6	90	20.00	0.34	18.9
7	105	35.00	0.57	31.7
8	120	50.00	0.76	42.3
9	135	65.00	0.91	50.6
10	150	80.00	0.98	54.5
11	165	95.00	0.99	54.5
12	180	110.00	0.94	52.3
13	195	125.00	0.82	45.6
14	210	140.00	0.64	35.6
15	225	155.00	0.42	23.6
16	240	170.00	0.17	09.5
17	255	185.00	-0.09	-05.0
18	270	200.00	-0.34	-18.9
19	285	215.00	-0.57	-31.7
20	300	230.00	-0.76	-42.3
21	315	245.00	-0.91	-50.6
22	330	260.00	-0.98	-54.5
23	345	275.00	-0.99	-55.5



Table 19  
Oscillatory Components of the Flow for the Remaining 5 Harmonics

r	2	3	4	5	6	$\Sigma$ 1 thru 6
0	-1.2	15.7	-4.9	-8.0	-0.74	-60.30
1	-14.7	15.9	1.9	-7.8	-0.26	-59.60
2	-24.3	6.8	6.8	4.0	-0.74	-50.30
3	-27.3	-6.3	4.9	9.9	0.26	-46.80
4	-23.1	-15.7	-1.9	1.1	0.74	-50.40
5	-12.6	-15.9	-6.8	-9.3	-0.26	-39.12
6	1.2	-6.8	-4.9	-5.9	-0.74	-18.90
7	14.7	6.3	1.9	6.2	0.26	67.70
8	24.3	15.7	6.8	9.2	0.74	107.80
9	27.3	15.9	4.9	-1.5	-0.26	106.90
10	23.1	6.8	-1.9	-9.9	-0.74	82.90
11	12.6	-6.3	-6.8	-3.7	0.26	62.60
12	-1.2	-15.7	-4.9	8.0	0.74	49.60
13	-14.7	-15.9	1.9	7.8	-0.26	33.50
14	-24.3	-6.8	6.8	-4.0	-0.74	14.90
15	-27.3	6.3	4.9	-9.9	0.26	2.40
16	-23.1	15.7	-1.9	-1.2	0.74	1.90
17	-12.6	15.9	-6.8	9.3	-0.26	-0.04
18	1.2	6.8	-4.9	5.9	-0.74	-14.50
19	14.7	-6.3	1.9	-6.2	0.26	-47.20
20	24.3	-15.7	6.8	-9.2	0.74	-44.20
21	27.3	-15.9	4.9	1.5	-0.26	-42.40
22	23.1	-6.8	-1.9	9.9	-0.74	-43.10
23	12.6	6.3	-6.8	3.7	0.26	-50.30

Figure 47

The first and second harmonic components of the  
computed flow curve and the sum of these components

- (A) is the sine wave representing the first or fundamental harmonic.  
The modulus (M) is 55.61 ml/sec and the phase ( $\phi$ ) is -1.22 radians.
- (B) is the sine wave representing the second harmonic and the  
synthesized flow curve (1 + 2). The modulus (M) of the second  
harmonic is 22.37 ml/sec and the phase ( $\phi$ ) is +3.19 radians.

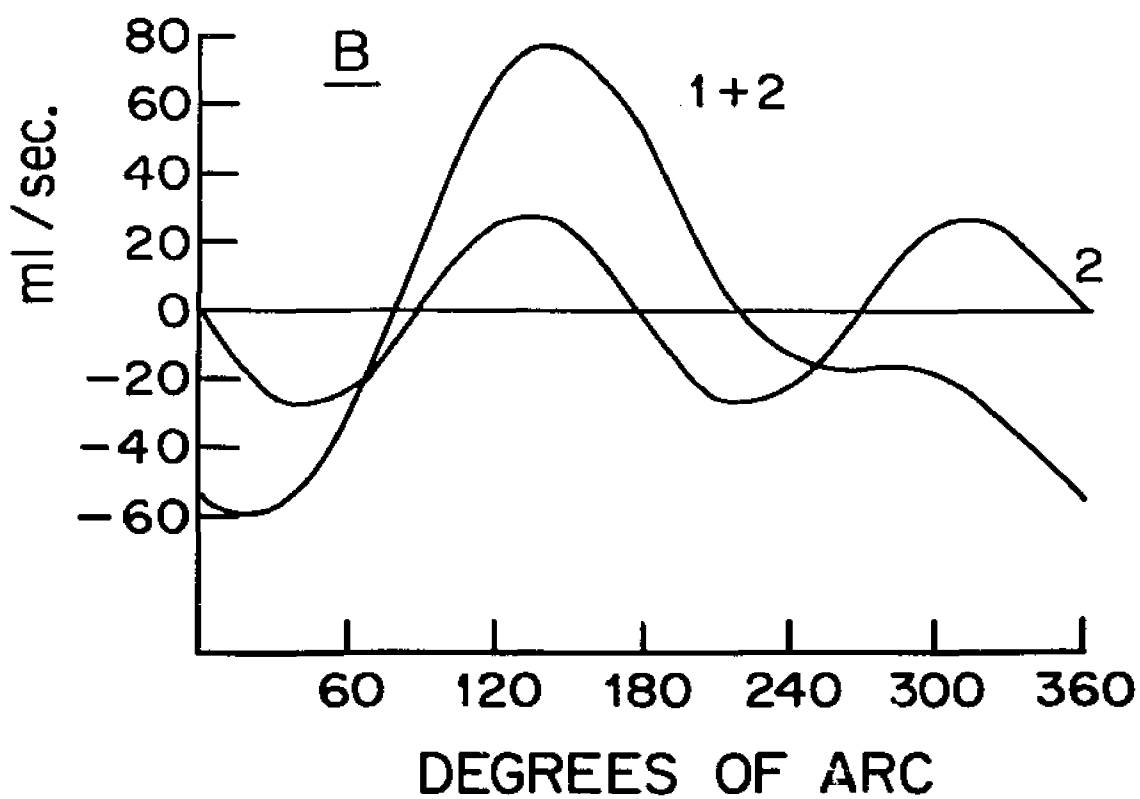
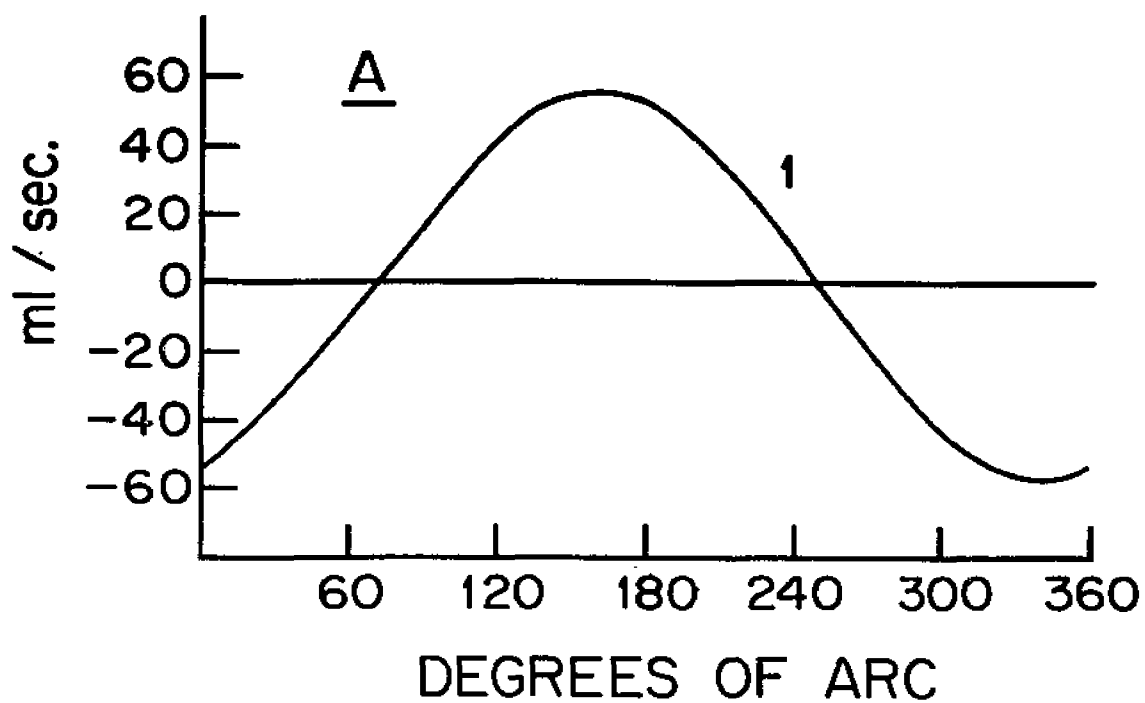


Figure 48

The third harmonic component of the computed flow curve. The sum of the first three harmonics and the final summation of the six harmonics

- (A) is the sine wave representing the third harmonic and the sum of the first three harmonic components (1 + 2 + 3). The modulus (M) of the third harmonic is 17.14 ml/sec and the phase ( $\phi$ ) is +1.16 radians.
- (B) is the final summation of the six harmonic components. The zero line has been shifted to represent the addition of the mean flow, as the sine waves only represent the oscillating part of the flow. The fourth, fifth, and sixth harmonics are too small to be shown on this graph.

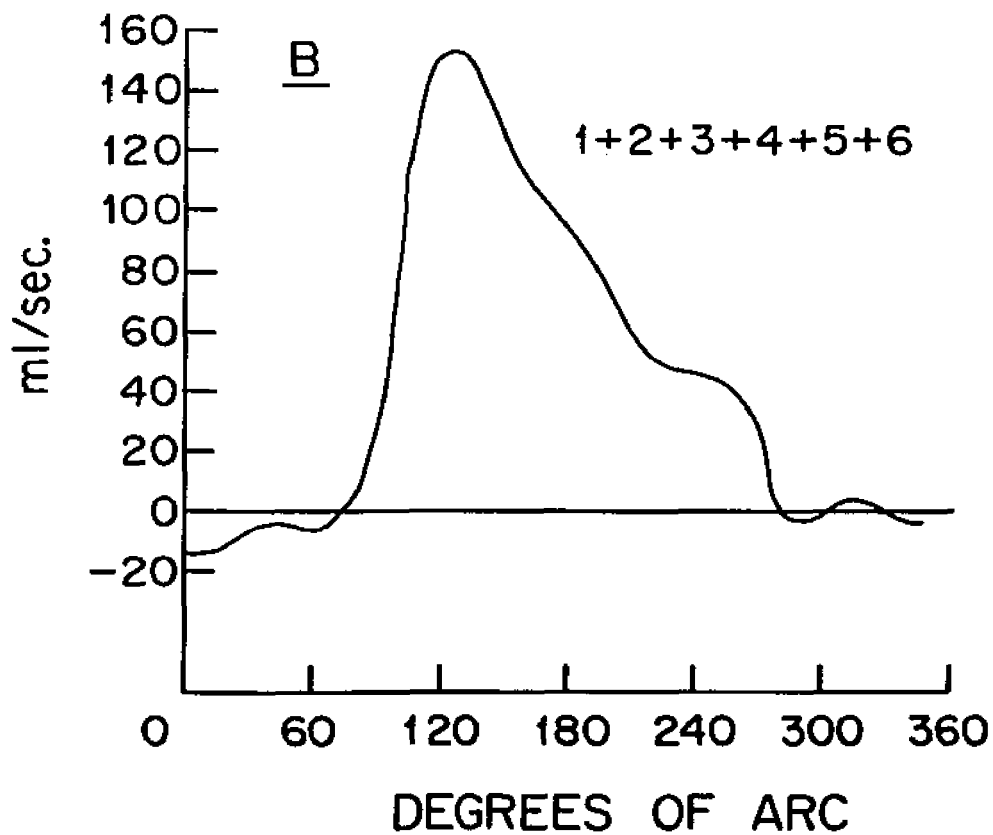
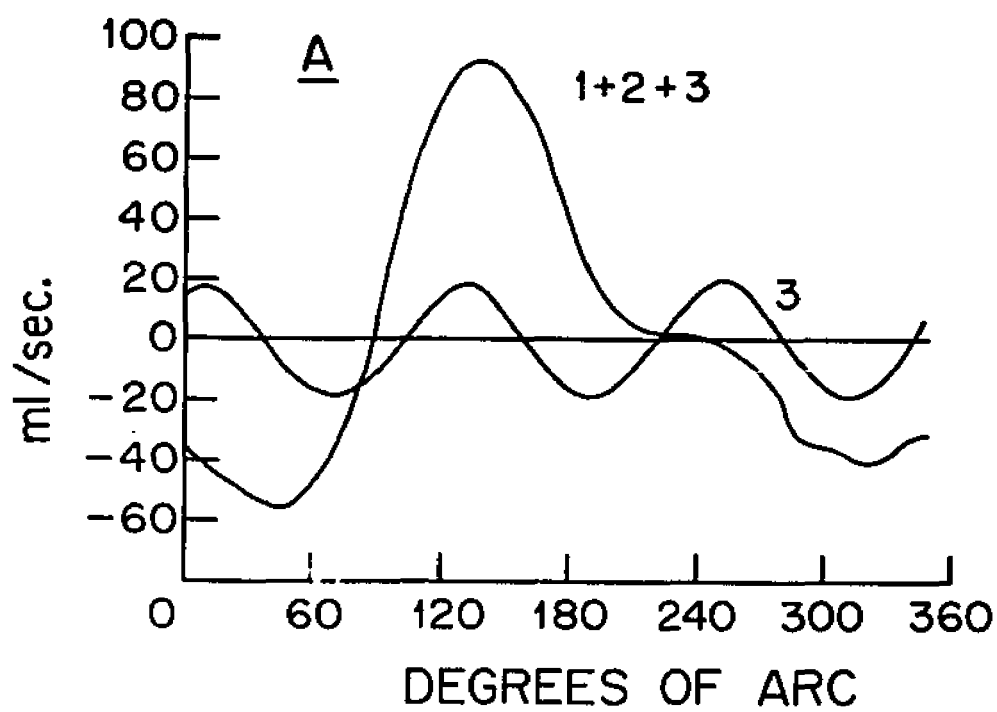
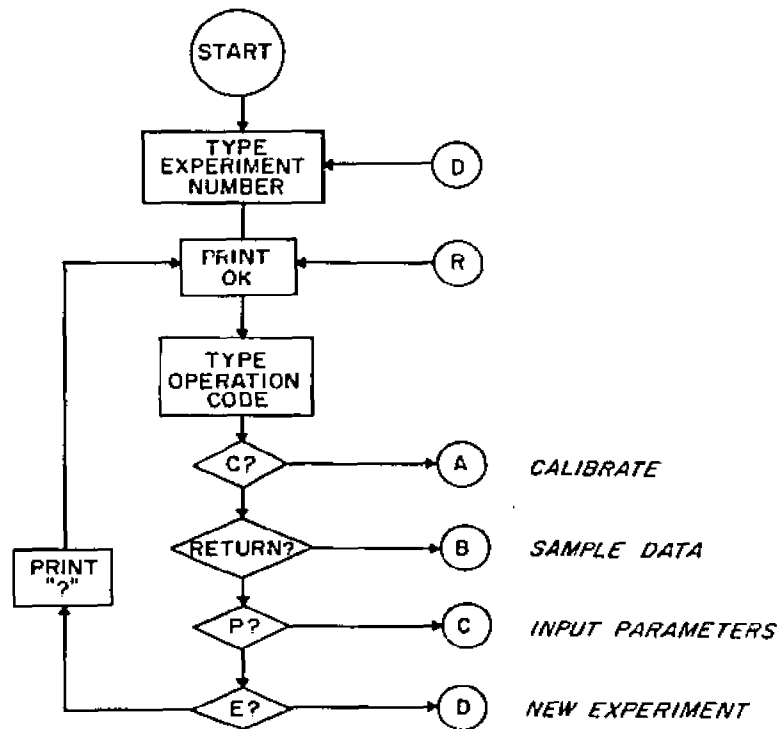
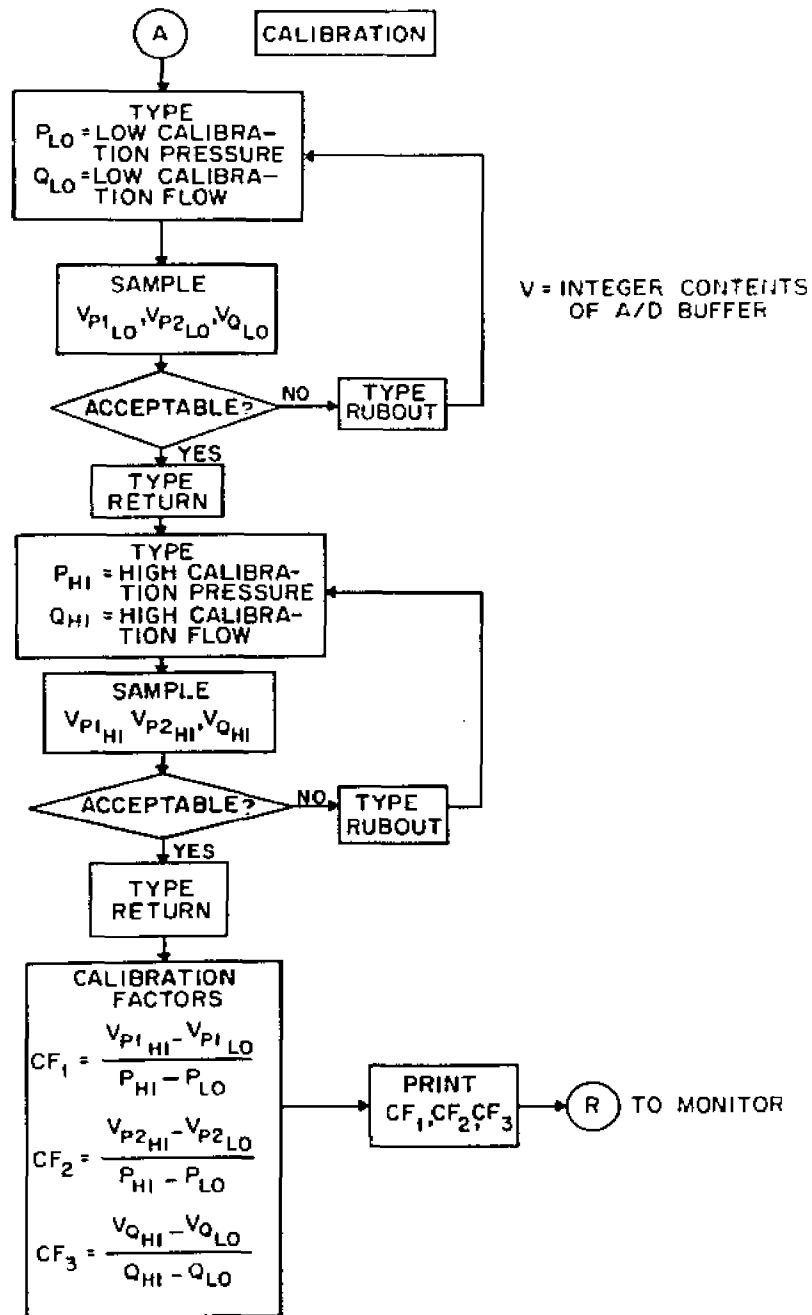


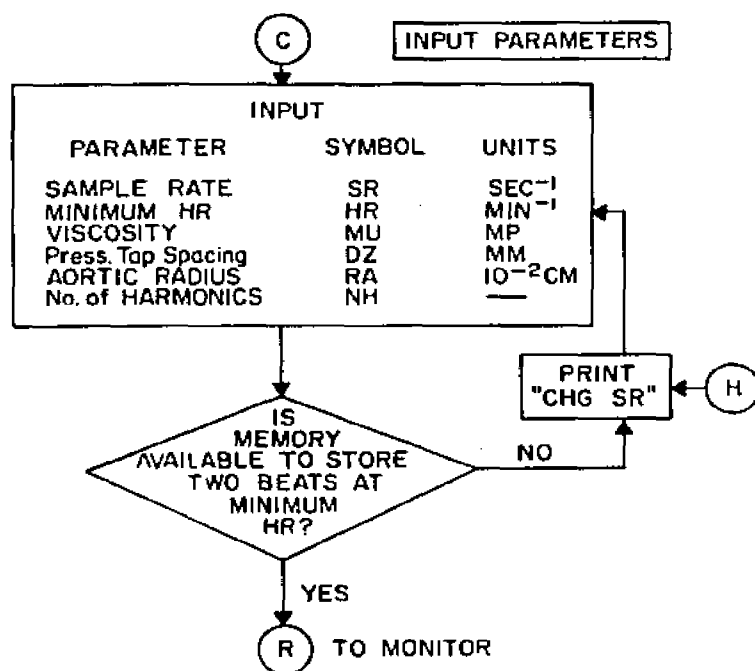
Figure 49

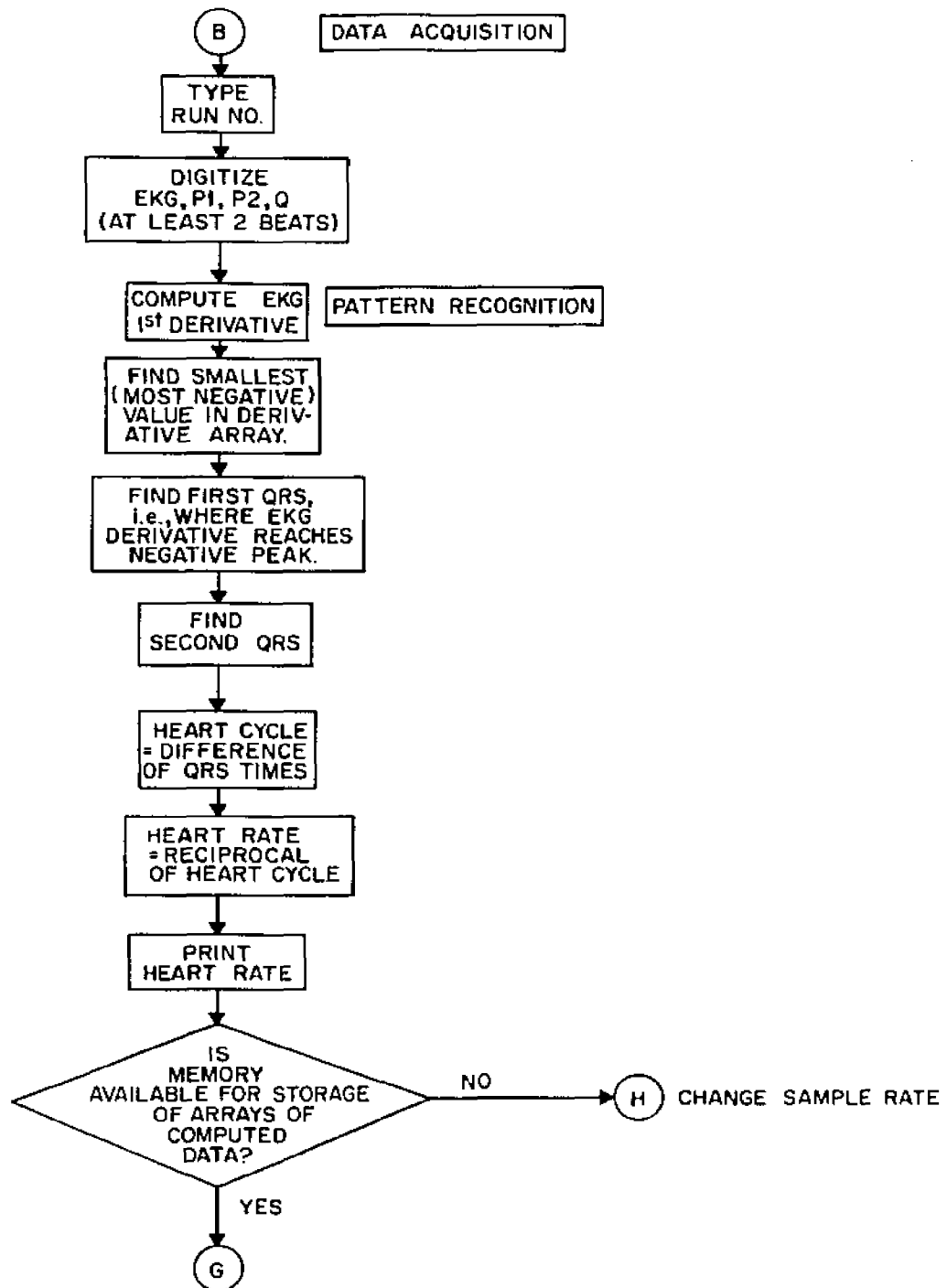
A flow chart of the computer program

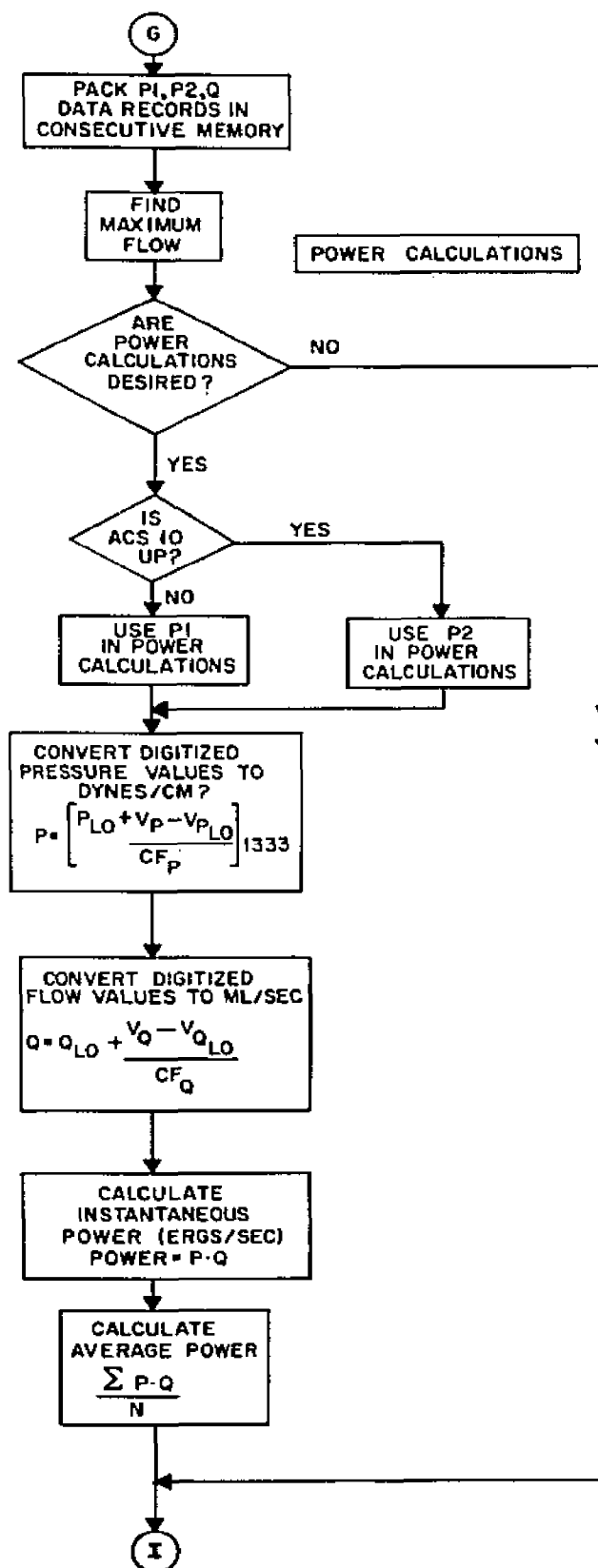


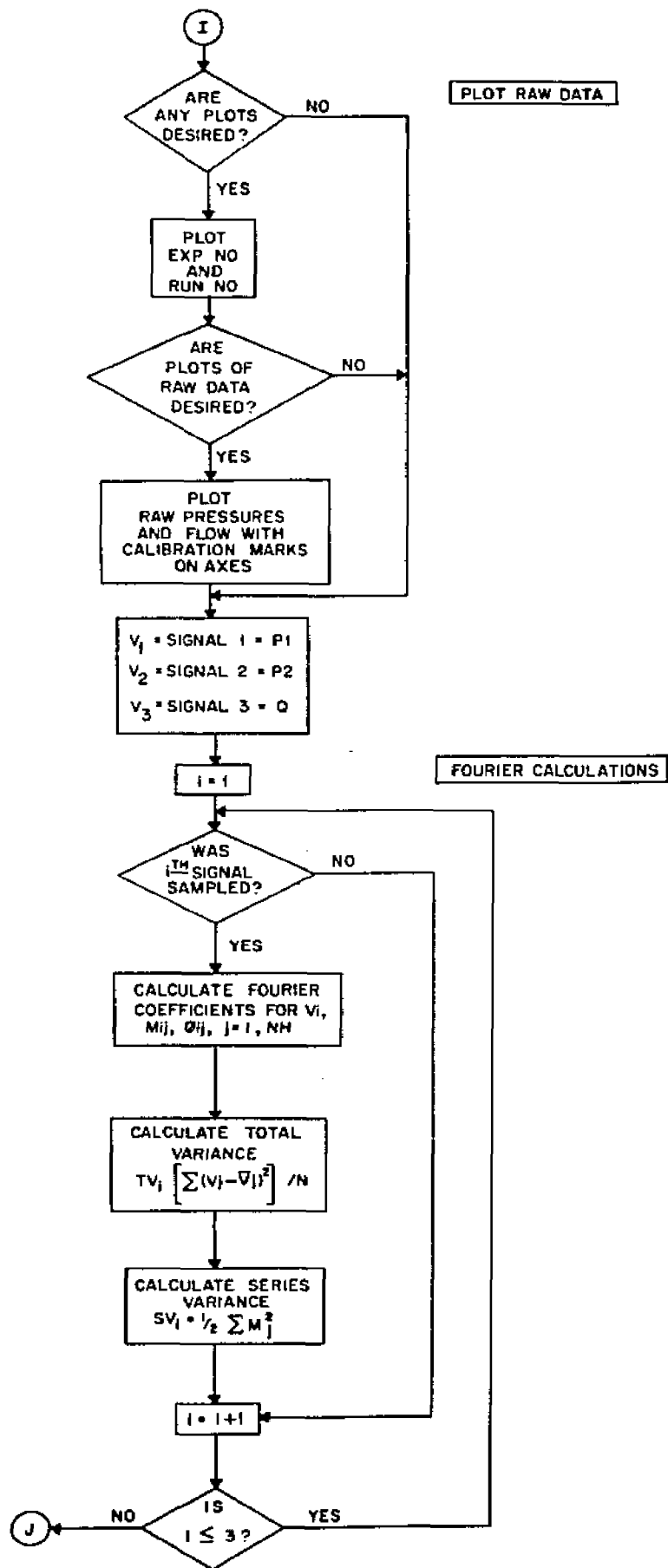


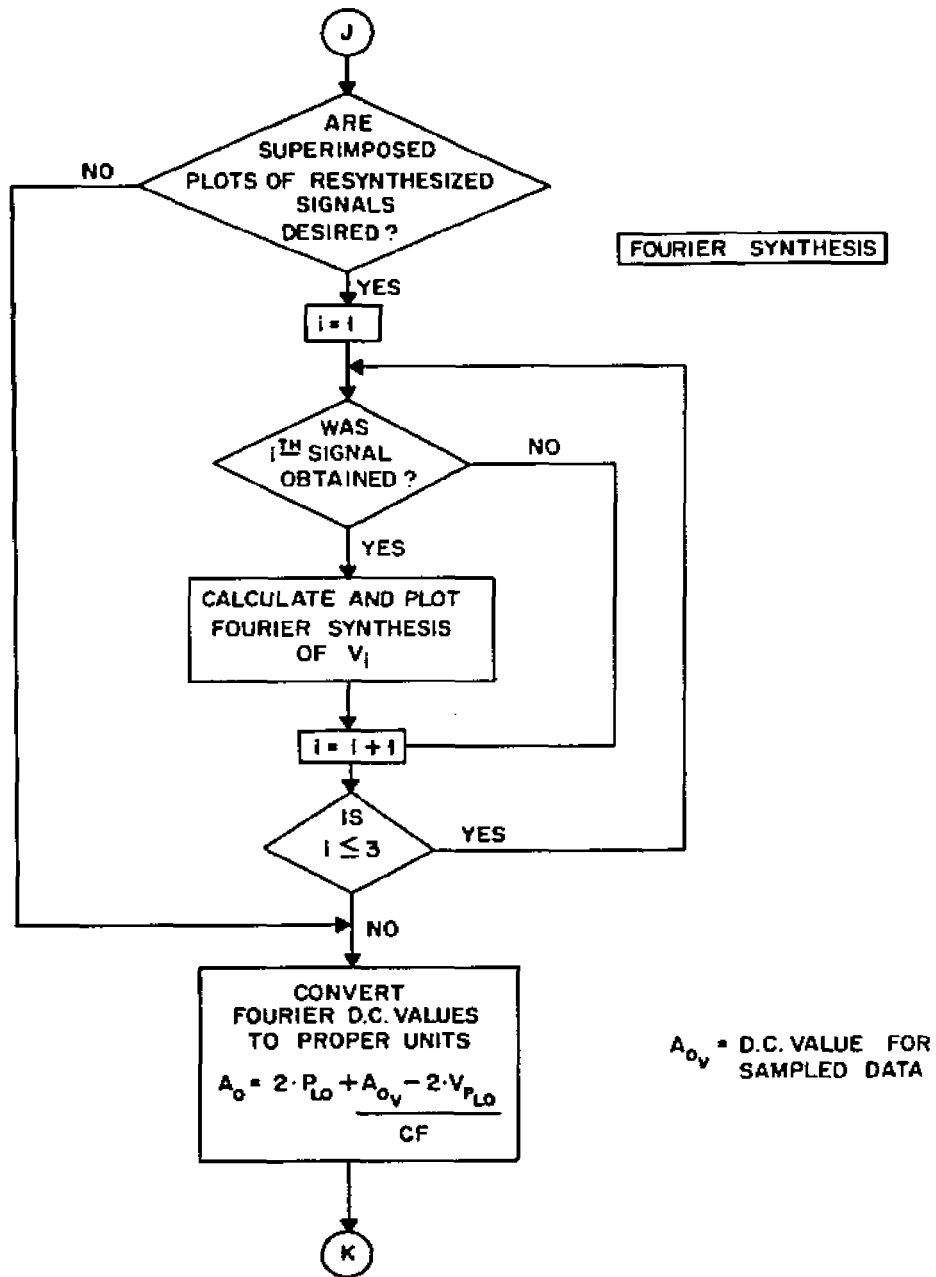


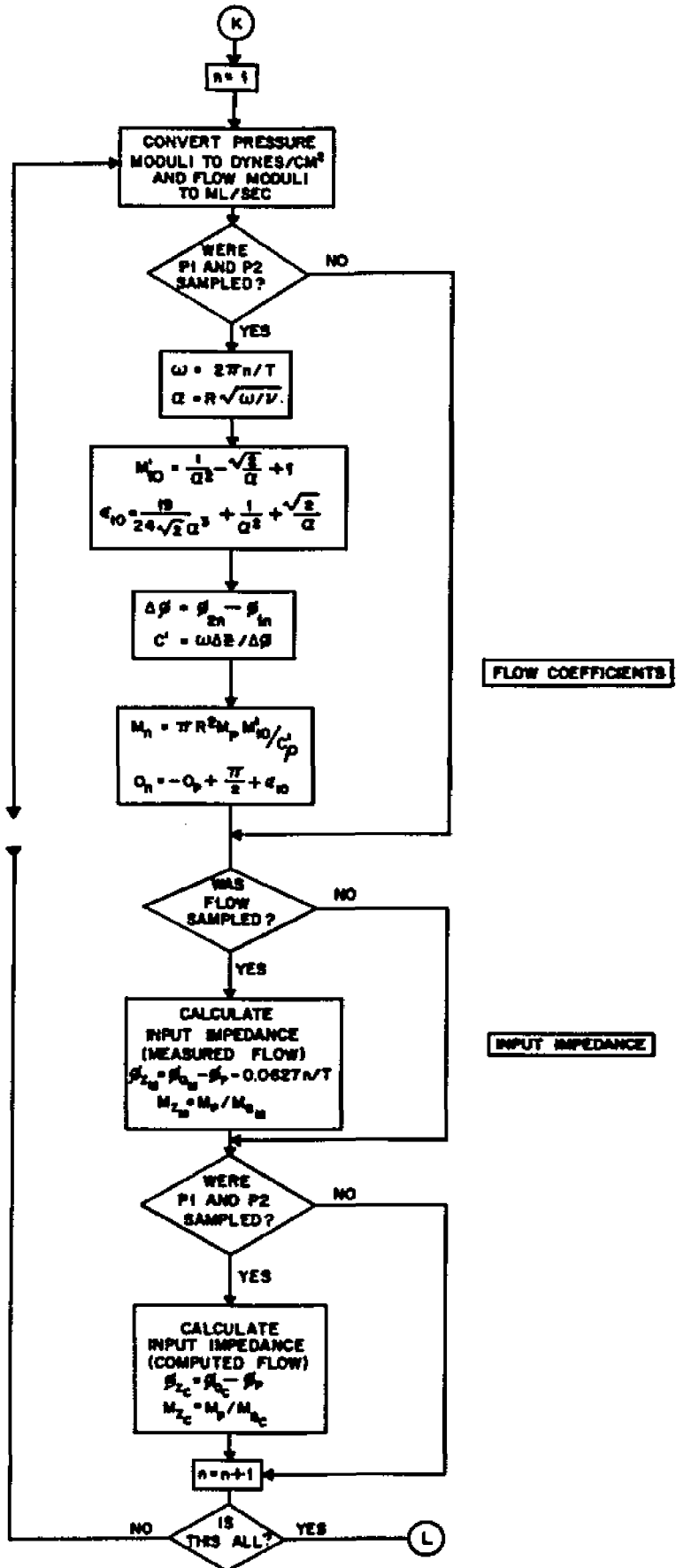


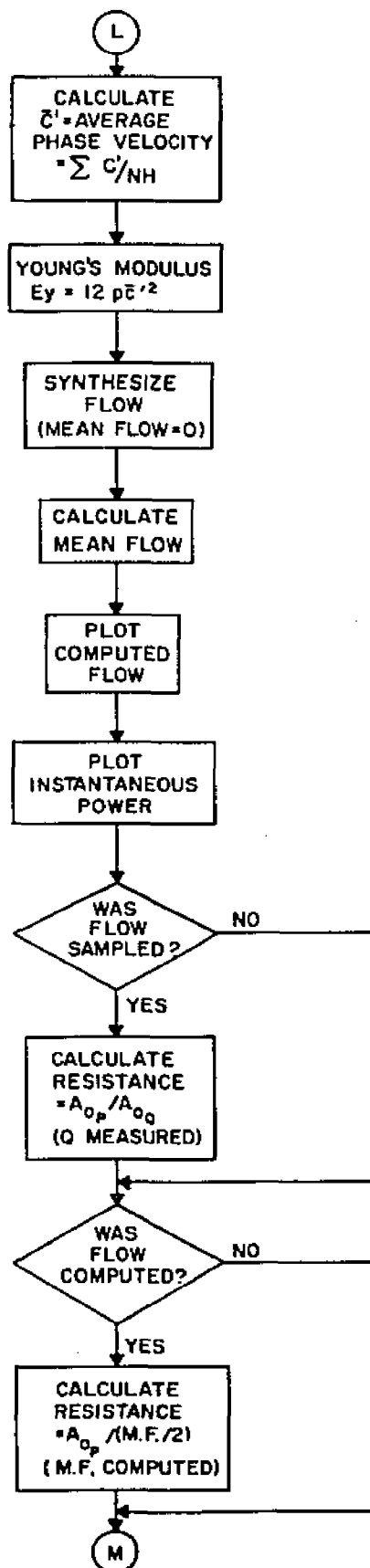




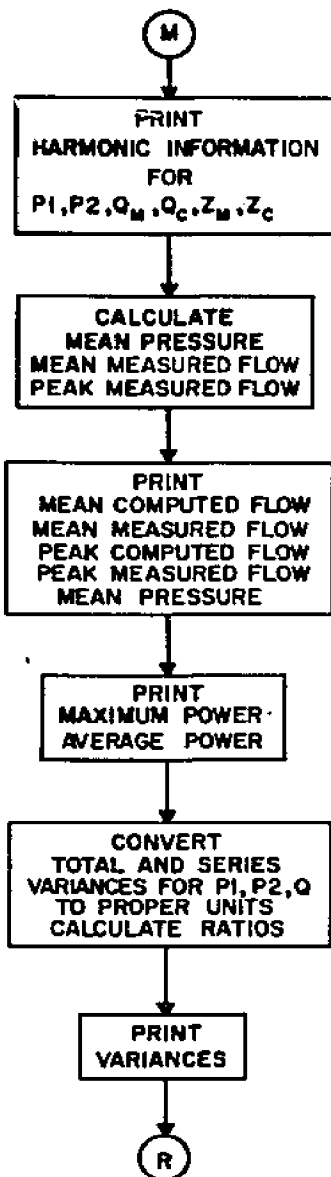








RESISTANCE



OUTPUT

VARIANCES



## BIBLIOGRAPHY

- Anliker, M., M. B. Histan and E. Ogden, 1968. Dispersion and attenuation of small artificial pressure waves in the canine aorta, *Circ. Res.* 28: 539.
- Attinger, E. O., A. Anne and D. A. McDonald, 1966. Use of Fourier series for the analysis of biological systems, *Biophys. J.* 6: 291.
- Barnett, G. O., J. C. Greenfield and S. M. Fox, 1961. The technique of estimating the instantaneous aortic blood velocity in man from the pressure-gradient, *Amer. Heart J.* 62: 359.
- Benchimol, A., H. F. Stegall, P. R. Maroko, J. W. Gartlan and L. Brewer, 1969. Aortic flow velocity in man during cardiac arrhythmias measured with the Doppler catheter-flowmeter system, *Amer. Heart J.* 78: 649.
- Berne, R. M. and M. N. Levy, 1967. Cardiovascular Physiology, C. V. Mosby Company, St. Louis.
- Bond, R. F. and C. A. Barefoot, 1967. Evaluation of an electromagnetic catheter tip velocity sensitive blood flow probe, *J. Appl. Physiol.* 23: 403.
- Boyett, J. E., D. E. Stowe and L. A. Becker, 1966. Evaluation of aortic blood velocity computed from the pressure pulse, *U.S.A.F. Sch. Aerospace Med. SAM-TR-66-75*: 1.
- Bramwell, J. C. and A. V. Hill, 1922. The velocity of the pulse wave in man, *Proc. Roy. Soc. B*, 93: 298.
- Brownlee, K. A., 1966. Statistical Theory and Methodology in Engineering, 2nd Ed, John Wiley & Sons, Inc., New York.
- Cournand, A., 1945. Measurement of cardiac output in man using right heart catheterization; description of technique; discussion of validity and of place in study of circulation, *Fed. Proc.* 4: 207.
- Cournand, A. and H. A. Ranges, 1941. Catheterization of right auricle in man, *Proc. Soc. Exper. Biol. Med.* 46: 462.

- Cournand, A., R. L. Riley, E. S. Breed, D. Baldwin and D. W. Richards, 1945. Measurement of cardiac output in man using technique of catheterization of right auricle or ventricle, *J. Clin. Invest.* 24: 106.
- Dawson, P. M. and L. W. Gorham, 1908. The pulse pressure as an index of the systolic output, *J. Exper. Med.* 10: 484.
- Dick, D. W., J. E. Kendrick, G. L. Matson and V. C. Rideout, 1968. Measurement of nonlinearity in the arterial system of the dog by a new method, *Circ. Res.* 22: 101.
- Erlanger, J. and D. R. Hooker, 1904. An experimental study of blood pressure and of pulse pressure in man, *Johns Hopkins Hosp. Rep.* 12: 145.
- Fick, A., 1870. Uber die Messung des Blutquantums in den Herzventrikeln, *Sitz. ber Physik. Med. ges. Wurzburg*, 16.
- Forssman, Q., 1929. Die Sondierung des rechten Herzens, *Klin. Wochschr.* 8: 2085.
- Franklin, D. E., W. Schlegel and R. F. Rushmer, 1961. Blood flow measured by Doppler frequency shift back scatter ultrasound, *Science*, 134: 564.
- Franklin, D. E., D. W. Baker and R. F. Rushmer, 1962. Ultrasonic transit time flowmeter, *Ins. Rad. Eng. Trans. Bio. Med. Elect. BME*: 9: 4.
- Franklin, D. E., W. Schlegel and N. W. Watson, 1963. Ultrasonic Doppler shift blood flowmeter circuitry and practical application, *Proc. ISA Biomed. Sci. Instrum. Symp.* 1.
- Fry, D. L., 1959. The measurement of pulsatile blood flow by the computed pressure-gradient technique, *IRE Trans. Med. Electron.* 6: 259.
- Fry, D. L. and J. C. Greenfield, 1964. The mathematical approach to hemodynamics, with particular reference to Womersley's theory, in Pulsatile Blood Flow, McGraw-Hill, New York, 85.
- Fry, D. L., A. J. Mallos and G. T. Casper, 1956. A catheter tip method for measurement of the instantaneous aortic blood velocity, *Circ. Res.* 4: 627.
- Fry, D. L., F. W. Noble and A. J. Mallos, 1957. An electric device for instantaneous and continuous computation of aortic blood velocity, *Circ. Res.* 5: 75.

- Gabe, I. T., 1965. An analogue computer deriving oscillatory arterial flow from the pressure-gradient, *Phys. Med. Biol.* 10: 407.
- Gabe, I. T., J. Karnell, I. G. Porjé and B. Rudewald, 1964. The measurement of input impedance and apparent phase velocity in the human aorta, *Acta Physiol. Scand.* 61: 73.
- Gessner, U. and D. H. Bergel, 1964. Frequency response of electromagnetic flowmeters, *J. Appl. Physiol.* 19: 1209.
- Goldstein, S., 1938a. Modern developments in fluid dynamics, Vol. I., Clarendon Press, Oxford.
- Goldstein, S., 1938b. Modern developments in fluid dynamics, Vol. II., Clarendon Press, Oxford.
- Greenfield, J. C., D. J. Patel, A. J. Mallos and D. L. Fry, 1962. Evaluation of Kolin type electromagnetic flowmeter and the pressure-gradient, *J. Appl. Physiol.* 17: 372.
- Greenfield, J. C. and D. L. Fry, 1965. Relationship between instantaneous aortic flow and the pressure-gradient, *Circ. Res.* 17: 340.
- Grehart, H. and C. E. Quinquaud, 1886. Recherches expérimentales sur la mesure du volume de sang qui traverse les paumons en un temps donné, *Compt. Rend. Soc. Biol.* 30: 159.
- Grollman, A., 1929. The determination of the cardiac output of man by the use of acetylene, *Amer. J. Physiol.* 88: 432.
- Grossman, J. R., E. Weston and L. Leiter, 1953. A method for determining cardiac output by the direct Fick principle without gas analysis, *J. Clin. Invest.* 32: 161.
- Guillemin, E., 1949. Mathematics of Circuit Analysis, J. Wiley & Sons, Inc., New York.
- Guthrie, D., 1945. A History of Medicine, Thomas Nelson & Sons, Ltd., New York.
- Guyton, A. C., 1963. Circulatory Physiology: Cardiac Output and Its Regulation, W. B. Saunders, Philadelphia.
- Guyton, A. C., C. A. Farish, and J. B. Abernathy, 1959. Continuous cardiac output recorder employing the Fick principle, *Circ. Res.* 1: 661.

- Hale, J. F., D. A. McDonald and J. R. Womersley, 1955. Velocity profiles of oscillating arterial flow, with some calculations of viscous drag and the Reynolds number, *J. Physiol.* 128: 629.
- Hales, S., 1733. Statical Essays, New York Academy of Medicine, The History of Medicine Series, Reprint 22, Hafner Publishing Co., 1964.
- Hamilton, W. F., 1953. The physiology of cardiac output, *Circulation*: 8: 527.
- Hamilton, W. F., 1962. Measurement of the cardiac output, Section 2, Vol. I, Handbook of Physiology, Amer. Physiol. Soc., Washington.
- Hamilton, W. F., J. W. Moore, J. M. Kinsman, and R. G. Spurling, 1928. Simultaneous determination of the greater and lesser circulation times, of the mean velocity of blood flow through the heart and lungs, of the cardiac output and an approximation of the amount of blood actively circulating in the heart and lungs, *Amer. J. Physiol.* 85: 377.
- Hamilton, W. F. and J. W. Remington, 1947. The measurement of the stroke volume from the pressure pulse, *Amer. J. Physiol.* 148: 14.
- Hamming, R. W., 1962. Numerical Methods for Scientists and Engineers, McGraw-Hill, New York.
- Helps, E. P. W. and D. A. McDonald, 1954. Arterial blood flow calculated from pressure-gradients, *J. Physiol.* 124: 30.
- Harvey, W., 1628. Exercitatio anatomica de motu cordis et sanguinis in animalibus, ed. with translation by K. J. Franklin, Blackwell's, Oxford, 1957.
- Hatschek, E., 1928. The Viscosity of Liquids, Bell, London.
- Henriques, V., 1913. Über die Verteilung des Blutes vom linken Herzen zwischen dem Herzen und dem übrigen Organismus, *Biochem. Z.* 56: 230.
- Hernandez, R. R., J. C. Greenfield, Jr. and B. W. McCall, 1964. Pressure-flow studies in hypertrophic subaortic stenosis, *J. Clin. Invest.* 43: 401.
- Indritz, J., 1963. Methods in Analysis, The MacMillan Co., New York.
- Jochim, K. E., 1948. Electromagnetic flowmeter, in Vol. I., Methods in Medical Research, ed. V. R. Potter, Year Book Publishers, Chicago, 108.

- Johnson, R. E. and F. L. Kiokemeister, 1962. Calculus, Allyn and Bacon, Boston.
- Jones, W. B., L. L. Hefner, J. R. Bancroft and W. Klip, 1959. Velocity of blood flow and stroke volume obtained from the pressure pulse, J. Clin. Invest. 38: 2087.
- Jones, W. B. and J. B. Griffin, 1962. Comparison of computed aortic blood velocity with that of electromagnetic flowmeter, J. Appl. Physiol. 17: 482.
- Jones, W. B., R. O. Russell, Jr. and D. H. Dalton, 1966. An evaluation of computed stroke volume in man, Amer. Heart J. 72: 746.
- Khoury, E. M. and D. E. Gregg, 1963. Miniature electromagnetic flowmeter applicable to coronary arteries, J. Appl. Physiol. 18: 224.
- Kinsman, J. M., J. W. Moore and W. F. Hamilton, 1929. Studies on the circulation: I. Injection method. Physical and mathematical considerations, Amer. J. Physiol. 89: 222.
- Klein, O., 1930. Für Bestimmung des zirkulatorischen Minutenvolums beim Menschen nach den Fickschen Prinzip mittels Herzsondierung, Münch. Med. Wochschr. 77: 1311.
- Kolin, A., 1936. An electromagnetic flowmeter: principles of the method and its application to blood flow measurements, Proc. Soc. Exper. Biol. Med. 35: 53.
- Kolin, A., 1945. An alternating field induction flowmeter of high sensitivity, Rev. Sci. Instrum. 16: 109.
- Kolin, A., 1960. Blood flow determinations by electromagnetic methods, Vol. III, in Medical Physics, ed. O. Glasser, Year Book Publishers, Chicago.
- Kolin, A., 1969. A radial field electromagnetic intravascular flow sensor, IEEE Trans. Biomed. Eng. 16: 220.
- Kolin, A. and R. Wisshaupt, 1963. Single coil coreless electromagnetic blood flowmeters, IRE Trans. Bio. Med. Electron. BME 10: 60.
- Kouchoukos, N. T., L. C. Sheppard, D. A. McDonald, and J. W. Kirklin, 1969. Estimation of stroke volume from the central arterial pressure contour in postoperative patients, Surg. Forum, 20: 180.

- Kouchoukos, N. T., L. C. Sheppard and D. A. McDonald, 1970.  
Estimation of stroke volume in the dog by a pulse contour method, *Circ. Res.* 26, in press.
- Lamb, H., 1932. Hydrodynamics, 6th ed., Dover Publications, New York.
- Lambossy, P., 1950. Aperçu historique et critique sur le problème de la propagation des ondes dans un liquide incompressible enfermé dans un tube elastique, *Helv. Physiol. Acta*, 8: 209.
- Lambossy, P., 1952. Oscillations forcées d'un liquide incompressible et visqueux dans un tube rigide et horizontal. Calcul de la force de frottement, *Helv. Physica Acta*, 25: 371.
- Luciani, L., 1911. Human Physiology, Vol. I, MacMillan, London.
- McDonald, D. A., 1955. The relation of pulsatile pressure to flow in arteries, *J. Physiol.* 127: 533.
- McDonald, D. A., 1960. Blood Flow in Arteries, Williams and Wilkins, Baltimore:
- McDonald, D. A., 1967. The continuous measurement of cardiac output, Digest 7th Int'l Conf. Med. Biol. Eng., Stockholm, 156 (abstract).
- McDonald, D. A., 1968a. Regional pulse-wave velocity in the arterial tree, *J. Appl. Physiol.* 24: 73.
- McDonald, D. A., 1968b. Chapter on Hemodynamics in Annual Review of Physiology, 30: 525.
- McDonald, D. A. and M. G. Taylor, 1959. The hydrodynamics of the arterial circulation, *Prog. in Biophys. & Biophys. Chem.* 9: 105.
- McDonald, D. A., N. T. Kouchoukos and W. W. Nichols, 1968a. Ventricular ejection computed from the time derivative of aortic pressure, *Proc. Int'l Union Physiol. Sciences*, XXIV Int'l Congr. 7: 287 (abstract).
- McDonald, D. A., W. W. Nichols and N. T. Kouchoukos, 1968b. Methods for monitoring cardiac output, *Proc. 21st Ann. Conf. on Eng. in Med. & Biol.* 10: 21A1 (abstract).

- McDonald, D. A., A. Navarro, S. Jedlicka and W. W. Nichols, 1970. The calibration of manometer-catheter systems; a comparison of the free-vibration and forced oscillation methods, J. Appl. Physiol., in preparation.
- McLachlan, N. W., 1941. Bessel Functions for Engineers, Oxford University Press.
- Malooly, D. A., D. E. Donald, H. W. Marshall and E. H. Wood, 1963. Assessment of an indicator dilution technique for quantitating aortic regurgitation by electromagnetic flowmeter, Circ. Res. 12: 487.
- Marshall, R. J. and J. T. Shepherd, 1959. Effect of injections of hypertonic solutions on blood flow through the femoral artery of the dog, Amer. J. Physiol. 197: 951.
- Medkins, J. and H. W. Davies, 1922. The influence of circulatory disturbances on the gaseous exchange in the blood. II. A method of measuring circulation rate in man, Heart, 9: 191.
- Mills, C. J., 1966. A catheter tip electromagnetic velocity probe, Phys. Med. Biol. 11: 323.
- Mills, C. J. and J. P. Shillingford, 1967. A catheter tip electromagnetic velocity probe and its evaluation, Cardiovasc. Res. 1: 263.
- Milnor, W. R., D. H. Bergel and J. D. Bargainer, 1966. Hydraulic power associated with pulmonary blood flow and its relation to heart rate, Circ. Res. 19: 467.
- Milnor, W. R., C. R. Conti, K. B. Lewis and M. F. O'Rourke, 1969. Pulmonary arterial pulse wave velocity and impedance in man, Circ. Res. 25: 637.
- Nichols, W. W., N. T. Kouchoukos and D. A. McDonald, 1968. Pulsatile flow in the ascending aorta computed from pressure, Fed. Proc. 27: 445 (abstract).
- Nichols, W. W., J. E. Webster and D. A. McDonald, 1969. Pulse wave velocity in the ascending aorta of the dog, Physiologist, 12: 315.
- Nichols, W. W. and D. A. McDonald, 1969. Aortic impedance derived from the apparent phase velocity, Fed. Proc. 28: 643 (abstract).
- Nichols, W. W. and D. A. McDonald, 1970. Wave velocity in the proximal aorta, J. Appl. Physiol. (in preparation).

- Nolan, S. P., R. D. Fisher, S. H. Dixon, Jr. and A. G. Morrow, 1969. Quantification of aortic regurgitation with a catheter tip velocitometer, Surgery, 65: 876.
- Oka, S., 1967. Rheology of blood, Koubunski, 16: 425.
- Olmstead, F., 1960. Measurement of cardiac output in unrestrained dogs by an implanted electromagnetic meter, in Medical Electronics, ed. C. N. Smyth, Charles C. Thomas, Springfield, Illinois.
- O'Rourke, M. F. and M. G. Taylor, 1967. Input impedance of the systemic circulation, Circ. Res. 20: 365.
- Pardue, D. R., A. L. Hedrich, J. C. Rose and P. A. Kot, 1967. Ultrasonic catheter-tip probe for measuring blood flow velocity, Circulation: Suppl. ii, 25 & 26: 204.
- Patel, D. J., F. M. deFreitas and D. L. Fry, 1963. Hydraulic input impedance to aorta and pulmonary artery in dogs, J. Appl. Physiol. 18: 134.
- Pipes, L. A., 1958. Applied Mathematics for Engineers and Physicists, McGraw-Hill, New York.
- Porjé, I. G., 1946. Studies of the arterial pulse wave, particularly in the aorta, Acta Physiol. Scand. 13: Suppl. 42: 1.
- Porjé, I. G. and B. Rudewald, 1957. Studies on a new theory of determination of some fundamental hemodynamic data in a circulation model, in normal persons and in aortic valvular diseases, Opuscula Medica, 2: 280.
- Porjé, I. G. and B. Rudewald, 1961. Hemodynamic studies with differential pressure technique, Acta Physiol. Scand. 51: 116.
- Randall, J. E., 1958. Statistical properties of pulsatile pressure and flow in the femoral artery of the dog, Circ. Res. 6: 689.
- Richardson, E. G. and E. Tyler, 1929. The transverse velocity gradient near the mouth of pipes in which an alternating or continuous flow of air is established, Proc. Phys. Soc. Lond. 42: 1.
- Rose, J. C., 1956. The Fick principle and the cardiac output, Gen. Practitioner, 14: 115.
- Rosen, I. T. and H. L. White, 1926. The relation of pulse pressure to stroke volume, Amer. J. Physiol. 78: 168.



- Rudinger, G., 1966. Review of current mathematical methods for the analysis of blood flow, in Biomed. Fluid Mech. Symp., New York, Amer. Soc. Mech. Engrs. 1.
- Scher, A. M., J. Zepada, and O. F. Brown, 1963. Square-wave electromagnetic flowmeter employing commercially available recorder, J. Appl. Physiol. 18: 1265.
- Schonfeld, J. C., 1948. Resistance and inertia of the flow of liquids in a tube or open canal, Appl. Sci. Res. Hagwe A, 1: 169.
- Schultz, D. L., D. S. Tunstall-Pedoe, G. de J. Lee, A. J. Gunning, and B. J. Bellhouse, 1969. Velocity distribution and transition in the arterial system, Ciba Foundation Symp. on Circulatory & Respiratory Mass Transport, J. & A. Churchill Ltd., London, 72.
- Shercliff, J. A., 1962. The Theory of Electromagnetic Flow Measurement, Cambridge University Press.
- Skalak, R., Wave-propagation in blood flow, in Biomechanics, ed. Y. C. Fung, Appl. Mechanics Div., Amer. Soc. Mech. Engrs., New York, 20, 1966.
- Snell, R. E. and P. C. Luchsinger, 1965. Determination of the external work and power of the left ventricle in intact man, Amer. Heart J. 69: 529.
- Sokolnikoff, I. S., 1939. Advanced Calculus, McGraw-Hill, New York.
- Spencer, M. P. and A. B. Denison, 1959. Square-wave electromagnetic flowmeter: theory of operation and design of magnetic probes for clinical and experimental application, IRE Trans, Med. Electron. 6: 220.
- Spiegel, M. R., 1958. Applied Differential Equations, Prentice-Hall, Inc., Englewood Cliffs, N.J.
- Starr, I., 1954. Clinical tests of the simple method of estimating cardiac stroke volume from blood pressure and age, Circulation, 9: 664.
- Starr, I. and A. Schild, 1954. A rough cardiac output method so simple that it could be performed by any doctor with the apparatus he now has, Trans. Assoc. Amer. Physicians, 67: 192.

- Starr, I., T. G. Schnabel, Jr., S. I. Askovitz, and A. Schild, 1954. Studies made by simulating systole at necropsy. IV. On the relation between pulse pressure and cardiac stroke volume, leading to a clinical method of estimating cardiac output from blood pressure and age, *Circulation*, 9: 648.
- Stegall, H. F., H. L. Store, V. S. Bishop and C. Laenger, 1967. A catheter-tip pressure and velocity sensor, *Proc. 20th Ann. Conf. Eng. Med. Biol.* 9: 27.4 (abstract).
- Stein, P. D. and W. H. Schuette, 1969. New catheter-tip flowmeter with velocity flow and volume flow capabilities, *J. Appl. Physiol.* 26: 851.
- Stewart, G. N., 1897. Researches on the circulation time and on the influences which affect it. IV. the output of the heart, *J. Physiol.* 22: 159.
- Stewart, G. N., 1921. The output of the heart in dogs, *Amer. J. Physiol.* 57: 27.
- Sugahara, H., 1968. Pulsatile Hemodynamics, *Nihon Rinsho*, 26: 242.
- Tang, K. Y., 1966. Alternating-Current Circuits, International Textbook Company, Serant, Pa.
- Taylor, M. G., 1957a. An approach to an analysis of the arterial pulse-wave. I. oscillations in an attenuating line, *Phys. Med. Biol.* 1: 258.
- Taylor, M. G., 1957b. An approach to an analysis of the arterial pulse-wave. II. fluid oscillations in an elastic pipe, *Phys. Med. Biol.* 1: 321.
- Taylor, M. G., 1967. The elastic properties of arteries in relation to the physiological functions of the arterial system, *Gastroenterology*, 52: 358.
- Walker, K., 1955. The Story of Medicine, Oxford University Press, New York.
- Warbasse, J. R., B. H. Hellman, R. E. Gillian, R. W. Hawley and H. I. Babitt, 1969. Physiologic evaluation of a catheter tip electromagnetic velocity probe, *Amer. J. Cardiol.* 23: 424.
- Warner, H. R., J. H. C. Swan, D. C. Connolly, R. G. Tompkins and E. H. Wood, 1953. Quantitation of beat-to-beat changes in stroke volume from the aortic pulse contour in man, *J. Appl. Physiol.* 5: 495.

- Weber, K. C., J. C. Engle, G. W. Lyons, A. C. Madsen and I. W. Fox, 1968. In vivo calibration of electromagnetic flowmeter probes on pulmonary artery and aorta, *J. Appl. Physiol.* 25: 455.
- Westerten, A., G. Herrold and N. S. Assali, 1960. Gated sine wave blood flowmeter, *J. Appl. Physiol.* 15: 533.
- Whitmore, R. L., 1968. Rheology of the Circulation, Pergamon Press Ltd., London.
- Wiley, C. R., Jr., 1960. Advanced Engineering Mathematics, McGraw-Hill, New York.
- Witzig, K., 1914. *Über erzwingene Wellenbewegungen zäher, inkompressibler Flüssigkeiten in elastischen Röhren*, Inaug. Dissert. Bern, Wyss.
- Womersley, J. R., 1954. Flow in the larger arteries and its relation to the oscillating pressure, *J. Physiol.* 124: 31.
- Womersley, J. R., 1955a. Method for the calculation of velocity, rate of flow and viscous drag in arteries when the pressure-gradient is known, *J. Physiol.* 127: 553.
- Womersley, J. R., 1955b. Oscillatory flow in arteries: effect of radial variation in viscosity on rate of flow, *J. Physiol.* 127: 38.
- Womersley, J. R., 1955c. Oscillatory motion of a viscous liquid in a thin-walled elastic tube, I. the linear approximation for long waves, *Phil. Mag.* 46: 199.
- Womersley, J. R., 1957. Oscillatory flow in arteries: the constrained elastic tube as a model of arterial flow and pulse transmission, *Phys. Med. Biol.* 2: 178.
- Womersley, J. R., 1958. The mathematical analysis of the arterial circulation in a state of oscillatory motion, Wright Air Dvpt. Center, Tech. Rept. WADC-TR56-614.
- Yanof, H. M., 1961. Trapezoidal-Wave electromagnetic blood flowmeter, *J. Appl. Physiol.* 16: 566.
- Yanof, H. M., A. L. Rosen, N. M. McDonald and D. A. McDonald, 1963. A critical study of the response of manometers to forced oscillations, *Phys. Med. Biol.* 8: 407.

Young, T., 1808. Hydraulic investigations subservient to an intended Croonian lecture on the motion of blood, Phil. Trans. 98: 164.

Young, T., 1809. The Croonian lecture. On the functions of the heart and arteries, Phil. Trans. 99: 1.